AD-A228 291

4

SECURITY CLASSIFICATION OF THIS PAGE (When Data Entered)

REPORT DOCUMENTATION PAGE		READ INSTRUCTIONS BEFORE COMPLETING FORM
1. REPORT NUMBER MAR 3	2. GOVT ACCESSION NO.	3. RECIPIENT'S CATALOG NUMBER
4. TITLE (and Subtitle) Theoretical Studies Relating to the Interaction of Radiation with Matter.		5. TYPE OF REPORT & PERIOD COVERED ANNUAL 10/01/89-9/15/90
		6. PERFORMING ORG. REPORT NUMBER
7. AUTHOR(s) P.R. Berman		8. CONTRACT OR GRANT NUMBER(s) N00014-87-K-0303
9. PERFORMING ORGANIZATION NAME AND ADDRESS Prof. P.R. Berman Physics Dept. - New York University 4 Washington Place, New York NY 10003		10. PROGRAM ELEMENT, PROJECT, TASK AREA & WORK UNIT NUMBERS 4124104....02
11. CONTROLLING OFFICE NAME AND ADDRESS Office of Naval Research, Resident Representative New York 715 Broadway, New York, NY 10003		12. REPORT DATE Sept. 15, 1989
		13. NUMBER OF PAGES 7
14. MONITORING AGENCY NAME & ADDRESS (if different from Controlling Office)		15. SECURITY CLASS. (of this report) Unclassified
		15a. DECLASSIFICATION/DOWNGRADING SCHEDULE

16. DISTRIBUTION STATEMENT (of this Report)

Approved for Public release: distribution unlimited

17. DISTRIBUTION STATEMENT (of the abstract entered in Block 20, if different from Report)

DTIC ELECTE NOV 01 1990 S C B D

18. SUPPLEMENTARY NOTES

19. KEY WORDS (Continue on reverse side if necessary and identify by block number)

Laser spectroscopy, collisions, pressure-induced resonances, dressed atoms, laser-assisted collisions, magnetic-state polarization, broadband noise, four-wave mixing, stochastic fields, quantum jumps, exchange collision kernel, optical Bloch Equations, coherent transients, laser cooling

20. ABSTRACT (Continue on reverse side if necessary and identify by block number)

1. Coherent transients
2. Collision-induced resonant structures in laser spectroscopy
3. Interactions with broadband noise
4. Laser cooling below the Doppler limit.

DD FORM 1 JAN 73 1473 EDITION OF 1 NOV 65 IS OBSOLETE
S/N 0102-LF-014-6601

SECURITY CLASSIFICATION OF THIS PAGE (When Data Entered)

ANNUAL REPORT (MAR 3)

Title: "Theoretical Studies Relating to the Interaction of Radiation with Matter"
Supported by: The U.S. Office of Naval Research
Contract No.: N00014-87-K-0303
Report Period: October 1, 1989 - September 15, 1990

Approved for public release; distribution unlimited.

During the past year, progress has been made in (1) the interpretation of pressure–induced resonances; (2) the theory of the interaction of broadband light with atoms; (3) the theory of coherent transients and (4) the theory of laser cooling below the Doppler limit.

1. Interpretation of pressure–induced resonances. (P.R. Berman).

Some of our earlier work on the interpretation of pressure–induced resonances using both semi–classical and quantized field dressed–atom approaches has been published.[1*,2*,3*] This work has been carried out in collaboration with G. Grynberg of the Ecole Normale in Paris. In the past year, we hav. completed this study by comparing calculations of pressure–induced resonances in four–wave mixing signals using both the Schrodinger and Heisenberg pictures in a fully quantized–field approach.[4*,5*] It is shown that the calculation takes only a few lines in the Heisenberg picture, but is much more involved in the Schrodinger picture. We believe that this is a general result for situations in which atomic state operators, averaged over all modes of the radiation field, are being evaluated.

While the Schrodinger calculation is more difficult, it brings out new features of the problem that are hidden in the Heisenberg picture. In the case of the pressure–induced resonances, the Schrodinger calculation provides new insights into the origin of the resonances. It is shown that the coherent four–wave mixing signals arise from interference of signals emitted at different atomic sites – this clearly shows the cooperative nature of the emission. The pressure–induced resonances arise from specific terms in which vacuum field modes *other* than those involved in the four–wave mixing signal are produced.[5] These results have implications for probe gain or absorption in the pressence of collisions. The Schrodinger picture may also prove useful in understanding mechanisms involved in laser cooling.

---

* An asterisk indicates that a reprint or preprint of this article has been forwarded to the Scientific Officer with this report. Reprints of articles have been furnished to DTIC with this report. Preprints or reprints of these articles are available on request to anyone receiving this report.

Our work has also led us to compare the Schrodinger and Heisenberg picture calculations of resonance fluorescence in the presence of a strong field. Again, the Schrodinger calculation is quite complicated and our work in this area is still in progress.

(2) Interaction of broadband light with atoms (V. Finkelstein, P.R. Berman).

The optical coherent transients that arise when a sample of two–level atoms is irradiated by a sequence of two or three broad–bandwidth pulses were studied theoretically.[6*] The first two pulses are correlated with one another and can be strong enough to saturate the two–level atomic transition. Taking into account the effects of inhomogeneous and homogeneous broadening, we calculate the intensity of the transient signals, emitted in different directions, as a function of delay time. In particular, it is shown for strong excitation pulses, that the strongest signals exhibit a peak having a width given by the cross–correlation time of the pulses, τ_c^{12}. The preliminary experimental results obtained at Laboratoire Aime Cotton (France) by the group of J.–L. LeGouet confirm our theoretical conclusions. In the case of two–pulse transient theory, the peak is found to disappear when the Doppler width of the atomic ensemble becomes sufficiently large[7*], in qualitative agreement with experiment.[8]

The optical coherent transients induced in a sample of three–level atoms by time–delayed fluctuating correlated pulses are also being considered. We have seen that the three–level dynamics leads to a signal which, as a function of the delay time, depends dramatically on the intensities of the excitation pulses. For strong pulses, the signal may vary significantly on a time scale much smaller than τ_c^{12}. This effect may permit one to obtain time resolution better than the cross–correlation time of the pulses. The results will be submitted for publication in the near future. This work was carried out in collaboration with P. Tchenio of Laboratoire Aime Cotton.

3. Theory of coherent transients (E. Block, P.R. Berman).

In trying to interpret the rotary echo data of A. Szabo,[9] we have carried out a detailed analysis of rotary echoes produced by atoms whose frequency is being perturbed in a stochastic manner. Good agreement with Szabo's data has been achieved and an article is in preparation. The analysis has been extended to include rotary echoes whose "off" time is arbitrarily long.

We have also analyzed the experiment of Itano *et al*[10], who claim to have demonstrated the quantum Zeno effect, inhibition of a transition produced by continuous observation of a system. It is shown that, while the Itano interpretation has some validity, the same conclusion is reached simply by studying the dynamics of the three–level system they consider, without any mention of wave–packet collapse. Moreover, their experiment does not really address the quantum Zeno paradox[11] – if one continuously observe a particle in a bubble chamber, why doesn't he affect its lifetime? We are proposing an atomic analogue to the bubble chamber experiment which should shed some new light on the quantum Zeno paradox.

4. Laser cooling below the Doppler limit (P.R. Berman).

Recently, laser cooling below the so–called Doppler limit has been achieved.[12] This came as somewhat of a surprise since it was in contradiction with the predictions of conventional theories. Subsequently, it was appreciated that the magnetic–state degeneracy of the transition levels was a critical feature in cooling below the Doppler limit. We have formulated a general theory for the interaction of several radiation fields with atoms having arbitrary level schemes.[13*,14*] The theory has been applied to a calculation of the friction force in 1–D cooling of atoms below the Doppler limit, both in the absence and presence of an external magnetic field. Analytic expressions have been obtained[14] which are in agreement with previous numerical results.[15] Our theory is formulated using an irreducible tensor basis for density matrix elements; this formalism is very effective for analyzing magnetically degenerate systems.

The formalism can also be applied to a study of collision effects in non–degenerate four–wave mixing. We hope to show that optical pumping produces the apparent discrepancy between theory and experiment observed in the four–wave mixing experiments of Liu and Steel.[16]

5. Miscellaneous

Earlier work on quantum jumps,[17*] the exchange collision kernel,[18*] and effects of magnetic–state degeneracy in radiative collisions[19*] have been published or submitted for publication.

REFERENCES

1. P.R. Berman and G. Grynberg, Phys. Rev. A**40**, 6921 (1989).
2. G. Grynberg and P.R. Berman, Phys. Rev. A**41**, 2677 (1990).
3. P.R. Berman and G. Grynberg, in *Laser Spectroscopy IX*; edited by M. Feld, A. Mooradian and J.E. Thomas (Academic Press, New York, 1989) pp 68–70.
4. P.R. Berman, in *Proceedings of Xth International Vavilov Conference on Nonlinear Optics*, to appear.
5. G. Grynberg and P.R. Berman, submitted to Phys. Rev. A.
6. V. Finkelstein and P.R. Berman, Phys. Rev. A**41**, 6193 (1990).
7. V. Finkelstein and P.R. Berman, Phys. Rev. Rapid. Comm. A**42**, 3145 (1990).
8. R. Beach, D. de Beer and S.R. Hartmann, Phys. Rev. A**32**, 3467 (1985).
9. T. Muramoto and S. Szabo, Phys. Rev. A**38**, 5928 (1989); A. Szabo, in *Proceedings of Xth International Vavilov Conference on Nonlinear Optics*, to appear.
10. W.M. Itano, D.J. Heinzen, J.J. Bollinger, and D.J. Wineland, Phys. Rev. A**34**, 3190 (1990).
11. B. Misra and E.C.G. Sudarshan, J. Math. Phys. **18**, 756 (1977).
12. See, for example, P.D. Lett, W.D. Phillips, S.L. Rolston, C.E. Tanner, R.N. Watts, and C.I. Westbrook, J. Opt. Soc. Amer. B**6**, 2084 (1989); J. Dalibard and C. Cohen–Tannoudji, J. Opt. Soc. Amer. B**6**, 2023 (1989); P.J. Ungar, D.S. Weiss, E. Riis, and S. Chu, J. Opt. Soc. Amer. B**6**, 2058 (1989); D.S. Weiss, E. Riis, Y. Shevy, P.J. Ungar and S. Chu, J. Opt. Soc. Amer. B**6**, 2072 (1989).
13. P.R.Berman, in Proceedings of Workshop on Light–Induced Kinetic Effects, to appear.
14. P.R. Berman, submitted to Phys. Rev. A.
15. D. Sheehy, S–Q. Shang, P. van der Staten, S. Hatamian and H. Metcalf, Phys. Rev. Lett. **64**, 858 (1990); S–Q. Shang, B. Sheehy, P. van der Straten and H. Metcalf, Phys. Rev. Lett. **65**, 317 (1990).
16. J. Liu and D.G. Steel, Phys. Rev. A**38**, 4639 (1988).
17. K. Yamada and P.R. Berman, Phys. Rev. A**41**, 2677 (1990).
18. G. Rogers and P.R. Berman, submitted to Phys. Rev. A.
19. P.R. Berman, F. Schuller and G. Neinhuis, Phys. Rev. A**42**, 459 (1990).

A list of publications and invited talks is appended.

Papers published in refereed journals

1. P. R. Berman and G.Grynberg, "Quantized field approach to pressure induced resonances," Phys. Rev. A40, 6921–6930 (1989) (additional support from NSF).
2. K. Yamada and P. R. Berman, "Macroscopic quantum jumps from a two–atom system," Phys. Rev. A41, 453–462 (1990) (additional support from NSF).
3. G. Grynberg and P. R. Berman, Pressure–induced extra resonances in nonlinear spectroscopy," Phys. Rev. A41, 2677–2686 (1990) (additional support from NSF).
4. V. Finkelstein and P. R. Berman, "Optical coherent transients induced by time–delayed fluctuating pulses. I: three–pulse transients," Phys. Rev. A41, 6193–6224 (1990) (additional support from NSF).
5. P. R. Berman, F. Schuller, and G. Neinhuis, "Generation of magnetic polarization in light induced collisional energy transfer," Phys. Rev. A42, 459–473 (1990).

Chapters of books published

P. R. Berman and G. Grynberg, "Dressed–atom approach to collision–induced resonances," in **Laser Spectoscopy IX**, edited by M. Feld, A. Mooradian and J. E. Thomas (Academic Press, New York, 1989) pp. 68–70 (additional support from NSF).

Papers submitted to refereed journals

1. P. R. Berman, "Nonlinear spectroscopy and laser cooling," submitted to Phys. Rev. A.
2. V. Finkelstein and P. R. Berman, "Optical transient signal induced by strong fluctuating pulses," Phys. Rev. Rapid Comm. A42, 3145 (1990).
3. G. Rogers and P. R. Berman, "The exchange collision kernel," submitted to Phys. Rev. A.
4. G. Grynberg and P. R. Berman, "Quantized–field approach to parametric mixing and pressure–induced resonances: the Schrodinger picture," submitted to Phys. Rev. A.

All the above articles acknowledge additional support from NSF.

Papers submitted as chapters of books

1. V. Finkelstein and P. R. Berman, "Stimulated photon echo induced by broad bandwidth pulses," in **Coherence and Quantum Optics 6**, edited by J. H. Eberly, L. Mandel and E. Wolf.
2. K. Yamada and P. R. Berman, "Macroscopic quantum jumps form a two–atom system," in **Coherence and Quantum Optics 6**, edited by J. H. Eberly, L. Mandel and E. Wolf.
3. V. Finkelstein, "Excitation into a Quasicontinuum by a Fluctuating Laser Field,"in **Coherence and Quantum Optics 6**, edited by J. H. Eberly, L. Mandel and E. Wolf.
4. P. R. Berman, "Narrow resonances in laser spectroscopy," in **Workshop on Light–Induced Kinetic Effects**, edited by E. Arimondo, C. Gabbanini, S. Gozzini, L. Moi, and F. Strumia.
5. P. R. Berman, "Pressure–induced resonances in multiwave mixing," in **Proceedings of Xth International Vavilov Conference on Nonlinear Optics**.

Papers 1,2,4,5 acknowledge additional support from NSF.

Invited papers

1. P. R. Berman, "Narrow resonances in laser spectroscopy," **Workshop on Light–Induced Kinetic Effects**, Marina Marciana, Elba, Italy, 1–5 may,1990.
2. P. R. Berman, "Pressure–induced resonances in multiwave mixing," **Xth International Vavilov Conference on Nonlinear Optics**, Novisibirsk, USSR, 31 May – 4 June,1990.

Optical coherent transients induced by time-delayed fluctuating pulses: Three-pulse transients

V. Finkelstein and P. R. Berman
Department of Physics, New York University, 4 Washington Place, New York, New York 10003
(Received 8 January 1990)

A theoretical analysis of the optical coherent transients that arise when a sample of two-level atoms is irradiated by a sequence of three broad-bandwidth pulses is presented. The first two pulses have a relative delay time of order of the correlation time of the pulse fluctuations and are sent into an atomic vapor from different directions. These pulses, whose temporal width is much greater than the delay time, can be correlated with one another and can be strong enough to saturate the two-level atomic transition. The third pulse is weak, noncorrelated with the first two, and is delayed in time so that it does not overlap them. We present a detailed examination of the transient signal that is produced when the third pulse is scattered by the spatial gratings in the population difference of atoms created by the first two pulses. Taking into account the effects of inhomogeneous and homogeneous broadening, we calculate the intensity of the transient signal, emitted in different directions, as a function of delay time. The signal is found to depend dramatically on the intensities of the excitation pulses. It is shown that, for strong excitation pulses, there is a direct dependence of the signal on the cross-correlation time of pulses τ_c^{12} that does not exist when the pulses are weak. In particular, the strongest signals exhibit a peak of width of order τ_c^{12}. This peak can have a very narrow dip near its maximum whose width is much smaller than τ_c^{12}, if the pulses are fully correlated. We develop a representation of the time evolution of the Bloch vector of a two-level atom, driven by time-delayed pulses, that enables us to explain our results. In this representation, the two time-delayed pulses are replaced by two fully overlapping pulses having some effective amplitudes and atomic field detunings.

I. INTRODUCTION

Experiments in which coherent transients are produced by time-delayed, correlated, fluctuating optical pulses[1-18] have received a great deal of attention in the last few years, owing to their potential as a source of subpicosecond time resolution. The advantage of using broad-bandwidtn light lies in the fact that under certain conditions, a time resolution may be achieved that is equal to the autocorrelation time τ_c of the applied fields. This autocorrelation time may be orders of magnitude smaller than the pulse duration t_p.

A convenient experimental configuration for observing such optical transients involves sending either two or three laser pulses into an atomic vapor. In this paper we consider only three-pulse transients (PT-3). Two pulses (which may be derived from a single laser), having wave vectors $\mathbf{k}_1$ (pulse 1) and $\mathbf{k}_2$ (pulse 2), respectively, are sent into a sample of two-level atoms [see Fig. 1(a)]. The wave vectors are chosen such that $|\mathbf{k}_1|=|\mathbf{k}_2|=k$ and $\theta=\angle(\mathbf{k}_1,\mathbf{k}_2)\ll 1$. Pulse 2 and pulse 1 have a relative time delay denoted by t_{12}. For $t_{12}>0$ ($t_{12}<0$), pulse 1 precedes (follows) pulse 2 [see Fig. 1(b)]. Under PT-3 conditions these pulses create spatial gratings in the population difference of atoms with Bragg vectors $n\mathbf{k}_d=n(\mathbf{k}_2-\mathbf{k}_1)$, $n=0,\pm 1,\ldots$. These gratings are subsequently probed by a third pulse with a wave vector $\mathbf{k}_3$ that is time delayed by $t_{13}>t_{12}+t_p$ relative to the first excitation pulse. The energy radiated in the directions $\mathbf{k}_3+n\mathbf{k}_d$ is studied

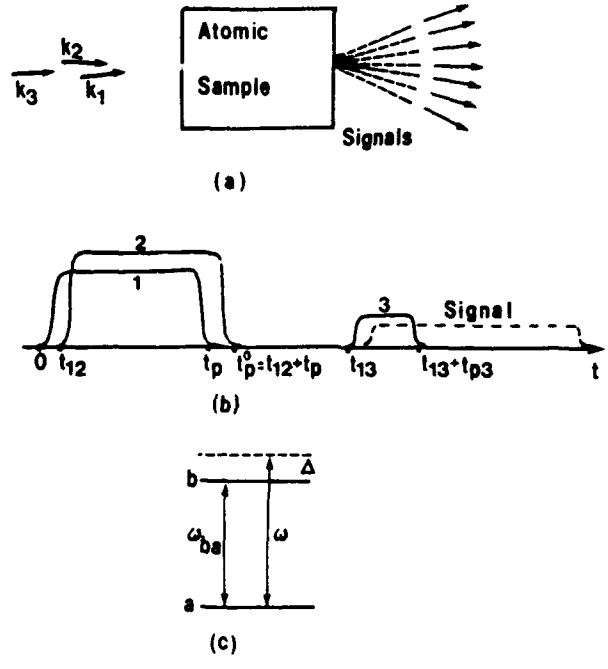

FIG. 1. The three-pulse transient (PT-3) configuration. (a) Angled-beam configuration. (b) The temporal sequence of pulses: for $t_{12}>0$ pulse 1 (wave vector $\mathbf{k}_1$) precedes pulse 2 (wave vector $\mathbf{k}_2$), the third pulse does not overlap the first two pulses. (c) A two-level atom having transition frequency ω_{ba} is driven by the pulses, each having central frequency ω.

as a function of t_{12}.

Although signals can be generated by scattering from nth-order gratings, most experimental work has concentrated on the signals originating from the first-order gratings ($n=\pm 1$). For weak incident pulses or for fully separated pulses, the first-order gratings provide the major contribution to the signal. However, for strong, overlapping incident pulses, higher-order gratings begin to contribute appreciably.

The early experimental results,[1-10] obtained for weak incident fields, have been interpreted in the context of perturbation theory. More recently, however, time-delayed two-pulse[11] and three-pulse transients[12-15] have been examined under conditions in which at least one of the pulses is strong; that is,

$$\alpha t_p \gg 1 ,$$

where $\alpha = f^2\tau_c$, and f is a Rabi frequency associated with a laser field interacting with a two-level atom. The three-pulse experiments are typically carried out at temperatures 300–500 K using excitation pulses having $t_p \approx 10$ ns, and with low buffer gas pressures; consequently, the Doppler width $\Delta_D = ku$ (u is the most probable atomic speed) satisfies the inequalities

$$\Delta_D \gg t_p^{-1}, T_1^{-1}, T_2^{-1} , \tag{1.1}$$

where T_1 and T_2 are longitudinal and transverse relaxation times, respectively.

In the strong-field regime the signal energy as a function of the delay time t_{12} may depend on the correlation time τ_c itself,[14,15] while the dependence of the signal on the Doppler width of the atomic ensemble is minimal. Such behavior differs sharply from that in a weak-field regime when the signal strongly depends on the Doppler width, and the correlation time does not play a separate role in the effects under consideration. Currently the nature of the phenomena observed in a strong-field regime remains unclear.

Theoretical analysis of the experimental results brings into play many profound theoretical problems concerned with studies of the stochastic Bloch equations in the intense field regime. A number of papers have been devoted to this problem in the last twenty-five years[19-40] and numerous effects have been discussed assuming fluctuating radiation fields (resonant fluorescence, double resonance, multiphoton ionization, optical induction decay, Hanle effect, etc.). In most of these calculations, the response of an atomic ensemble to a fluctuating field has been studied as a function of the noise properties of the fields. In many cases the noise was assumed to be Markovian in nature. The problem under consideration herein differs in that atoms are subjected to two time-delayed noise fields which may be correlated. Thus, the atoms retain some memory of the first field when the second field acts. Even if the noise of each field is Markovian, the combined effect of the two fields is non-Markovian, in general, owing to these memory effects. This feature greatly complicates the calculations. Initial attempts at solutions employed diagrammatic methods.[14,41] Later, a decorrelation approximation[42] was used and results were obtained[15] in the limit of stationary atoms subjected to fully correlated, time-delayed fields, one of which was weak, while another was strong: $\alpha_1 t_p \ll 1 \ll \alpha_2 t_p$ [$\alpha_i = |f_i|^2\tau_c$ ($i=1,2$), f_i is Rabi frequency associated with field i]. It was shown theoretically, and has been confirmed experimentally, that under these conditions the radiated energy $W_1^{(3)}(t_{12})$ exhibits a narrow dip centered at $t_{12}-0$, superimposed on a broad background signal. The dip has a width of order τ_c and relative depth equal to 0.5

This observation motivates us to consider the limiting, but important, case in which the correlation and delay times are sufficiently small to satisfy

$$\tau_c, t_{12} \ll \alpha^{-1}, t_p, \Delta_D^{-1}, T_1, T_2 . \tag{1.2}$$

No restriction is imposed on the ratio t_{12}/τ_c. Under these conditions we have found a closed form solution for the signal energy, valid for arbitrary field intensities and relaxation rates. Some direct dependence of the observed signal on τ_c will be shown to exist in the strong-field regime; the interpretation of this effect is given in terms of some additional detuning parameter that appears in the Bloch equations as a result of the time delay of the pulses. The conditions required for observation of the studied phenomena are discussed.

In Sec. II we derive the laser fields and quantum system to be considered, and present the general expressions for the measured energy of the signal in the PT-3 case in terms of a single-time, two-atom correlation function. Using the Bloch vector model, in Sec. III we develop a new representation which permits us to analyze the dynamics of a two-level atom driven by the time-delayed pulses as if the pulses are fully overlapping. The equations for single-time two-atom correlation functions averaged over field fluctuations, which are needed in the calculation, are derived in Sec. IV. In Sec. V we describe a general solution to the problem. A weak-relaxation limit is discussed in Sec. VI. An explanation of the dependence of the signal on time delay t_{12} is presented in Sec. VII and the relative dephasing of the Bloch vectors in a strong-field regime that leads to the results obtained in Sec. VI is considered qualitatively. The results obtained in a strong-relaxation limit are discussed in Sec. VIII.

II. BASIC ASSUMPTIONS AND EQUATIONS

A. Laser field

We consider an ensemble of two-level atoms each having transition frequency ω_{ba} [excited state b, ground state a, as shown in Fig. 1(c)]. Atoms interact with two laser pulses of duration t_p, time delayed relative to each other by an interval t_{12}. These classical incident fields can be represented as

$$\mathcal{E}(\mathbf{r},t) = \frac{e^{-i\omega t}}{2}\{\mathcal{E}_1(t)\exp(i\mathbf{k}_1\cdot\mathbf{r}) + \mathcal{E}_2(t-t_{12})\exp[i(\omega t_{12}+\mathbf{k}_2\cdot\mathbf{r})]\} + \text{c.c.} , \tag{2.1}$$

where, without loss of generalization, we take all fields having parallel polarization. It is assumed that the atom-field detuning, $\Delta=\omega_{ba}-\omega$, satisfies $|\Delta|\ll\omega$, and that $\mathcal{E}_1$ and $\mathcal{E}_2$ are slowly varying complex field amplitudes satisfying

$$|\dot{\mathcal{E}}_1/\mathcal{E}_1|,|\dot{\mathcal{E}}_2/\mathcal{E}_2|\ll\frac{c|\mathbf{k}_1|}{L|\mathbf{k}_d|},\omega\ ,$$

where c is the speed of light, L is a characteristic length of the sample, and

$$\mathbf{k}_d=\mathbf{k}_2-\mathbf{k}_1\ .$$

We introduce the Rabi frequency $f_i=\mu_{ab}\mathcal{E}_i\hbar^{-1}$ $(i=1,2)$ associated with field $\mathcal{E}_i$; μ_{ab} is the dipole moment matrix element of the $a\rightarrow b$ transition. Both of the pulses are characterized by a broad spectrum, and the amplitudes $\mathcal{E}_1$ and $\mathcal{E}_2$ and, consequently, the Rabi frequencies f_1 and f_2 are treated as complex stationary stochastic processes that may be correlated with each other. In particular, we assume that

$$\begin{aligned}&\langle f_1^*(t)f_1(t-\tau)\rangle=\alpha_1 g_{11}(\tau)\ ,\\&\langle f_2^*(t)f_2(t-\tau)\rangle=\alpha_2 g_{22}(\tau)\ ,\\&\langle f_1(t)f_1(t-\tau)\rangle=0,\quad\langle f_2(t)f_2(t-\tau)\rangle=0\ ,\end{aligned}\tag{2.2}$$

and

$$\begin{aligned}&\langle f_1(t)f_2(t-\tau)\rangle=0,\quad\langle f_1(t)\rangle=\langle f_2(t)\rangle=0\ ,\\&\langle f_1^*(t)f_2(t-\tau)\rangle=\alpha_{12}g_{12}(\tau)\ ,\end{aligned}\tag{2.3}$$

where the average is over all possible realizations of the fluctuating fields. The quantity $g_{ij}(\tau)$ $(i,j=1,2)$ is a correlation function normalized such that

$$\int_0^\infty g_{ij}(\tau)d\tau=1,\quad i,j=1,2$$

and the autocorrelation parameters α_1 and α_2 are given by

$$\alpha_i=\langle|f_i(t)|^2\rangle\tau_c^{ii},\quad i=1,2$$

while the cross-correlation parameter α_{12} that determines the mutual coherence of the Rabi frequencies is equal to

$$\alpha_{12}=\langle f_1^*(t)f_2(t)\rangle\tau_c^{12}\ .\tag{2.4}$$

Correlation times are defined by

$$\tau_c^{ij}=g_{ij}^{-1}(0)\ .\tag{2.5}$$

The cross-correlation time τ_c^{12} cannot be larger than autocorrelation times τ_c^{11},τ_c^{22}, and it follows that

$$\Phi=\frac{\alpha_{12}^2}{\alpha_1\alpha_2}\ ,\tag{2.6}$$

which is a measure of the relative coherence of the pulses, satisfies

$$0\le\Phi\le1\ .$$

For fully correlated pulses $\Phi=1$, while for noncorrelated pulses $\Phi=0$.

According to Eqs. (2.2) and (2.3), the statistical properties of the total field (2.1) are characterized not only by the correlation time τ_c^{ij} but also by the delay time t_{12}, provided the correlation parameter $\Phi\neq0$. In this paper the correlation times τ_c^{ij} as well as the delay time t_{12} are assumed to be much smaller than any characteristic time in the problem [see Eq. (1.2)], but can be comparable to each other; that is

$$\tau_c^{ij},t_{12}\ll\Delta_D^{-1},t_p,\alpha_1^{-1},\alpha_2^{-1},\Delta^{-1},T_1,T_2\ .\tag{2.7}$$

In the three-pulse transient, the third pulse is assumed to be weak $(\alpha_3 t_p\ll1)$, to have a broad bandwidth $(\tau_c^{33}\sim\tau_c^{ij})$, and to be uncorrelated with the first two pulses. It is switched on after both the first two excitation pulses and any transients associated with them have already died out. Equation (2.7) defines the delay times for which the theory is applicable.

It is also assumed that the transverse Doppler effect is negligible:

$$\frac{|\mathbf{k}_d|}{|\mathbf{k}_1|}\Delta_D t_p\ll1\ ,$$

enabling us to set $\mathbf{k}_1,\mathbf{k}_2\approx\frac{1}{2}(\mathbf{k}_1+\mathbf{k}_2)=\mathbf{k}$ in certain expressions.

B. Dynamical equations

In the rotating-wave approximation the following equations then hold for density matrix elements of a two-level atom having velocity $\mathbf{v}$:

$$\begin{aligned}\dot\rho_1&=-\gamma_t\rho_1+\delta\rho_2+Y\rho_3\ ,\\\dot\rho_2&=-\delta\rho_1-\gamma_t\rho_2-X\rho_3\ ,\\\dot\rho_3&=-Y\rho_1+X\rho_2-\gamma_l(\rho_3-\rho_{3e})\ ,\end{aligned}\tag{2.8}$$

where

$$\begin{aligned}&\rho_1=2\,\mathrm{Re}(\rho_{ab}e^{i(\omega t-\mathbf{k}_2\cdot\mathbf{r})})\ ,\\&\rho_2=2\,\mathrm{Im}(\rho_{ab}e^{i(\omega t-\mathbf{k}_2\cdot\mathbf{r})})\ ,\\&\rho_3=\rho_{aa}-\rho_{bb},\quad\rho_{aa}+\rho_{bb}=1\ ,\end{aligned}$$

and

$$\begin{aligned}&X(t)=X_1(t)+X_2(t-t_{12})\ ,\\&Y(t)=Y_1(t)+Y_2(t-t_{12})\ ,\\&X_1=-\mathrm{Re}[f_1(t)e^{-i\phi}],\quad Y_1=-\mathrm{Im}[f_1(t)e^{-i\phi}]\ ,\\&X_2=-\mathrm{Re}[f_2(t-t_{12})],\quad Y_2=-\mathrm{Im}[f_2(t-t_{12})]\ ,\\&\phi=\mathbf{k}_d\cdot\mathbf{r}-\omega t_{12},\quad\delta=\Delta+kv_z\ ,\\&f_i(t)=\mu_{ab}\mathcal{E}_i(t)\hbar^{-1},\quad i=1,2\end{aligned}\tag{2.9}$$

and ρ_{3e} is the population difference ρ_3 at thermal equilibrium. The transverse relaxation rate $\gamma_t=T_2^{-1}$ can be expressed as the sum of the spontaneous relaxation rate, $\gamma_l=T_1^{-1}$, of level b and a collisional contribution γ_{coll} as

$$\gamma_t=\frac{\gamma_l}{2}+\gamma_{\mathrm{coll}}\ .$$

All the dependence on position of the atoms is contained in the phase parameter ϕ; the z axis is taken in the $\mathbf{k}_d$ direction.

Equations (2.8) can be represented as

$$\dot{\rho}_m = \sum_k a_{mk}\rho_k + \gamma_l \rho_{3e}\delta_{m3}, \quad m=1,2,3 , \tag{2.10}$$

where

$$\underline{A} = [a_{mk}] = \underline{A}^0 - \underline{\Gamma} ,$$

$$\underline{A}^0 = [a^0_{mk}] = \begin{bmatrix} 0 & +\delta & Y \\ -\delta & 0 & -X \\ -Y & X & 0 \end{bmatrix} , \tag{2.11}$$

$$\underline{\Gamma} = \begin{bmatrix} \gamma_t & 0 & 0 \\ 0 & \gamma_t & 0 \\ 0 & 0 & \gamma_l \end{bmatrix} .$$

The components (ρ_1,ρ_2,ρ_3) are the standard components of the Bloch vector $\mathbf{R}(t;\phi,\delta)$, which, according to Eqs. (2.8)–(2.10), may be written in series form as

$$\mathbf{R}(t;\phi,\delta) = \sum_{k=-\infty}^{+\infty} \mathbf{R}^{(k)}(t;\delta)\exp(ik\phi) , \tag{2.12}$$

where $\mathbf{R}^{(k)}$ has components $(\rho_1^{(k)},\rho_2^{(k)},\rho_3^{(k)})$ and

$$\mathbf{R}^{(k)} = (\mathbf{R}^{(-k)})^* . \tag{2.13}$$

We often will refer to $\rho_3^{(n)}$ as the nth-order population grating, even though it is a Fourier component corresponding to the nth-order spatial grating.

C. Signal energy

The aim of this paper consists in studying the signal emitted in the direction $\mathbf{k}_3 + n\mathbf{k}_d$. In particular, it is the pulse intensity as a function of a delay time which is the subject of investigation. When deriving the general expressions for this quantity, we do not restrict ourselves to any particular shape of the pulse envelopes.

It is shown in Appendix A that, if the third pulse is weak and is not correlated with the first two excitation pulses, the PT-3 signal intensity in the direction $\mathbf{k}_3 + n\mathbf{k}_d$ is proportional to the quantity defined by

$$W_n^{(3)} = \frac{\sqrt{2}}{\Delta_D \pi\sqrt{\pi}} \int\int \frac{\psi(\delta-\Delta)\psi(\tilde{\delta}-\Delta)}{2\gamma_t + i\delta_-} \times \langle T_{33}^{(n,-n)}(t_p^0;\delta,\tilde{\delta})\rangle d\delta\, d\tilde{\delta} , \tag{2.14}$$

where

$$\langle T_{33}^{(n,-n)}(t;\delta,\tilde{\delta})\rangle = \langle \rho_3^{(n)}(t;\delta)\rho_3^{(-n)}(t;\tilde{\delta})\rangle \tag{2.15}$$

and

$$\psi(\delta) = \exp\left[-\frac{\delta^2}{\Delta_D^2}\right]$$

is a Maxwellian distribution function, $t_p^0 = t_p + t_{12}$ is the time immediately following the two-excitation pulse sequence, and

$$\delta_- = \delta - \tilde{\delta} .$$

We refer to $W_n^{(3)}(t_{12})$ as the PT-3 signal intensity. It is seen from Eq. (2.14) that the signal depends on the average product of Fourier components (2.12) of two Bloch vectors, associated with different atoms. In Eq. (2.14) and all subsequent equations, a tilde denotes variables of a second atom, i.e., $\tilde{\delta} = \Delta + k\tilde{v}_z$.

The problem is reduced to obtaining a two-atom signal-time correlation function for the population difference ρ_3. It will be shown that in a strong-field regime, the gratings in the population difference fluctuate considerably; consequently, the correlation function (2.15) cannot be factorized. In order to solve the problem, we have to consider the second moments of the density matrix elements defined by

$$T_{mm'} = \rho_m(t;\phi,\delta)\rho_{m'}(t;\tilde{\phi},\tilde{\delta}) = \rho_m\tilde{\rho}_{m'} .$$

It follows from Eqs. (2.10) that components of the matrix $T_{mm'}$ evolve as

$$\dot{T}_{mm'} = \sum_k (a_{mk}T_{km'} + \tilde{a}_{m'k}T_{mk}) + \gamma_l(\rho_m\delta_{m'3} + \tilde{\rho}_{m'}\delta_{m3}) . \tag{2.16}$$

The solution of this equation averaged over field fluctuations gives the function

$$T = \langle T_{33}(t;\phi,\tilde{\phi},\delta,\tilde{\delta})\rangle ,$$

from which one can extract the Fourier component

$$T^{(n,-n)}(t;\delta,\tilde{\delta}) = \frac{1}{4\pi^2}\int\int_{-\pi/2}^{3\pi/2} T(t;\phi,\tilde{\phi},\delta,\tilde{\delta}) \times e^{-in(\phi-\tilde{\phi})} d\phi\, d\tilde{\phi} \tag{2.17}$$

needed in Eq. (2.14). It also will prove useful to introduce the change of variables

$$\phi_- = \tfrac{1}{2}(\phi-\tilde{\phi}), \quad \phi_+ = \tfrac{1}{2}(\phi+\tilde{\phi}) , \tag{2.18}$$

and rewrite Eq. (2.17) as

$$T^{(n,-n)}(t;\delta,\tilde{\delta}) = \frac{1}{2\pi^2}\int_{-\pi/2}^{\pi/2} d\phi_- \int_{-\pi/2}^{3\pi/3} d\phi_+ e^{-i2n\phi_-} T(t;\phi_-,\phi_+,\delta,\tilde{\delta}) . \tag{2.19}$$

Hereafter we take ϕ and $\tilde{\phi}$ in the simplified form

$$\phi=\mathbf{k}_d\cdot\mathbf{r},\quad \tilde{\phi}=\mathbf{k}_d\cdot\tilde{\mathbf{r}}$$

instead of using the rigorous definition (2.9), as the term ωt_{12} leads only to a shift of origin of coordinates and does not affect the Fourier component (2.19) and, consequently, the PT-3 signal.

The signal (2.14) can be written as a sum of two terms, one an even function of t_{12} and the other an odd function of t_{12}. Using both Eq. (2.13) and the fact that T is unchanged if α_1 and α_2 are interchanged, one can show that $T^{(n,-n)}\equiv\langle T_{33}^{(n,-n)}\rangle$ can be written as

$$T^{(n,-n)}(t_p^0;\delta,\tilde{\delta})=N_1(\delta_-,\delta_+)+is\delta_-N_2(\delta_-,\delta_+) \tag{2.20}$$

with N_1 and N_2 being real functions which are even with respect to t_{12}, $\delta_-=\delta-\tilde{\delta}$, and $\delta_+=\delta+\tilde{\delta}$. The parameter s is given by

$$s=\begin{cases}1 \text{ if } t_{12}\geq 0\\ -1 \text{ if } t_{12}<0\end{cases}. \tag{2.21}$$

If γ_t is much smaller than any characteristic spectral width in the system, Eq. (2.14) can be simplified by using the following approximation:

$$(2\gamma_t+i\delta_-)^{-1}=\pi\delta(\delta_-)-iP\left[\frac{1}{\delta_-}\right] \tag{2.22}$$

with $\delta(\ )$ being the δ function and P denoting a principal value. Taking into account Eqs. (2.22) and (2.20), we finally obtain from Eq. (2.14)

$$W_n^{(3)}=(\Delta_D\sqrt{2\pi})^{-1}\int_{-\infty}^{\infty}\psi\left[\frac{\delta_+}{\sqrt{2}}-\sqrt{2}\Delta\right]\left[N_1(0,\delta_+)+\frac{2s}{\pi}\int_0^{\infty}\psi\left[\frac{\delta_-}{\sqrt{2}}\right]N_2(\delta_-,\delta_+)d\delta_-\right]d\delta_+ . \tag{2.23}$$

The first term in (2.23), which is an even function of t_{12}, involves a single integral over δ_+ (or, equivalently, over velocity); consequently, this term can be interpreted as arising independently from the different velocity groups of atoms. The second term in (2.23) is responsible for an asymmetry in the signal as a function of the delay time t_{12}; it involves a double integral over velocities.

III. FULLY OVERLAPPING PULSES VERSUS TIME-DELAYED PULSES: WHAT IS THE DIFFERENCE?

If the excitation pulses fully overlap, i.e., $t_{12}=0$, the non-Markovian nature of the problem related to the time delay is removed. As a result, all the standard methods for treating fields with short correlation times can be applied. What may be less obvious, however, is that, owing to conditions (2.7), these methods also work for nonzero delay times. Before going into the details of such a calculation, we introduce a model which enables us to gain some physical insight into the dynamics of two-level atoms interacting with time-delayed pulses. We do not take into account the relaxation processes at this point, as they play no role in the particular phenomena discussed in this section.

For nonzero delay time we would like to represent the position of the Bloch vector at time t_p^0 as a result of some rotation performed under the influence of two pulses which are fully overlapping rather than spaced apart in time as is the actual case. In other words, we replace the two time-delayed pulses by two, modified simultaneous ones. The new pulses produce the same effect as the two time-delayed pulses. This representation will let us formulate the effect of the time delay in a simple and systematic manner.

It is well known that in the absence of relaxation Eqs. (2.8) can be rewritten in a vector form as

$$\dot{\mathbf{R}}=[\mathbf{H}\times\mathbf{R}],\quad \mathbf{H}=\begin{bmatrix}X\\ Y\\ -\delta\end{bmatrix}, \tag{3.1}$$

where X and Y as defined in Eq. (2.9) are the real and imaginary parts, respectively, of the Rabi frequency associated with the electric field amplitude, taken with the negative sign.

Let us consider the rotation of the Bloch vector $\mathbf{R}$ under the influence of two arbitrary time delayed pulses. It is always possible to find a time t_0, such that the Rabi frequency $f(t)$ of any pulse is negligibly small for $t<t_0$. The exact value of t_0 does not play any role, so we put it equal to zero.

According to Eqs. (2.9) the angular velocity $\mathbf{H}$ equals

$$\mathbf{H}=\mathbf{H}_1(t)+\mathbf{H}_2^-(t),$$

where

$$\mathbf{H}_2^-(t)=\mathbf{H}_2(t-t_{12}),$$

$$\mathbf{H}_1=\begin{bmatrix}X_1(t)\\ Y_1(t)\\ -\delta\end{bmatrix},\quad \mathbf{H}_2=\begin{bmatrix}X_2(t)\\ Y_2(t)\\ 0\end{bmatrix}. \tag{3.2}$$

At time $t=2t_{12}$ the position of the Bloch vector $\mathbf{R}(2t_{12})$ results from two consecutive rotations, each of duration t_{12}. During the first one, an atom is driven by the first excitation pulse only. The Bloch vector rotates with angular velocity

$$\mathbf{H}=\mathbf{H}_1(t),\quad 0\leq t\leq t_{12},$$

and, at $t=t_{12}$, takes the form

$$\mathbf{R}(t_{12})=\mathbf{R}(0)+\int_0^{t_{12}}[\mathbf{H}_1(t')\mathbf{R}(t')]dt' . \tag{3.3}$$

The second rotation is performed under the influence of both pulses (see Fig. 2) with angular velocity

$$\mathbf{H}=\mathbf{H}_1(t)+\mathbf{H}_2(t-t_{12}),\quad t_{12}\le t\le 2t_{12} .$$

The position of the Bloch vector at $t=2t_{12}$ is then given by

$$\mathbf{R}(2t_{12})=\mathbf{R}(t_{12})+\int_{t_{12}}^{2t_{12}}\{[\mathbf{H}_1(t')+\mathbf{H}_2(t'-t_{12})]\mathbf{R}(t')\}dt' . \tag{3.4}$$

We would like to represent the same transition from the starting position $\mathbf{R}(0)$ to the final one $\mathbf{R}(2t_{12})$ as a result of a different sequence of rotations. The second rotation is performed under the influence of the *first* pulse only:

$$\mathbf{H}=\mathbf{H}_1(t),\quad \text{for } t_{12}\le t\le 2t_{12} \tag{3.5}$$

while the first rotation is carried out with an angular velocity

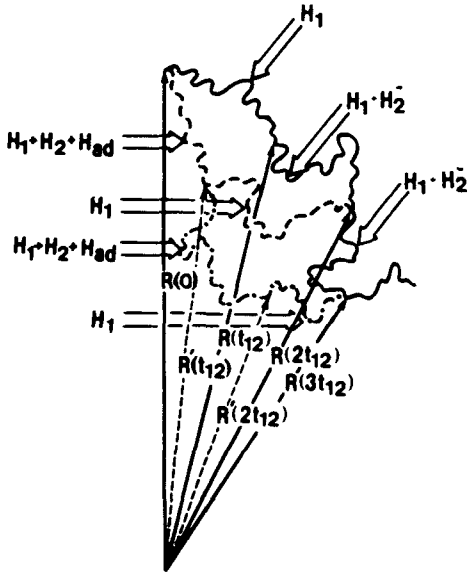

FIG. 2. Schematic representation of stochastic rotation of a Bloch vector **R** for given time-delayed fluctuating excitation pulses. Solid curve, the trajectory of the tip of this vector on the surface of a unit sphere. Positions of the Bloch vector at time $t=0,t_{12},2t_{12},3t_{12}$ are represented by solid arrows. Trajectory of the tip of the Bloch vector are shown for $0\le t\le 2t_{12}$ (dashed curve) and $t_{12}\le t\le 3t_{12}$ (dot-dashed curve) using an effective angular velocity corresponding to fully overlapping pulses (see text). Dashed arrows represent the modified intermediate positions $\mathbf{R}'(t_{12})$ and $\mathbf{R}'(2t_{12})$ of the Bloch vector. Note that at the end of each step of the transformation the position of the actual and modified Bloch vectors coincides, even though they differ throughout the intervals. The wide arrows labeled by various values of **H** give the angular velocity in each interval.

$$\mathbf{H}=\mathbf{H}_1(t)+\mathbf{H}_2(t)-\mathbf{H}_{ad}(t),\quad \text{for } 0\le t\le t_{12} , \tag{3.6}$$

where an additional angular velocity component is introduced to achieve the same final position of the Bloch vector (see Fig. 2). In terms of the new angular velocities, the modified intermediate position $\mathbf{R}'(t_{12})$ of the Bloch vector is given by

$$\mathbf{R}'(t_{12})=\mathbf{R}(0)+\int_0^{t_{12}}\{[\mathbf{H}_1(t')+\mathbf{H}_2(t')-\mathbf{H}_{ad}(t')]\mathbf{R}(t')\}dt' \tag{3.7}$$

and may not coincide with the true value $\mathbf{R}(t_{12})$. Using Eq. (3.5), one finds that the final position of the Bloch vector at $t=2t_{12}$ is given by

$$\mathbf{R}(2t_{12})=\mathbf{R}'(t_{12})+\int_{t_{12}}^{2t_{12}}[\mathbf{H}_1(t')\mathbf{R}(t')]dt' . \tag{3.8}$$

Since the delay time satisfies condition (2.7) the Bloch vector rotates only slightly in a time period t_{12} and Eqs. (3.3), (3.4), (3.7), and (3.8) can be solved by iteration. Carrying out the iterations to second order gives us two expressions for $\mathbf{R}(2t_{12})$ in terms of $\mathbf{R}(0)$. These expressions are identical provided that

$$\mathbf{H}_{ad}(t)=\int_t^{t+t_{12}}[\mathbf{H}_1(t')\mathbf{H}_2(t)]dt' . \tag{3.9}$$

From the geometrical point of view, the appearance of $\mathbf{H}_{ad}\neq 0$ is simply a consequence of the fact that two successive rotations with different angular velocity vectors $\mathbf{H}_1$ and $\mathbf{H}_2$ do not coincide with that of a single rotation with $\mathbf{H}=\mathbf{H}_1+\mathbf{H}_2$.

We can carry out a similar transformation for the next time period $t_{12}\le t\le 3t_{12}$ and so forth (see Fig. 2). At each step we obtain the same result (3.9) for the time intervals $nt_{12}\le t\le(n+1)t_{12}$, $n=1,2\ldots$. When this transformation is completed up to the time $t=t_p^0$ we get the correct position of the Bloch vector, $\mathbf{R}(t_p^0)$, although all the intermediate values $\mathbf{R}'(nt_{12})$ differ from their true values. The vector $\mathbf{R}(t_p^0)$ can be regarded now as a result of the rotation performed under the influence of the two fully overlapping modified pulses along with some modified atom-field detuning. The modification of the field components and the detuning is given by Eq. (3.9).

If the laser field is fluctuating, the vector $\mathbf{H}_{ad}$ is also a fluctuating function of time. It turns out that the fluctuating part of $\mathbf{H}_{ad}(t)$ results in contributions which are negligible in the limits discussed in this paper. Consequently, the signal depends only on $\langle\mathbf{H}_{ad}\rangle$. Taking into account definitions (2.9) one finds that the only nonzero component of the averaged vector $\langle\mathbf{H}_{ad}\rangle$ lies along the 3 axis and thus describes some additional detuning. This component $h_{ad,3}$, is given by

$$h_{ad,3}=\langle\mathbf{H}_{ad}\rangle_3=G(t_{12})\alpha_{12}\sin\phi , \tag{3.10}$$

where

$$G(t_{12})=\int_0^{t_{12}}g_{12}(\tau)d\tau;\quad G(\pm\infty)=\pm 1 . \tag{3.11}$$

The additional detuning $h_{ad,3}$ is nonzero only for time-delayed pulses ($t_{12}\neq 0$), if both $\alpha_{12}\neq 0$ (the pulses are correlated) and $\phi=\mathbf{k}_d\cdot\mathbf{r}\neq 0$. It depends strongly on the

position $\mathbf{r}$ of the atom and on the delay time t_{12} through the functions ϕ and $G(t_{12})$, respectively. Owing to its dependence on $G(t_{12})$, the absolute value of this additional detuning rises from 0 to $\alpha_{12}|\sin\phi|$ as $|t_{12}|$ varies from 0 to $|t_{12}|>\tau_c^{12}$. Hence, if this additional detuning significantly modifies the dynamics of the two-level atom, we can also expect the PT-3 signal to depend on t_{12} even if $T_{12}\sim\tau_c^{12}$. The implications of this model are explored below.

IV. AVERAGED EQUATIONS FOR THE CORRELATION FUNCTIONS

The single-time two-atom correlation functions $\langle T_{nm}(t)\rangle$ are the solutions of Eqs. (2.16) averaged over histories of the laser fields. A solution for $\langle T_{nm}\rangle$ for the general case of arbitrary t_{12} will be discussed elsewhere.

In this paper we obtain exact results for delay times t_{12} satisfying Eq. (2.7), i.e., sufficiently small that the Bloch vector $\mathbf{R}$, as well as the tensor T_{nm}, varies only slightly during this time period. Nevertheless, it will be shown that the signal (2.14) can vary significantly as a function of t_{12} even under this restriction.

Owing to condition (2.7) we can use the decorrelation approximation[42] when deriving equations for $\langle T_{nm}\rangle$. We follow the method described in Refs. 15 and applied there to this particular problem, extending the method to include effects of relaxation and atomic motion. We obtain the following differential equations for $\langle T_{lm}\rangle$ and $\langle\rho_l\rangle$ that hold true for pulses of arbitrary shape:

$$\langle\rho_1\rangle=\langle\rho_2\rangle=0\ ,$$

$$\dot\rho=-2\alpha(\phi)\rho+\gamma_l(\rho_{3e}-\rho)\ , \tag{4.1}$$

$$\dot T=-2(x+\gamma_l)T+Q(\phi,\tilde\phi)Z+Q^*(\phi,\tilde\phi)Z^*+\gamma_l\rho_{3e}(\rho+\tilde\rho)\ , \tag{4.2}$$

$$\dot Z=-(x+2\gamma_t+i\delta_f)Z+4Q^*T\ , \tag{4.3}$$

where

$$\begin{aligned}&\rho=\langle\rho_3(\delta,\phi)\rangle,\quad\tilde\rho=\langle\rho_3(\tilde\delta,\tilde\phi)\rangle\ ,\\&T=\langle\rho_3(\delta,\phi)\rho_3(\tilde\delta,\tilde\phi)\rangle=\langle\rho_3\tilde\rho_3\rangle=\langle T_{33}\rangle\ ,\\&Z=\langle(\rho_1+i\rho_2)(\tilde\rho_1-i\tilde\rho_2)\rangle\\&\quad=\langle T_{11}+T_{22}+i(T_{21}-T_{12})\rangle\ ,\end{aligned} \tag{4.4}$$

and

$$\alpha(\phi)=\tfrac{1}{2}(\alpha_1+\alpha_2+2\alpha_{12}\cos\phi)\ , \tag{4.5}$$

$$x=\alpha(\phi)+\alpha(\tilde\phi)=\alpha_1+\alpha_2+\alpha_{12}(\cos\phi+\cos\tilde\phi)\ ,$$

$$Q=\tfrac{1}{2}[\alpha_2+\alpha_1e^{i(\phi-\tilde\phi)}+\alpha_{12}(e^{i\phi}+e^{-i\tilde\phi})]\ , \tag{4.6}$$

$$\begin{aligned}\delta_f&=[\delta+G(t_{12})\alpha_{12}\sin\phi]-[\tilde\delta+G(t_{12})\alpha_{12}\sin\tilde\phi]\\&=\delta_-+G(t_{12})\alpha_{12}(\sin\phi-\sin\tilde\phi)\ .\end{aligned} \tag{4.7}$$

The function $G(t_{12})$ is given by Eqs. (3.11).

Equations (4.1)–(4.3) describe the first- and second-order density-matrix correlation functions of two atoms located at points $\mathbf{r}$ and $\tilde{\mathbf{r}}$, respectively. We present only three of the nine equations for T_{lm} because, under the approximation applied here, the rest of the equations are decoupled from Eqs. (4.2) and (4.3) and do not play any role in this problem. We shall discuss solutions of Eqs. (4.1)–(4.3) in Sec. V. Before doing so, let us consider the coefficients appearing in these equations. The parameter $2\alpha(\phi)$ which appears in Eq. (4.1) is proportional to the mean intensity of interference fringes at the location of the atom. This parameter is responsible for the decay of $\rho=\langle\rho_3\rangle=\langle\rho_{aa}-\rho_{bb}\rangle$; in other words, $(2\alpha)^{-1}$ is a relaxation parameter whose origin can be traced to the combined action of the fluctuating excitation pulses. In Eqs. (4.2) and (4.3) the parameter x, equal to the sum $\alpha(\phi)+\alpha(\tilde\phi)$ ($\phi=\mathbf{k}_d\cdot\mathbf{r}$, $\tilde\phi=\mathbf{k}_d\cdot\tilde{\mathbf{r}}$), leads to the decay of the averaged, single-time, two-atom correlation function T. Another parameter, Q, proportional to the correlation between interference fringes at different points $\mathbf{r}$ and $\tilde{\mathbf{r}}$, provides coupling between the population correlation function T and the coherence correlation function Z. As $\alpha(\phi)$, x, and Q depend on the cross-correlation parameter α_{12}, we expect the solution of Eqs. (4.1)–(4.3) to differ substantially for correlated ($\alpha_{12}\neq0$) and uncorrelated ($\alpha_{12}=0$) pulses. Finally, we note that quantity δ_f defined as a difference of modified detunings in Eq. (4.7), appears in Eq. (4.3). In Eq. (4.7), one sees that the atom-field detuning δ is altered by a term $G(t_{12})\alpha_{12}\sin\phi$ [see Eq. (3.10)], whose origin was explained in the previous section and which is the only parameter in Eqs. (4.1)–(4.3) that depends on the delay time t_{12}.

V. RECTANGULAR PULSES

In this paper we consider pulses with rectangular envelopes

$$f(t)=\text{const}\neq0\quad\text{for } 0\le t\le t_p\ ,$$

for which the coefficients (4.5) in Eqs. (4.1)–(4.3) do not vary with time. Although the assumption of rectangular pulses may seen to be a severe restriction, it turns out that many of the results obtained are independent of pulse shape.

The ensemble of two-level atoms is assumed to be in thermal equilibrium before the excitation pulses are applied at $t=0$. The corresponding initial conditions are

$$\begin{aligned}&\rho_3(0)=\rho_{aa}(0)-\rho_{bb}(0)=\rho_{3e}\ ,\\&\rho_1(0)=2\,\mathrm{Re}[\rho_{ab}(0)e^{-i\mathbf{k}_2\cdot\mathbf{r}}]=0\ ,\\&\rho_2(0)=2\,\mathrm{Im}[\rho_{ab}(0)e^{-i\mathbf{k}_2\cdot\mathbf{r}}]=0\ ,\end{aligned} \tag{5.1}$$

implying that

$$\rho(0)=\rho_{3e},\quad\langle T(0)\rangle=\rho_{3e}^2,\quad Z(0)=0\ . \tag{5.2}$$

From Eq. (4.1) we find an averaged population difference

$$\rho=\frac{\rho_{3e}}{2\alpha(\phi)+\gamma_l}(\gamma_l+2\alpha e^{-[2\alpha(\phi)+\gamma_l]t}) . \tag{5.3}$$

The solution for the averaged second moment of the population difference can be represented in a general form as

$$T=T_0+\sum_{i=1}^{3} e^{\lambda_i t}T_i+e^{-\gamma_l t}(T_4e^{-2\alpha t}+T_5e^{-2\bar{\alpha}t}) , \tag{5.4}$$

where T_0 is the steady-state solution

$$T_0=\frac{\gamma_l^2\rho_{3e}^2(x+\gamma_l)[(x+2\gamma_t)^2+\delta_f^2]}{(2\alpha+\gamma_l)(2\bar{\alpha}+\gamma_l)\{[(x+2\gamma_t)^2+\delta_f^2](x+\gamma_l)-4|Q|^2(x+2\gamma_t)\}} . \tag{5.5}$$

The exponents $\lambda_{1,2,3}$ are the roots of the equation

$$(\lambda+2\gamma_t)(\lambda+2\gamma_t+x)(\lambda+2\gamma_t+3x)=-2y(\lambda+2\gamma_t+x)-\delta_f^2(\lambda+2\gamma_l+2x)-2(\gamma_l-\gamma_t)(\lambda+2\gamma_t+x)^2 \tag{5.6}$$

with

$$y=x^2-4|Q|^2$$
$$=2\alpha_1\alpha_2[1-\cos(\phi-\bar{\phi})]=\alpha_{12}^2(\sin\phi-\sin\bar{\phi})^2 . \tag{5.7}$$

The functions T_i $(i=1,2,3)$ are solutions of the homogeneous equations (4.2) and (4.3) $(\rho_{3e}=0)$; they correspond to the roots λ_i and take into account the initial conditions (5.2). The exact expressions for $T_{1,2,3}$ are too complicated to be presented here. Limiting values for T_1, T_2, T_3 are given in Sec. VI and Appendix C.

Finally, $T_4(\alpha,\bar{\alpha})=T_5(\bar{\alpha},\alpha)$ is given by

$$T_4=\frac{2\gamma_l\rho_{3e}^2\alpha(z^2+\delta_f^2)}{(2\alpha+\gamma_l)[(z^2+\delta_f^2)(2\bar{\alpha}+\gamma_l)-8|Q|^2z]} , \tag{5.8}$$

where $z=\bar{\alpha}-\alpha-\gamma_l+2\gamma_t$.

In principle, a numerical integration (2.19) of the general solution (5.4) over ϕ and $\bar{\phi}$ gives us the desired PT-3 signal. However, to understand the dependence of this signal on the numerous parameters involved, it is useful to obtain some analytical results. They can be obtained for large or small values of a parameter n_0 which characterizes the number of population gratings of comparable amplitude which are generated in the sample, each grating of order n contributing to the signal in direction $\mathbf{k}_3\pm n\mathbf{k}_d$. For $n_0\ll 1$, only the gratings of the first order, $n=\pm 1$, are important. For $n_0\gg 1$, it is possible to integrate (2.19) by noting that regions where $\cos\phi\approx\cos\bar{\phi}$ give maximum contributions to the PT-3 signal.

Hereafter, we replace $t_p^0=t_p+t_{12}$ by t_p, since under conditions (2.7) the difference between them does not affect the results. We assume that at thermal equilibrium a two-level atom is in its ground state and thus

$$\rho_{3e}=1 . \tag{5.9}$$

Deviation from condition (5.9) leads only to decrease of the PT-3 signal by the factor ρ_{3e}^2. In addition, we drop the $(\phi,\bar{\phi},\delta,\bar{\delta})$ arguments and write $T(t;\phi,\bar{\phi},\delta,\bar{\delta})$ simply as $T(t)$.

VI. QUANTITATIVE RESULTS IN THE WEAK-RELAXATION LIMIT $\gamma_l T_p\ll 1;\gamma_T T_p\ll 1$

In this section we assume that

$$\gamma_l,\gamma_t\ll t_p^{-1} \tag{6.1}$$

and consequently, the role of relaxation in the formation of the PT-3 signal is negligible, and the signal can be calculated using Eq. (2.23). Most experiments have been carried out in this "weak-relaxation" limit.

A. Weak-field regime

The weak-field regime is defined by

$$\alpha_1,\alpha_2\ll t_p^{-1} . \tag{6.2}$$

In this limit, the population gratings of order $n=\pm 1$ lead to the strongest PT-3 signals. The signals, originating from the $n=1$ and $n=-1$ gratings, are of equal intensity. In the weak-field regime, one can interpret the signals in terms of a four-wave mixing process involving one interaction with each of the three excitation pulses. If inequalities (6.1) and (6.2) hold, one finds (see Appendix B)

$$T^{(1,-1)}(t_p;\delta,\bar{\delta})=\alpha_{12}^2t_p^2+2\alpha_1\alpha_2\frac{1-\cos(\delta_-t_p)}{\delta_-^2} . \tag{6.3}$$

As $T^{(1,-1)}$ given by (6.3) is a real even function of δ_-, it follows that $N_2=0$ in Eq. (2.20). Hence, to obtain the PT-3 signal from Eq. (2.23), one needs only the expression (6.3) with equal detunings, that is $T^{(1,-1)}(t_p;\delta,\delta)=N_1(\delta_-=0)$, given by

$$T^{(1,-1)}(t_p;\delta,\delta)=t_p^2(\alpha_{12}^2+\alpha_1\alpha_2) . \tag{6.4}$$

To interpret (6.4), one can use Eqs. (2.15) and (2.13) to rewrite $T^{(1,-1)}(t_p;\delta,\delta)$ as

$$T^{(1,-1)}(t_p;\delta,\delta)=\langle|\rho_3^{(1)}(t_p;\delta)|^2\rangle$$
$$=[\rho^{(1)}(t_p)]^2+\langle|\rho_3^{(1)}(t_p;\delta)-\rho^{(1)}(t_p)|^2\rangle , \tag{6.5}$$

where $\rho^{(1)}(t_p)$ is the *mean* amplitude of the population

difference grating, $\rho^{(1)}(t_p)=\langle\rho_3^{(1)}(t_p;\delta)\rangle$. From Eqs. (2.12) and (5.3), and under condition (6.2), one finds that $\rho^{(1)}(t_p)$ is given by

$$\rho^{(1)}(t_p)=\alpha_{12}t_p \ . \tag{6.6}$$

The correlation function (6.4) consists of the two parts. The first term $\alpha_{12}^2t_p^2$ depends on the mutual correlation of the pulses and is equal to the first term in Eq. (6.5), that is, to the square of the mean amplitude $\rho^{(1)}(t_p)$ of the population difference grating. The second term of expression (6.4) equals the average of the square of the fluctuating part of the population difference grating and is independent of the mutual correlation of the pulses. For fully correlated pulses these two contributions are equal.

From Eqs. (2.23) and (6.5) one obtains the PT-3 signal

$$W_1^{(3)}=t_p^2(\alpha_{12}^2+\alpha_1\alpha_2) \tag{6.7}$$

which does not depend on the delay time t_{12}. One might have anticipated this result since, in a weak-field regime, the significant asymmetry of the signal occurs only for long delay times $|t_{12}|\geq\Delta_D^{-1}$,[3,8] for which the Bloch vector can acquire a non-negligible Doppler phase (of order $\Delta_D t_{12}>1$). For t_{12} satisfying inequality (2.7), however, this asymmetry is negligible. For fully correlated pulses ($\Phi=1$), Eq. (6.7) coincides with a previously obtained result.[12]

The important feature of the weak-field result is the absence of a direct dependence of the signals on the correlation time. This dependence emerges only in third order of the parameter αt_p and can be neglected.

One can also see from Eq. (6.7) and the definition of α_{12} that the part of the signal proportional to α_{12}^2, which depends on the correlation of the pulses, cannot be larger than the part proportional to $\alpha_1\alpha_2$, which is independent of this correlation. In a strong field, these properties of the signals are changed dramatically.

B. Strong-field regime

The main objective of this work is to study the regime when at least one of the excitation pulses is strong. In the weak-relaxation limit (6.1), the strong-field criterion is

$$\alpha_{\max}=\max(\alpha_1,\alpha_2)\gg t_p^{-1} \ . \tag{6.8}$$

The PT-3 signal is determined from Eq. (2.17) [which gives $T^{(n,-n)}(t_p)$ in terms of the averaged correlation function $T(t_p)$], Eq. (2.20) [which represents $T^{(n,-n)}(t_p)$ in terms of N_1 and N_2], and Eq. (2.23) (which gives the PT-3 signal as an integral of N_1 over δ_+ and N_2 over $\delta_\pm$). It is shown in Appendix C that $T(t_p)$ is approximately given by

$$T(t_p)=\tfrac{1}{3}e^{\lambda_1 t_p} \ , \tag{6.9}$$

where

$$\begin{aligned}\lambda_1=-\tfrac{2}{3}\{&2\alpha_1\alpha_2[1-\cos(\phi-\tilde{\phi})]\\&-[1-G^2(t_{12})]\alpha_{12}^2(\sin\phi-\sin\tilde{\phi})^2+\delta_-^2\\&+2\delta_- G(t_{12})\alpha_{12}(\sin\phi-\sin\tilde{\phi})\}\\&\times[\alpha_1+\alpha_2+\alpha_{12}(\cos\phi+\cos\tilde{\phi})]^{-1} \ .\end{aligned} \tag{6.10}$$

All the other terms in the general expression (5.4) provide corrections to the PT-3 signal which are at most of order $(\alpha_{\max}t_p)^{-1}\ll 1$.

An important feature of the strong-field signal is tied to the two terms in Eq. (6.10) that contain the function $G(t_{12})$. For correlated pulses ($\alpha_{12}\neq 0$; i.e., $\Phi\neq 0$), these terms lead to the variation of the signal on a time scale of τ_c^{12}, since $G(t_{12})$ has been shown to vary over such a time scale. As noted above, Eq. (2.23) is a valid starting point for an analysis of the PT-3 signal in the weak-relaxation limit. The part of the signal which is asymmetrical about $t_{12}=0$ arises from the N_2 term in Eq. (2.23). Both of the terms in Eq. (6.10) depending on $G(t_{12})$ affect this part of the PT-3 signal. It can be shown, however (see Appendix D), that in a strong-field regime the strongest PT-3 signals are characterized by small orders n and are almost symmetrical for $|t_{12}|\leq\alpha^{-1}$. Although the asymmetrical contribution to the signal is usually small, there are certain cases (to be discussed) where it cannot be neglected. If we do not consider this small asymmetry, then according to Eq. (2.23) the PT-3 signal is determined by its symmetrical part, N_1, that depends only on λ_1 ($\delta_-=0$) from Eq. (6.10). Consequently, N_1 is affected only by the term in Eq. (6.15) which is proportional to the parameter $[1-G^2(t_{12})]\alpha_{12}^2$ that varies from α_{12}^2 to 0 as t_{12} varies from 0 to values $\geq\tau_c^{12}$. Thus, for $t_{12}>\tau_c^{12}$ this factor vanishes. Consequently, the numerator of Eq. (6.10) becomes independent of Φ once $t_{12}>\tau_c^{12}$. There is an additional dependence on α_{12} contained in the denominator of Eq. (6.10); however, it turns out this dependence does not significantly modify the signal for small order n. As a result, the signal is nearly independent of Φ for $t_{12}>\tau_c^{12}$; in other words, both correlated or uncorrelated pulses, characterized by $\Phi=1$ and $\Phi=0$, respectively, give rise to almost equal signals for $t_{12}>\tau_c^{12}$.

The detailed calculations of the PT-3 signal are carried out in Appendix D. Below we present the results in the most important cases.

1. *One strong and one weak pulse*

As α_1 and α_2 enter Eq. (6.10) in a symmetric way, the PT-3 signal does not depend on which pulse is strong, and this case is characterized by

$$\alpha_{\max}\gg t_p^{-1}\gg\alpha_{\min} \ , \tag{6.11}$$

where $\alpha_{\min}=\min(\alpha_1,\alpha_2)$. Taking into account Eqs. (6.11) and expanding expression (6.10) to first order in $\alpha_{\min}t_p$, we get the correlation function

$$T(t_p)=\tfrac{1}{3}\exp\left[-\frac{2\delta_-^2 t_p}{3\alpha_{\max}}\right]\left\{1+\frac{2\alpha_{\min}t_p}{3}\left[[\cos(\phi-\tilde{\phi})-1][2-(1-G^2)\Phi[1+\cos(\phi+\tilde{\phi})]\right]-\frac{2G\Phi\delta_-}{\alpha_{12}}\left[1-\frac{\alpha_{12}}{\alpha_{\max}}(\cos\phi+\cos\tilde{\phi})\right](\sin\phi-\sin\tilde{\phi})\right]\right\}. \tag{6.12}$$

The strongest signals ($n\neq 0$) are emitted in the directions $k_3\pm k_d$. Picking up the terms proportional to $\exp\{i(\phi-\tilde{\phi})\}$ needed in Eq. (2.19) one finds

$$T^{(1,-1)}(t_p)=\frac{\alpha_{\min}t_p}{9}\exp\left[-\frac{2\delta_-^2 t_p}{3\alpha_{\max}}\right]\times\left[2-[1-G^2(t_{12})]\Phi-i\frac{2\Phi G\delta_-}{\alpha_{\max}}\right]. \tag{6.13}$$

The signal obtained from Eqs. (2.20) and (2.23) is given by

$$W_1^{(3)}=\frac{\alpha_{\min}t_p}{9}\left[2-[1-G^2(t_{12})]\Phi-\frac{2\Phi G}{\sqrt{\pi}}\left[\frac{\alpha_{\max}^2}{2\Delta_D^2}+\tfrac{2}{3}\alpha_{\max}t_p\right]^{-1/2}\right]. \tag{6.14}$$

Thus, when one of the fields is weak, the PT-3 transient consists of a background signal and a narrow dip of width τ_c^{12} and relative depth $\Phi/2$ centered at zero delay time, $t_{12}=0$ (see Fig. 3). The dip is produced only for correlated pulses ($\Phi\neq 0$) while the background signal exists for either noncorrelated or correlated pulses. The result (6.14) coincides with that obtained earlier[15] for fully correlated pulses, when $\Phi=\alpha_{12}^2(\alpha_1\alpha_2)^{-1}=1$, and for $\alpha_{\max}t_p=\infty$. Owing to condition (6.11), the signal (6.14) is almost symmetrical around $t_{12}=0$ for any Doppler width Δ_D; however, there is a small negative asymmetry which arises from the last term in Eq. (6.14) [the signal at $t_{12}<0$ is larger than at $t_{12}>0$]. Such an asymmetry cannot appear in a weak-field regime.

2. *Both pulses are strong*

This case is described by the condition

$$\alpha_{\min}=\min(\alpha_1,\alpha_2)\gg t_p^{-1}. \tag{6.15}$$

Population gratings of order $n\leq n_0$, with $n_0\gg 1$, are created by these strong fields; consequently, the signal intensity in many directions, $\mathbf{k}_3\pm n\mathbf{k}_d$ with $n\leq n_0$, can be comparable. We need consider only $n\geq 0$, since the signals in the $\mathbf{k}_3-n\mathbf{k}_d$ directions are related to those at $\mathbf{k}_3+n\mathbf{k}_d$ by

$$W_n^{(3)}(t_{12})=W_{-n}^{(3)}(-t_{12}). \tag{6.16}$$

It is possible to obtain analytical expressions for the signal in some important limiting cases provided

$$n\ll\alpha_{\min}t_p. \tag{6.17}$$

If mutual correlation of the pulses is moderate or weak, that is, if

$$\Phi\leq 0.5, \tag{6.18}$$

the PT-3 signal takes the form (see Appendix D)

$$W_n^{(3)}=\frac{e^{-n^2/2\eta^2}}{3\eta\sqrt{2\pi}}\left\{1+\frac{\Phi}{4}\left[[1-G^2(t_{12})]\left[1-\frac{n^2}{\eta^2}\right]-\frac{\beta^2}{4}\left[1+\frac{2n^2}{\eta^2}-\frac{n^4}{\eta^4}\right]+\frac{2Gn\beta}{\eta\sqrt{2\pi(D+1)}}\left[\frac{2+D}{1+D}-\frac{n^2}{\eta^2}\right]\right]\right\}, \tag{6.19}$$

where

$$\eta=\left[\frac{4\alpha_1\alpha_2 t_p}{3(\alpha_1+\alpha_2)}\right]^{1/2},\qquad \beta=\frac{2(\alpha_1\alpha_2)^{1/2}}{\alpha_1+\alpha_2}, \tag{6.20}$$

and

$$D=\frac{3(\alpha_1+\alpha_2)}{4\Delta_D^2 t_p},$$

and all the terms in parentheses that are proportional to Φ are assumed to be small compared to 1. Note that $D\ll 1$ corresponds to a relatively large Doppler width, and $D\gg 1$ to a relatively small Doppler width.

In the limit that $\Phi=0$ (noncorrelated pulses) the signal (6.19) reduces to

$$W_n^{(3)}(\Phi=0)=\frac{e^{-n^2/2n^2}}{3\eta\sqrt{2\pi}}. \tag{6.21}$$

The signal (6.21) does not depend on t_{12}, and Eq. (6.21) is valid for all $n\ll\eta^2$ [see Eqs. (6.17) and (6.20)].

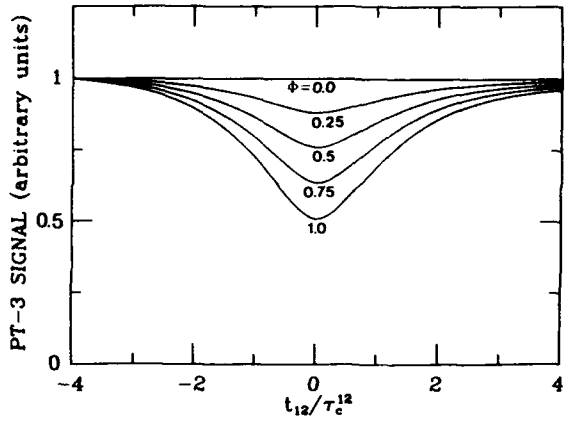

FIG. 3. Signals corresponding to order $n=1$ vs t_{12}/τ_c^{12} in a weak-relaxation limit ($\gamma_l t_p=0.02$ and $\gamma_t t_p=0.01$ in this figure and Figs. 4–10) in the case of one strong and one weak pulse $\alpha_{max}t_p=300$, $\alpha_{min}t_p=0.05$, for different degrees of mutual correlation Φ of the pulses; $\Delta_D t_p=14$. All curves in this and all other figures represent numerical solutions of Eqs. (4.1)–(4.3).

The signal (6.19) for correlated pulses differs only slightly from that for uncorrelated pulses, but the difference between the two is a function of t_{12}. The PT-3 signal (6.19) in a direction characterized by $n \ll \eta$ exhibits a small peak having width τ_c^{12} and relative height

$$S=\frac{W_n^{(3)}(t_{12}=t_{12}^{max})-W_n^{(3)}(t_{12}\gg\tau_c)}{W_n^{(3)}(t_{12}\gg\tau_c)}=\tfrac{1}{4}\Phi\ll 1 \qquad (6.22)$$

(see Fig. 4). The signal has positive asymmetry which is small for any Doppler width and ratio of the pulse intensities. Owing to this asymmetry the central peak maximum of the signal is slightly shifted to positive delay time, that is

$$t_{12}^{max}=\frac{n\beta}{\eta}\frac{(2+D)}{(1+D)^{3/2}}\tau_c^{12}\ll\tau_c^{12}\ . \qquad (6.23)$$

It is also seen in Eq. (6.19) that the background signal for $t_{12}>\tau_c$ does not exactly equal that for noncorrelated pulses. This difference reaches its maximum value $-\Phi/16\ll 1$ when the pulses have equal intensities, $\alpha_1=\alpha_2$, and the background signal decreases with increasing Φ.

In contrast to the signals corresponding to small n, the signal in a direction characterized by $n\gg\eta$ exhibits a dip (see curve a in Fig. 5), if

$$\frac{n\beta}{\eta\sqrt{1+D}}\ll 1\ . \qquad (6.24)$$

Condition (6.24) can be satisfied if the Doppler distribution is narrow, $D\gg 1$, or the pulses have very different intensities, $\beta\ll 1$ [or $\alpha_{max}/\alpha_{min}>10$, see expression (6.20)]. The signal has a small negative asymmetry; the dip is positioned at $t_{12}\approx 0$ and has relative depth

$$|S|=\frac{W_n^{(3)}(t_{12}\gg\tau_c)-W_n^{(3)}(t_{12}=0)}{W_n^{(3)}(t_{12}\gg\tau_c)}=\tfrac{1}{4}\Phi\frac{n^2}{\eta^2}\ll 1\ . \qquad (6.25)$$

However, as soon as condition (6.24) is violated, the dip vanishes and the signal continuously decreases as t_{12} varies from negative to positive values (see curve c in Fig. 5).

If the pulses are strongly correlated, that is if

$$(1-\Phi)\ll 1\ , \qquad (6.26)$$

the qualitative behavior of the PT-3 signal is similar to that considered above; however, all the features are more clearly defined as we proceed to discuss.

First, we consider the strongest signal, characterized by small n, $n\ll\eta$. The intensity of the signal is given by

$$W_n^{(3)}(t_{12})=W_S+W_{AS}\ , \qquad (6.27)$$

where W_S and W_{AS} are correspondingly the symmetrical and asymmetrical parts of the signal

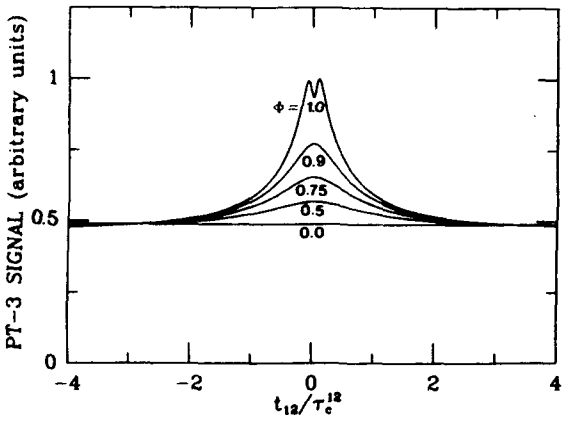

FIG. 4. Signals corresponding to small order $n=1\ll\eta$ vs t_{12}/τ_c^{12} in a weak-relaxation limit in the case when both pulses are strong: $\alpha_{max}t_p=10^3$, $\alpha_{min}t_p=10^2$ for different degrees of mutual correlation Φ of the pulses; $\Delta_D t_p=14$.

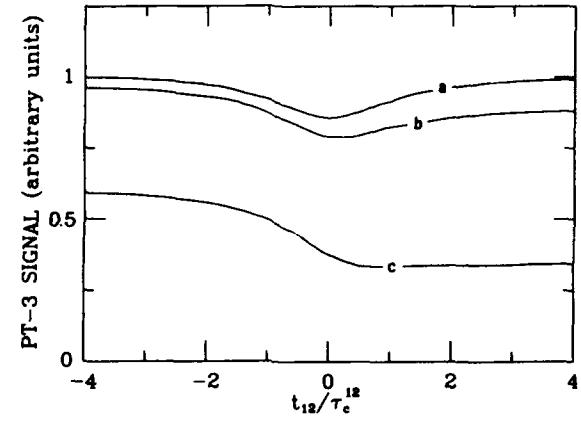

FIG. 5. Signals corresponding to high order $n=20>\eta$ vs t_{12}/τ_c^{12} in a weak-relaxation limit in the case when both pulses are strong: $\alpha_{min}t_p=100$ and $\alpha_{max}t_p=10^4$ (curve a), 10^3 (curve b), and 110 (curve c). Degree of mutual correlation of the pulses is moderate: $\Phi=0.25$; $\Delta_D t_p=14$.

$$W_S(t_{12})=W_S(-t_{12});\ W_{AS}(t_{12})=-W_{AS}(-t_{12})\ . \quad (6.28)$$

For $n \ll \eta$, W_S is much larger than W_{AS}, and for $t_{12} \leq \tau_c^{12}$ it can be represented in the form (see Appendix D)

$$W_S=\frac{1}{3\pi\sqrt{2\pi}}\left[W_+ + W_- + \frac{\beta^2}{4\eta}\right], \quad (6.29)$$

with

$$W_\pm=\frac{1}{\eta_\pm}\ln\frac{4\eta_\pm}{n\{\exp(-Z_\pm/2)+[Z_\pm+\exp(-Z_\pm)]^{1/2}\}}, \quad (6.30)$$

and

$$\eta_\pm=\left[\frac{4\alpha_1\alpha_2 t_p}{3(\alpha_1+\alpha_2\pm 2\alpha_{12})}\right]^{1/2} \gg 1\ ,$$
$$Z_\pm=\frac{[1-\Phi(1-G^2)]\eta_\pm^2}{n^2}\ . \quad (6.31)$$

If the pulses are strongly correlated, that is, if $(1-\Phi)<n^2/\eta_\pm^2$, and if the delay time is very small,

$$t_{12} \ll \tau_c^{12}\left[\frac{n^2}{\eta_\pm^2}-(1-\Phi)\right]^{1/2}, \quad (6.32)$$

then $Z_\pm \ll 1$ in Eq. (6.30), and $W_\pm$ increases with increasing t_{12} as

$$W_\pm=\frac{1}{\eta_\pm}\left[\ln\frac{2\eta_\pm}{n}+\frac{[1-\Phi+(t_{12}/\tau_c^{12})^2]\eta_\pm^2}{2n^2}\right]. \quad (6.33)$$

However, when

$$\tau_c^{12} \geq t_{12} > \tau_c^{12}\left[\frac{n^2}{\eta_\pm^2}-(1-\Phi)\right]^{1/2}, \quad (6.34)$$

then $Z_\pm > 1$, and $W_\pm$ is given by

$$W_\pm=\frac{1}{2\eta_\pm}\ln\frac{16}{[1-\Phi+(t_{12}/\tau_c^{12})^2]}, \quad (6.35)$$

and decreases with increasing t_{12}. Consequently, $W_\pm$ reaches its maximum for

$$t_{12}^{\max} \approx \tau_c^{12}\left[\frac{n^2}{\eta_\pm^2}-(1-\Phi)\right]^{1/2}. \quad (6.36)$$

If the pulses have very different intensities ($\alpha_{max} \gg \alpha_{min}$ or $\beta \ll 1$), the asymmetrical part of the signal W_{AS} can be neglected, since $W_{AS} \ll \beta/\eta \ll \eta^{-1}$ (see Appendix D). Thus the signal is completely determined by its symmetrical part W_S. The condition $\beta \ll 1$ holds when $\eta_+ \approx \eta_- \approx \eta$; in this limit $W_+ \approx W_-$, and the signal, obtained from Eqs. (6.29)–(6.35), exhibit a peak centered at $t_{12}=0$. The peak has temporal width $|t_{12}| \approx \tau_c^{12}$ and, moreover, for fully correlated pulses ($\Phi=1$) there is an *additional* very narrow dip that appears in the middle of this central peak. This dip has width $|t_{12}| \approx (n/\eta)\tau_c^{12}$, depth $\sim 0.02\eta^{-1}$, and is very sensitive to the degree of mutual correlation of the pulses, since the dip vanishes as soon as $(1-\Phi) > n^2/\eta^2$, as shown in Fig. 4. For fully correlated pulses, the peak is approximately $2\pi^{-1}\ln(2\eta/n)$ times higher than the background signal [see Eq. (D17)]:

$$W_n^{(3)}(|t_{12}| \gg \tau_c^{12}) = \frac{1}{3\eta\sqrt{2\pi}}\ , \quad (6.37)$$

which is reached for $|t_{12}| > \tau_c^{12}$ and which would be obtained for noncorrelated pulses [$\Phi=0$, see Eq. (6.21) for $n \ll \eta$].

In Fig. 6 the signal for order $n=1$ is shown as a function of intensity of the weaker pulse. The transition from a dip of width τ_c^{12} [$\alpha_{min}t_p \ll 1$; Eq. (6.14)] to the peak ($1 \ll \alpha_{min}t_p \ll \alpha_{max}t_p$) occurs for $\alpha_{min}t_p \approx 1$. The absolute intensity of the background signal varies with $\alpha_{min}t_p$ as

$$W_1^{(3)}=\tfrac{1}{3}\exp\left[-\frac{4\alpha_{min}t_p}{3}\right]I_1\left[\frac{4\alpha_{min}t_p}{3}\right], \quad (6.38)$$

where I_1 is a modified Bessel function, and reaches its maximum 0.07 for $\alpha_{min}t_p = 1.1$

If the pulses have nearly equal intensities, such that

$$1-\beta=[(\alpha_1)^{1/2}-(\alpha_2)^{1/2}]^2/(\alpha_1+\alpha_2) \ll 1\ ,$$

one can see from Eq. (6.30) that $W_+ \gg W_-$ and thus $W_S \approx W_+$. The asymmetrical part W_{AS} of the signal is still small. However, it cannot be neglected if the pulses are fully correlated [$(1-\Phi)<n^2/\eta^2 \ll 1$] and the Doppler width of the atomic ensemble is large ($D \ll 1$).

In this case W_{AS} is given by

$$W_{AS}=\frac{2nG}{3\pi^2(4n^2-1)}\left[-D+\frac{8G^2\eta^2}{3}\right], \quad \text{if } |G| \ll \eta^{-1}\ , \quad (6.39)$$

$$W_{AS}=\frac{G}{6\pi n\sqrt{\pi}}, \quad \text{if } \eta^{-1} \ll |G| \ll n\eta^{-1}\ , \quad (6.40)$$

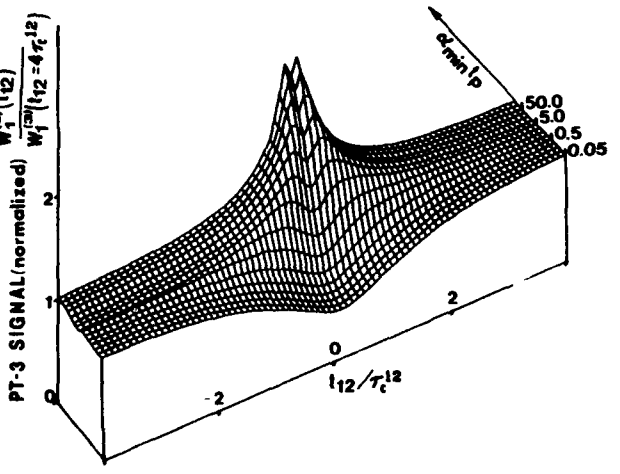

FIG. 6. Signal of order $n=1$ as a function of t_{12}/τ_c^{12} and $\alpha_{min}t_p$ in a weak-relaxation limit in the case when one of the fully correlated ($\Phi=1$) pulses is strong $\alpha_{max}t_p=500$, while the intensity of another varies, $0.05 < \alpha_{min}t_p < 170$; $\Delta_D t_p = 7$.

$$W_{AS}=\frac{1}{3\pi\eta G\sqrt{\pi}}\left[y_0+\frac{2n}{\eta\sqrt{\pi}}\ln\frac{2|G|}{y_0+(y_0^2+2G^2D)^{1/2}}\right],$$
$$\text{if } n\eta^{-1}\ll|G|\ , \quad (6.41)$$

where

$$y_0=\frac{n}{\eta}\exp\left[-\frac{DG^2\eta^2}{n^2}\right].$$

One can see from Eqs. (6.39)–(6.41) that W_{AS} is much smaller than W_S. However, when $|t_{12}|\le(n/\eta)\tau_c^{12}$, W_{AS} is comparable with the part of W_S which depends on delay time [see Eq. (6.33)]. As a result, the narrow dip in the middle of the peak practically vanishes (see Fig. 7) and the maximum of the signal shifts to

$$t_{12}^{\max}\approx\frac{n}{\eta}\tau_c^{12}.$$

For $|t_{12}|>\tau_c^{12}$ the signal reaches its background value given by

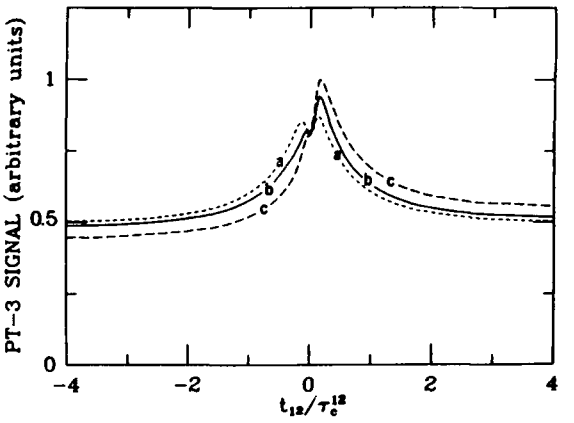

FIG. 7. Signals corresponding to order $n=1$ vs t_{12}/τ_c^{12} in a weak-relaxation limit in the case of fully correlated ($\Phi=1$) strong pulses with almost equal intensities ($\alpha_1 t_p=120$, $\alpha_2 t_p=100$) for different Doppler widths of the atomic ensemble: curve *a*, $-\Delta_D t_p=1.4$ ($D=118$); curve *b*, $-\Delta_D t_p=14$ ($D=1.2$); curve *c*, $-\Delta_D t_p=70$ ($D=0.05$).

$$W_n^{(3)}(|t_{12}|\gg\tau_c^{12})=\frac{1}{3\pi\eta\sqrt{2\pi}}\left[2\sqrt{2}+s\frac{n}{\eta\sqrt{2}}\ln\left\{\min\left[\left[\frac{\eta e}{n}\right]^2,\frac{2}{D}\right]\right\}\right], \quad (6.42)$$

where s is defined by Eq. (2.21). Comparing Eqs. (6.37) and (6.42), one can see that even in the case of equal intensities of the fully correlated pulses the background signal differs only slightly from that corresponding to noncorrelated pulses.

In Fig. 8 for $\alpha_1/\alpha_2=\text{const}\approx1$ the evolution of the signal with increasing intensity of both pulses is shown. The transition from the signal with no dependence on t_{12} [weak-field regime, $\alpha_{1,2}t_p\ll1$; Eq. (6.7)] to the signal with a well-defined peak (strong-field regime, $1\ll\alpha_{1,2}t_p$) occurs in the intermediate range of intensities; that is, when $\alpha_{1,2}t_p\approx1$. For these intensities the asymmetry of the signal and its absolute intensity reach their maximum values.

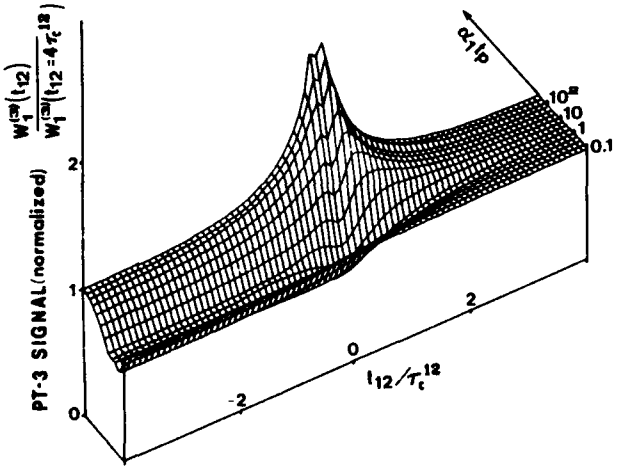

FIG. 8. Signal of order $n=1$ as a function of t_{12}/τ_c^{12} and $\alpha_1 t_p$ in a weak-relaxation limit; $\Delta_D t_p=7$. The fully correlated ($\Phi=1$) pulses have nearly equal intensities $\alpha_2/\alpha_1=1.2$ that vary from small to large values ($0.1<\alpha_1 t_p<500$).

The above discussion is valid for orders n satisfying $0<n\ll\eta$. The signal of order $n=0$ is difficult to detect, as it is emitted simultaneously with the third pulse in the same direction, but it is the strongest of the PT-3 signals. It is given completely by its symmetrical part, and at zero delay time can be expressed as

$$W_0^{(3)}(t_{12}=0)=W_1^{(3)}(t_{12}=0)+\frac{1}{3\eta\sqrt{2\pi}}. \quad (6.43)$$

For $t_{12}>\tau_c^{12}[n^2/2\eta_\pm^2-(1-\Phi)]^{1/2}$, the difference between PT-3 signals of zero and first order vanishes, and $W_0^{(3)}(t_{12})$ coincides with the symmetrical part of the signal $W_1^{(3)}(t_{12})$ given by Eq. (6.35). The zero-order signal always decreases with increasing $|t_{12}|$.

Let us now consider the PT-3 signals of higher order, that is, with $n\gg\eta$. These signals are relatively weak; nevertheless, they have some features that deserve discussion. For the sake of simplicity we consider fully correlated pulses ($\Phi=1$) in two limiting cases: (1) the pulses have very different intensities $\alpha_{\max}\gg\alpha_{\min}$, and (2) the pulses have equal intensities $\alpha_1=\alpha_2=\alpha$.

In the first case ($\alpha_{\max}\gg\alpha_{\min}$), if

$$\frac{n^4\alpha_{\min}}{\eta^4\alpha_{\max}} \ll 1 , \tag{6.44}$$

the signal is given by

$$W_n^{(3)}(t_{12}) = \frac{1}{3\eta\sqrt{2\pi}} \exp\left[-\frac{n^2(3-G^2)}{4\eta^2}\right] \times I_0\left[\frac{n^2(1-G^2)}{4\eta^2}\right] , \tag{6.45}$$

where I_0 is a modified Bessel function. As shown in Fig. 9, the signal (6.45) exhibits a profound dip of relative depth $|S| = (1-2\eta/\pi n) \approx 1$ centered at $t_{12}=0$; for $|t_{12}| > \tau_c^{12}$ the signal practically coincides with that for noncorrelated pulses.

When

$$\frac{n^4\alpha_{\min}}{\eta^4\alpha_{\max}} > 1 , \tag{6.46}$$

the background signal acquires a negative asymmetry if $D\eta^2/n^2 < 1$ [see Eq. (D36)].

In the second case (equal pulse intensities) the signal is given approximately by

$$W_n^{(3)} = \frac{\eta}{3\pi n^2\sqrt{\pi}}\left[|G| - G\,\mathrm{erf}\left[\frac{n}{\eta[2(DG^2+2)]^{1/2}}\right]\right] + \frac{\sqrt{2}\exp(-n^2/4\eta^2)}{3\pi n}\left[1-\mathrm{erf}\left[\frac{n|G|}{4\eta}\right]\right] , \tag{6.47}$$

where erf is the error function.[43]

If the Doppler width of the atomic ensemble is sufficiently small, such that

$$\frac{n^2}{D\eta^2} = \left[\frac{n\Delta_D}{\alpha}\right]^2 \ll 1 , \tag{6.48}$$

then, as in the first limit ($\alpha_{\max} \gg \alpha_{\min}$), the PT-3 signal for equal intensities exhibits a dip whose minimum is shifted to positive t_{12}. The dip has relative depth close to unity, since the background signal

$$W_n^{(3)}(t_{12} > \tau_c^{12}) = \frac{\eta}{3n^2\pi\sqrt{\pi}} \tag{6.49}$$

is much larger than the value at zero delay time.

If the Doppler width is sufficiently large, such that condition (6.48) is violated, the signal (6.47) becomes strongly negatively asymmetric and the dip vanishes (see Fig. 10).

The remarkable feature of Eq. (6.49) is the power-law-type dependence of the signal on n for $t_{12} > \tau_c^{12}$, rather than the Gaussian-like dependence seen in Eq. (6.45) for pulses having different intensities. As a result, it may be easier to detect signals corresponding to large n if equal pulse intensities are used. By comparing Eqs. (6.49) and (6.21), one sees that the background signal for equal intensity, fully correlated pulses differs from that for noncorrelated pulses. This is the only limit where such a marked deviation occurs; the origin of this effect can be traced to the increasing importance of the α_{12} term in the denominator of Eq. (6.10), a term that was ignored in the qualitative discussion following that equation.

When both fields are strong, the PT-3 signal differs in almost every respect from the analogous signal in the weak-field regime. The strong-field PT-3 signals are emitted with comparable intensities in many directions (corresponding $n < n_0 \lesssim \eta$), while the weak-field signals only in the $\mathbf{k}_3 \pm \mathbf{k}_d$ directions. The signal for correlated pulses can be much stronger than that for noncorrelated in the strong-field regime but not in the weak-field regime. Only the strong-field result depends directly on the cross-correlation time τ_c^{12} exhibiting a well-defined narrow peak ($n \ll \eta$), dip ($n \gg \eta$), or combination of them ($n \sim \eta$) at $t_{12}=0$. A negative asymmetry of the signal also occurs only in a strong-field regime.

Finally, it is possible to show that, in sharp contrast to the weak-field regime, for strong fields the signal induced

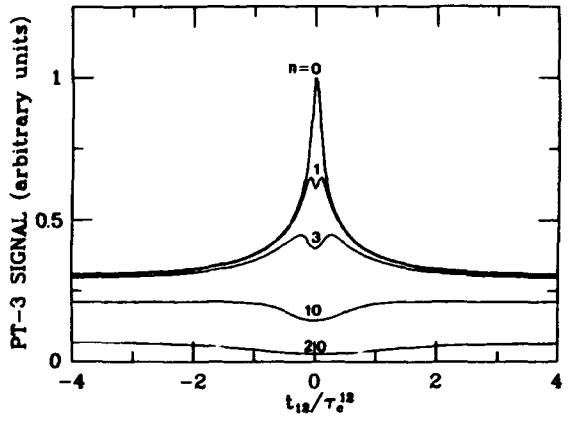

FIG. 9. Signals corresponding to different orders n vs t_{12}/τ_c^{12} in a weak-relaxation limit. Both pulses are strong and have very different intensities $\alpha_{\max}t_p = 10^4$, $\alpha_{\min}t_p = 100$ ($\beta = 0.2$); $\Delta_D t_p = 14$, $\Phi = 1$.

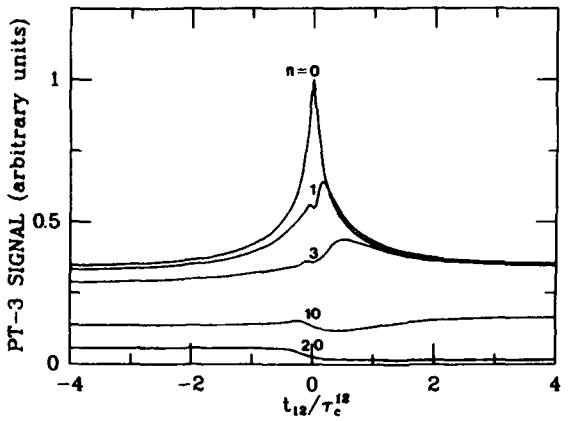

FIG. 10. Signals corresponding to different orders n vs t_{12}/τ_c^{12} in a weak-relaxation limit. Both pulses are strong and have nearly equal intensities $\alpha_{\max}t_p = 120$, $\alpha_{\min}t_p = 100$ ($\beta = 0.996$). All other parameters and notations are the same as in Fig. 9.

by the correlated pulses originates from the stochastic part of the population grating $[\rho_3^{(n)}(t_p)-\langle\rho_3^{(n)}(t_p)\rangle]$, while the contribution from the constant part of the grating, $\langle\rho^{(n)}(t_p)\rangle$, is negligible. In the weak-field regime, the constant and stochastic parts of the population grating induced by the fully correlated pulses provide signals of the same intensity [see Eqs. (6.6) and (6.7)]. To understand the strong-field results one can consider the mean amplitude $\rho^{(n)}=\langle\rho_3^{(n)}(t_p)\rangle$ for the grating of the order n.

Since the spontaneous relaxation is assumed to be negligible ($\gamma_l \ll t_p^{-1}$) we obtain from Eq. (5.3)

$$\rho^{(n)}=(-1)^n e^{-(\alpha_1+\alpha_2)t_p} I_n(2\alpha_{12}t_p) , \tag{6.50}$$

where I_n is a modified Bessel function. In contrast to the two-atom correlation function $T^{(n,-n)}=\langle\rho_3^{(n)}(t_p)\bar{\rho}_3^{(n)}(t_p)\rangle$, the single-atom amplitude (6.50) does not depend on either delay time t_{12} or the detuning δ.

As long as condition

$$(\alpha_1+\alpha_2-2\alpha_{12})t_p=\alpha(\pi)t_p \gg 1 \tag{6.51}$$

is satisfied [$\alpha(\phi)$ is defined in Eq. (4.5)], the mean grating amplitude $\rho^{(n)}(t_p)$ given by (6.50) is exponentially small for any n, namely

$$\rho^{(n)}(t_p) \ll e^{-(\alpha_1+\alpha_2-2\alpha_{12})t_p} \ll 1 .$$

However, if the pulses are almost fully correlated ($\Phi\approx 1$) with nearly equal intensities ($\alpha_1\approx\alpha_2\approx\alpha_{12}$), inequality (6.51) can be violated to the point that

$$(\alpha_1+\alpha_2-2\alpha_{12})t_p \lesssim 1 . \tag{6.52}$$

For $\max\{n,1\} \ll \alpha_{12}t_p$ it follows from Eq. (6.50) that

$$\rho^{(n)}(t_p)=\frac{(-1)^n\exp(-n^2/4\alpha_{12}t_p)}{(4\pi\alpha_{12}t_p)^{1/2}} \times e^{-(\alpha_1+\alpha_2-2\alpha_{12})t_p} , \tag{6.53}$$

and, owing to condition (6.52), the gratings characterized by $n<(2\alpha t_p)^{1/2}$ have nonexponentially small mean amplitudes $\sim(\alpha t_p)^{-1/2}$.

It is not too difficult to understand the physical origin of Eq. (6.51). The atoms in the sample see interference fringes produced by the excitation pulses. Atoms at points other than interference minima are saturated by the fields. If the pulse amplitudes are unequal, the intensity at the minima of the interference fringes is still sufficiently high (in the strong-field regime) to saturate even these atoms. These saturated atoms produce exponentially small contributions to the mean grating amplitude. On the other hand, for equal pulse amplitudes, atoms near the interference minima see an arbitrarily small effective total field; these atoms are not saturated. As a result, the mean amplitude $\rho(t_p;\phi)$ of the spatial population grating has narrow groves in the vicinity of the minima $\phi\approx(2m+1)\pi$ ($m=0,\pm1\ldots$) of the interference fringes.

If the nth-order population grating $\rho_3^{(n)}(t_p;\delta)$ is written as the sum of the constant and stochastic contributions,

$$\rho_3^{(n)}(t_p;\delta)=\rho^{(n)}(t_p)+[\rho_3^{(n)}(t_p)-\rho^{(n)}(t_p)] , \tag{6.54}$$

the correlation function $T^{(n,-n)}=\langle\rho_3^{(n)}(t_p;\delta)\rho_3^{(-n)}(t_p;\tilde{\delta})\rangle$ is given by

$$T^{(n,-n)}(t_p)=[\rho^{(n)}(t_p)]^2 + \langle[\rho_3^{(n)}(t_p;\delta)-\rho^{(n)}(t_p)] \times[\rho_3^{(-n)}(t_p;\tilde{\delta})-\rho^{(n)}(t_p)]\rangle . \tag{6.55}$$

We did not take into account the first term in Eq. (6.55) when deriving the results in the strong-field regime, owing to the fact that this contribution is (a) exponentially small if condition (6.52) is violated and (b) still small relative to the second term of Eq. (6.55) [compare Eqs. (6.53) and (6.49)] even if condition (6.52) is satisfied. In other words, for all $\alpha_1,\alpha_2,\alpha_{12}$, the signal in the strong-field regime is produced by the stochastic part of the populating grating, i.e.,

$$W_n^{(3)} \approx T^{(n,-n)}(t_p,\delta,\delta) \approx\langle|\rho_3^{(n)}(t_p;\delta)-\rho^{(n)}(t_p)|^2\rangle \gg[\rho^{(n)}(t_p)]^2 . \tag{6.56}$$

VII. QUALITATIVE EXPLANATION OF THE STRONG-FIELD RESULTS

To give a qualitative explanation of the strong-field results obtained in Sec. VI, we recall that the PT-3 signal depends directly on the correlation function $T(t_p)=\langle\rho_3(t_p;\phi,\delta)\rho_3(t_p;\tilde{\phi},\tilde{\delta})\rangle$ of population differences of two atoms. In general, these atoms are characterized by different positions ($\phi\neq\tilde{\phi}$) and velocities ($\delta\neq\tilde{\delta}$). More precisely, according to Eqs. (2.19), (2.20), and (2.23), the part of the signal symmetrical relative to t_{12} and n depends only on the correlation $\langle\rho_3(t_p;\phi,\delta)\rho_3(t_p;\tilde{\phi},\delta)\rangle$ of atoms having the same velocity. The asymmetrical part of the signal can arise when

$$\langle\rho_3(t_p;\phi,\delta)\rho_3(t_p;\tilde{\phi},\tilde{\delta})\rangle \neq\langle\rho_3(t_p;\tilde{\phi},\delta)\rho_3(t_p;\phi,\tilde{\delta})\rangle . \tag{7.1}$$

To explain the obtained results, we first consider the behavior of the correlation function $T(t_p)$ as a function of $\phi,\tilde{\phi},\delta,\tilde{\delta}$ and t_{12}. Since in a strong-field regime the population difference $\rho_3(t_p;\phi,\delta)$ is a stochastic quantity with $\langle\rho_3(t_p;\phi,\delta)\rangle\approx 0$, only those atoms that satisfy the condition $\rho_3(t_p;\phi,\delta)\approx\rho_3(t_p;\tilde{\phi},\tilde{\delta})$ contribute to the signal. To determine the range of ϕ and $\tilde{\phi}$ and δ and $\tilde{\delta}$ that contribute to $W_n^{(3)}(t_{12})$ for a given t_{12}, let us consider fully correlated excitation pulses ($\alpha_{12}=\sqrt{\alpha_1\alpha_2}$), when the PT-3 signal reveals the most profound dependence on t_{12}.

First we analyze the case of zero delay time, $t_{12}=0$. The behavior of the correlation function $T(t_p)$ depends implicitly on the spatial dependence of the incident fields, which in turn is represented by the total Rabi frequency $f(t,\phi)$. As the pulses are assumed to be fully correlated, $f(t,\phi)$ can be represented in the form

$$f(t,\phi)=f_1 e^{-i\phi}+f_2 =|f_1(t)|\left|\frac{\alpha(\phi)}{\alpha_1}\right|^{1/2}\exp\{i[\theta+\arg f_1(t)]\} , \tag{7.2}$$

where

$$\alpha(\phi)=\alpha_1+\alpha_2+2(\alpha_1\alpha_2)^{1/2}\cos(\phi)\ , \tag{7.3}$$

and

$$\tan\theta=-\frac{\alpha_1\sin\phi}{\alpha_1\cos\phi+(\alpha_1\alpha_2)^{1/2}}\ .$$

The phase θ does not depend on time and thus cannot affect the evolution of atomic population, while $\arg f_1(t)$ is the same for all atoms. Thus, all the essential dependence on ϕ is contained only in the absolute value of the Rabi frequency $|f(t,\phi)|$, which in turn represents a fixed spatial grating (or interference fringes) proportional to $\alpha(\phi)$, whose amplitude fluctuates in time according to $|f_1(t)|$.

The larger the difference in $|f(t,\phi)|$ and $|f(t,\tilde{\phi})|$ for atoms characterized by ϕ and $\tilde{\phi}$, the faster is the decorrelation of their populations. A difference in detunings (velocities) leads to the same decorrelation. Namely, for $\alpha(\phi)\approx\alpha(\tilde{\phi})$, only those atoms which satisfy the condition [see Eq. (C8)]

$$\tfrac{1}{3}(\sqrt{\alpha(\phi)}-\sqrt{\alpha(\tilde{\phi})})^2t_p+\frac{(\delta-\tilde{\delta})^2t_p}{3\alpha(\phi)}<1 \tag{7.4}$$

contribute to the signal. At $t_{12}=0$, however, the asymmetrical part of the signal vanishes, and only correlations between atoms with equal velocities are important. Thus, one need consider only the first term in Eq. (7.4) when $t_{12}=0$.

For $\alpha(\phi)\approx\alpha(\tilde{\phi})$, it follows from Eq. (7.3) one needs to have $\cos\phi\approx\cos\tilde{\phi}$. Consequently, the population correlations can be of two types. For a given atom, characterized by "location" $\phi=\mathbf{k}_d\cdot\mathbf{r}(-\pi/2\le\phi\le3\pi/2)$, the first type of correlation occurs with a neighboring atom having

$$\tilde{\phi}\approx\phi\ . \tag{7.5}$$

The second type of correlation arises for an atom located at ϕ and another one at

$$\begin{aligned}&\tilde{\phi}\approx-\phi,\ \text{ if } -\frac{\pi}{2}\le\phi\le\frac{\pi}{2}\ ,\\ &\tilde{\phi}\approx2\pi-\phi,\ \text{ if } \frac{\pi}{2}\le\phi\le\frac{3\pi}{2}\ .\end{aligned} \tag{7.6}$$

These correlations are illustrated qualitatively in Fig. 11. According to Eqs. (7.5) and (7.6), all atoms are naturally separated into two subensembles: those which are closer to maxima $-\pi/2\le\phi<\pi/2$ or minima $\pi/2\le\phi<3\pi/2$ of the interference fringes, respectively. The atomic populations are correlated only within these subensembles, which therefore contribute to the PT-3 signal independently:

$$W_n^{(3)}=W_{n,\max}^{(3)}+W_{n,\min}^{(3)}\ , \tag{7.7}$$

where max and min designate "maxima" and "minima" subensembles, respectively.

To continue the analysis, one must distinguish between two limiting cases, that of (1) pulses with very different intensities ($\alpha_{\max}\gg\alpha_{\min}$), and (2) pulses with nearly equal intensities ($\alpha_1\approx\alpha_2$). In the first case one can see from Fig. 11(a) that the spatial modulation of the interference fringes is small compared with its average amplitude. Hence, one can expect the behavior of the correlation function $T(t_p)$ to be almost identical for the "maxima" and "minima" subensembles. In the second case the "minima" subensemble is driven by a considerably weaker field than the "maxima" one [see Fig. 11(b)]; this can result in different contributions to $T(t_p)$ from the two subensembles.

If the pulses have very different intensities, condition (7.4) takes the form ($\delta=\tilde{\delta}$)

$$\frac{\alpha_{\min}t_p}{3}(\cos\phi-\cos\tilde{\phi})^2<1\ . \tag{7.8}$$

The fact that expression (7.8) is not changed under the substitution $\phi\to\phi+\pi$; $\tilde{\phi}\to\tilde{\phi}+\pi$ proves the behavior of $T(t_p)$ to be identical for the two subensembles. Suppose

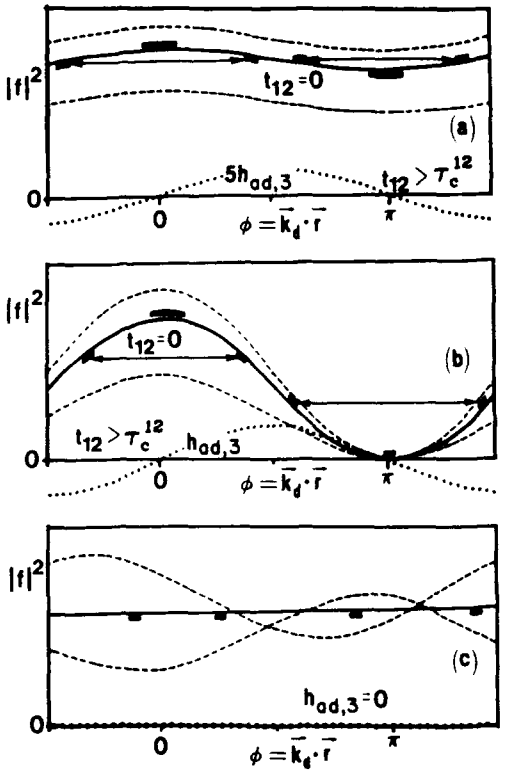

FIG. 11. Schematic representation of the two types of population correlations for $t_{12}=0$ for different excitation pulses. (a) The pulses are strong, fully correlated, and have very different intensities. Rectangles depict the range of correlations of the first type, while arrows depict the correlations of the second type. The solid curve represents the averaged interference fringes $\langle|f(t)|^2\rangle$, while the dashed curves depict nonaveraged interference fringes $|f(t)|^2$ for two different times. The effective detuning, which arises at $t_{12}\neq0$, is shown by the dotted curve. (b) The pulses have equal intensities. All other conditions and notations are the same as in (a). (c) The pulses are noncorrelated; only the correlations of the first type exist, and the effective detuning vanishes.

an atom is located near an extremum of the interference fringes ($\phi \approx 0$ or $\phi \approx \pi$). Then, $\tilde{\phi} \approx \phi$ holds for the both types of population correlations. Since $\sqrt{\alpha(\phi)}$ varies slowly near extrema, the amount of $(\phi - \tilde{\phi})$ that can still contribute to $T(t_p)$ is relatively large. According to Eq. (7.8) this range is given by

$$|\phi - \tilde{\phi}| < (\alpha_{\min} t_p)^{-0.25} \ll 1 . \tag{7.9}$$

On the other hand, if an atom characterized by ϕ is located at a slope of the interference fringes, then the correlations of the different types are well separated in space, and only the atoms satisfying

$$|\phi - \tilde{\phi}| < (\alpha_{\min} t_p)^{-0.5} \ll 1$$

(first type of correlations) (7.10)

and

$$|\phi + \tilde{\phi}| < (\alpha_{\min} t_p)^{-0.5} \ll 1 ,$$
$$|\phi + \tilde{\phi} - 2\pi| < (\alpha_{\min} t_p)^{-0.5} \ll 1 , \tag{7.11}$$

(second type of correlations)

can contribute to the signal. The ranges (7.10) and (7.11) are much smaller than (7.9).

For pulses with equal intensities ($\alpha_1 = \alpha_2 = \alpha$), condition (7.4) for atoms to contribute is

$$\frac{4\alpha t_p}{3} \left| \cos\frac{\phi}{2} - \cos\frac{\tilde{\phi}}{2} \right|^2 < 1 . \tag{7.12}$$

Comparing Eqs. (7.8) and (7.12), one finds that for the "maxima" subensemble, the behavior of correlations is not changed significantly compared to the case $\alpha_{\max} \gg \alpha_{\min}$. However, for the "minima" subensemble, that is, for an atom located close to a minimum of the interference fringes ($\phi \approx \pi$), the amount of $(\phi - \tilde{\phi})$ that can still lead to a contribution to $T(t_p)$ decreases drastically. According to Eq. (7.12), this range is given by

$$|\phi - \tilde{\phi}| < (\alpha t_p)^{-0.5} \ll 1 , \tag{7.13}$$

and does not differ from that of an atom located at a slope of the interference fringes.

To consider what happens to the population correlations when the pulses become time delayed ($t_{12} \neq 0$), we use the model developed in Sec. III, in which, for $0 < t_{12} \ll \alpha_{1,2}^{-1}$, the pulses can be still regarded as fully overlapping and the Rabi frequency, $f(t,\phi)$, is still given by Eq. (7.2). In this model, every two-level atom acquires an additional detuning $h_{\text{ad},3}(\phi) = G(t_{12})(\alpha_1\alpha_2)^{1/2}\sin\phi$; consequently, the second term in Eq. (7.4) is modified, and the condition for atoms to contribute to $T(t_p)$ becomes

$$\tfrac{1}{3}[\sqrt{\alpha(\phi)} - \sqrt{\alpha(\tilde{\phi})}]^2 t_p + \frac{[\delta - \tilde{\delta} + h_{\text{ad},3}(\phi) - h_{\text{ad},3}(\tilde{\phi})]^2 t_p}{3\alpha(\phi)} < 1 . \tag{7.14}$$

The additional ϕ-dependent detuning alters the symmetrical part of the signal since it results in an additional dephasing for atoms having equal detunings $\delta = \tilde{\delta}$. First one notes that the additional detuning varies as $\sin\phi$ (see Fig. 11). This implies that correlations of the type 2 for atoms located at the slopes of the interference fringes are destroyed for relatively small values of t_{12}. For example, for the atoms characterized by $\phi \approx -\tilde{\phi} \approx \pi/2$ and $\phi \approx 2\pi - \tilde{\phi} \approx \pi/2$ the difference in additional detunings [see Eq. (7.14)] is maximal, and the correlation of their populations is already destroyed at $t_{12} \approx \tau_c^{12}/(\alpha_{\min} t_p)^{1/2} \ll \tau_c^{12}$. For larger delay time and pulses having very different intensities, the range $(\phi - \tilde{\phi})$ that contributes to the signal for the atoms located in the vicinity of the extrema of the interference fringes decreases from $(\alpha_{\min} t_p)^{-0.25}$ to $(\alpha_{\min} t_p)^{-0.5}$ as t_{12} varies from 0 to $t_{12} \gg \tau_c^{12}$. For $t_{12} > \tau_c^{12}$ the range $(\phi - \tilde{\phi})$ which contributes to the signal is the same for atoms at the extrema and the slopes of the interference fringes (in contrast to the situation at $t_{12} = 0$). This result also holds for atoms near the maxima in the case of equal pulse intensities. However, the range $(\phi - \tilde{\phi})$ of the correlations for the atoms near the minima ($\phi \approx \pi$) shrinks from the value (7.13) to an even smaller value $\cos(\phi/2)(\alpha t_p)^{-0.5}$.

In general, when $\alpha(\phi) \approx \alpha(\tilde{\phi})$, the detuning term [second term of Eq. (7.14)] leads to eventual decorrelation for $t_{12} \neq 0$. However, for certain unequal detunings $\delta \neq \tilde{\delta}$, this decorrelation can be significantly reduced. If

$$\delta - \tilde{\delta} \approx h_{\text{ad},3}(\tilde{\phi}) - h_{\text{ad},3}(\phi) \tag{7.15}$$

the second term of Eq. (7.14) vanishes and the correlation of the populations coincides with that for the atoms with equal detunings at $t_{12} = 0$. For detunings $\delta \neq \tilde{\delta}$ which satisfy (7.15), there is always a contribution to the asymmetrical part of the signal.

The analysis of the population correlations presented above and the representation of the atomic ensemble as a sum of "maxima" and "minima" subensembles helps to explain the dependence of the signal on time delay t_{12} and grating order N. First, using Eq. (7.7), one can show that, owing to Eqs. (2.19), (2.23), and (6.9), the total PT-3 signals emitted in all directions by these subensembles are given by

$$\sum_{n=-\infty}^{\infty} W_{n,\max}^{(3)} = \sum_{n=-\infty}^{\infty} W_{n,\min}^{(3)} = \tfrac{1}{6} , \tag{7.16}$$

such that the total signal satisfies

$$\sum_{n=-\infty}^{\infty} W_n^{(3)} = \tfrac{1}{3} . \tag{7.17}$$

The sum rules (7.16) and (7.17) are valid independent of the delay time or correlation properties of the pulses. For any given delay time t_{12} and correlation parameter Φ, one can regard $W_{n,\max}^{(3)}$, $W_{n,\min}^{(3)}$, and $W_n^{(3)}$ as some "distribution" functions of the signal intensity relative to N. Consequently, knowledge of $W_n^{(3)}(t_{12})$ for a given n allows one to draw conclusions about $W_n^{(3)}(t_{12})$ for other values of n.

A. Pulses with very different intensities

In this case it has been shown that at $t_{12}=0$ the behavior of $T(t_p)$ in both ("maxima" and "minima") subensembles is identical [see Fig. 12(a)], and thus

$$W^{(3)}_{n,\max}(t_{12}=0)=W^{(3)}_{n,\min}(t_{12}=0)=0.5W^{(3)}_{n}(t_{12}=0)\ ,$$

where, according to Eqs. (2.23) and (2.19), $W^{(3)}_n$ is given by

$$W^{(3)}_n(0)=T^{(n,-n)}(t_p,\delta,\delta)=\frac{1}{4\pi^2}\int_{-\pi/2}^{3\pi/2}d\phi\int_{-\pi/2}^{3\pi/2}d\tilde{\phi}\langle\rho_3(t_p,\phi,\delta)\rho_3(t_p,\tilde{\phi},\delta)\rangle\cos n(\phi-\tilde{\phi})\ . \tag{7.18}$$

The correlation function appearing in Eq. (7.18) is always positive, as is $W^{(3)}_0$. Owing to the oscillatory behavior of $\cos n(\phi-\tilde{\phi})$ for $n\neq 0$ the distribution $W^{(3)}_n(t_{12}=0)$ is a smoothly decreasing symmetrical function of n, characterized by width n_0 with $n_0\gg 1$.

For $t_{12}>0$ the two subensembles lead to the distributions $W^{(3)}_{n,\max}(t_{12})$ and $W^{(3)}_{n,\min}(t_{12})$ which acquire some asymmetry [see Fig. 12(b) and Eq. (7.15)]. However, the asymmetry of the "maxima" distribution is positive $[W^{(3)}_{n,\max}(t_{12})>W^{(3)}_{-n,\max}(t_{12})]$, while that of the "minima" is negative, such that they are exactly compensated in the joint "distribution" $W^{(3)}_n(t_{12})$, which is symmetrical relative to n (and t_{12}).

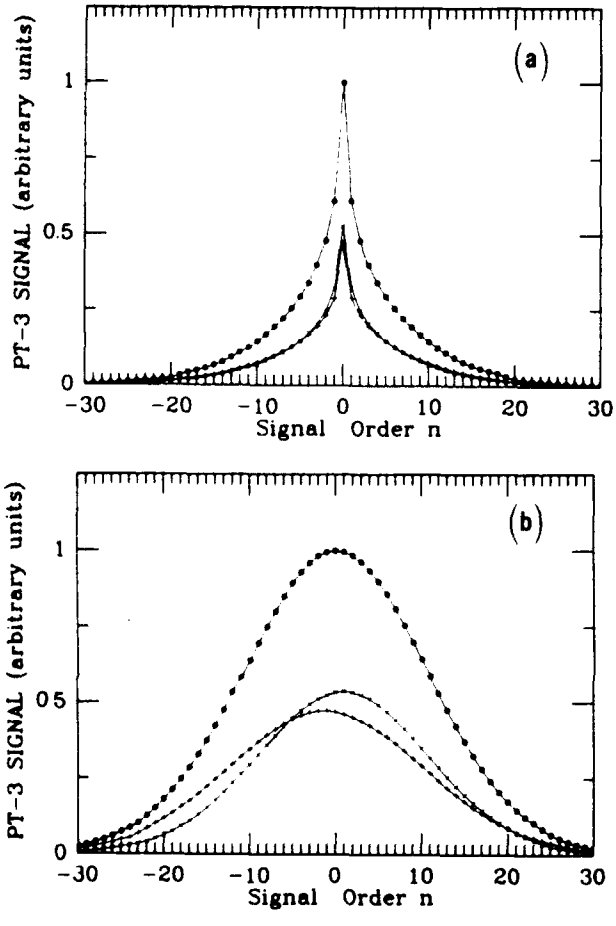

FIG. 12. Distribution of the signal intensity as a function of order N for delay time (a) $t_{12}=0$ and (b) $t_{12}=2\tau_c^{12}$ ●, the total signal intensity $W^{(3)}_n$; +, the signal intensity $W_{n,\min}$ corresponding to the "minima" ensemble; ×, the signal intensity $W_{n,\max}$ corresponding to the "maxima" ensemble ($W^{(3)}_n=W_{n,\min}+W_{n,\max}$). The pulses are fully correlated and have very different intensities: $\Phi=1$, $\alpha_1 t_p=10^4$, $\alpha_2 t_p=10^2$, $\Delta_D t_p=14$.

Some insight into $W^{(3)}_n(t_{12})$ can be obtained by first considering $W^{(3)}_0(t_{12})$. In light of the discussion above about the destruction of correlations with increasing t_{12}, one finds that the signal $W^{(3)}_0(t_{12}\neq 0)<W^{(3)}_0(0)$. When t_{12} becomes larger than τ_c^{12}, only the correlations of the first type survive, and the signal $W^{(3)}_0(t_{12})$ tends to its minimum, $W^{(3)}_0(\infty)$. Thus, the signal $W^{(3)}_0(t_{12})$ exhibits a peak of width τ_c^{12} [see Figs. 8–10 and the discussion that follows Eq. (6.43)].

To see the connection between $W^{(3)}_n(T_{12})$ $(n\neq 0)$ and $W^{(3)}_0(t_{12})$, one can use the fact that in the strong-field regime the number n_0 of the PT-3 signals of comparable intensity is large, and owing to relation (7.17) can be expressed as

$$n_0(t_{12})\sim[W^{(3)}_0(t_{12})]^{-1}\ . \tag{7.19}$$

Since the signal $W^{(3)}_0$ decreases with increasing t_{12}, it follows that n_0 increases with increasing t_{12} (in the limit $\alpha_{1,2}t_{12}\ll 1$ considered in this paper), i.e., $n_0(0)=n_0(t_{12}=0)<n_0(\infty)=n(t_{12}\gg\tau_c^{12})$. Now it is possible to get a qualitative understanding of the dependence of the signal $W^{(3)}_n$ with a given n on t_{12}. As t_{12} varies from 0 to $t_{12}>\tau_c^{12}$, n_0 rises from $n_0(0)$ to $n_0(\infty)$ and the "distribution" function $W^{(3)}_n$ becomes wider and, consequently, lower in the center (small n) and higher at the wings (large n) (see Fig. 12). For fixed $n\lesssim n_0(0)$, $W^{(3)}_n$ decreases with increasing t_{12}, while for $n\gtrsim n_0(\infty)$, the signal $W^{(3)}_n$ increases with increasing t_{12}. Thus in the former case there is a peak centered at t_{12} and in the latter case a dip. In the intermediate range of n, $n_0(0)<n<n_0(\infty)$, the signal first increases and then decreases with increasing t_{12}. For $t_{12}>\tau_c^{12}$ the signal $W^{(3)}_n$ reaches the background value shown in Fig. 12(b). The narrow dip in the central peak that can occur for fully correlated pulses and small n can be traced to the fact that at $t_{12}=0$ the contribution of the correlations of the second type to the signal is negative, and they are destroyed on a time scale $t_{12}\ll\tau_c^{12}$. For example, at $t_{12}=0$ this contribution to the first-order signal $W^{(3)}_1$ is characterized by $(\phi-\tilde{\phi})\approx\pi$ and is negative as $\cos(\phi-\tilde{\phi})\approx -1$ in Eq. (7.18). Since these correlations are destroyed as t_{12}

varies from 0 to $t_{12} \approx \tau_c^{12}/(\alpha_{\min} t_p)^{1/2}$, this leads to the dip in the central peak having this width.

B. Pulses with equal intensities

In this case the behavior of $T(t_p)$ is different for the two subensembles even at $t_{12}=0$ [see Fig. 11(b)], and consequently $W^{(3)}_{n,\max}(t_{12}=0) \neq W^{(3)}_{n,\min}(t_{12}=0)$. As these signals represent Fourier transforms (phase factor $\exp[in(\phi-\tilde{\phi})]$) of $T(t_p)$, and, as discussed previously, the range of $(\phi-\tilde{\phi})$ that contributes to the signal is much narrower for the "minima" subensemble, it follows that the distribution $W^{(3)}_{n,\min}(t_{12}=0)$ over n is much wider and lower than $W^{(3)}_{n,\max}(t_{12}=0)$; that is, $n_{0,\min}(t_{12}=0) \gg n_{0,\max}(t_{12}=0)$ [see Fig. 13(a)]. Hence, $W^{(3)}_{n,\max}(t_{12}=0)$ and $W^{(3)}_{n,\min}(t_{12}=0)$ determines the signals of small and high orders, respectively. As in the case of pulses with very different intensities, the distributions $W^{(3)}_{n,\max}(t_{12})$ and $W^{(3)}_{n,\min}(t_{12})$ acquire some positive and negative asymmetry, respectively, as t_{12} increases. However, the asymmetrical parts of these signals are not canceled in $W^{(3)}_n(t_{12})$. As t_{12} tends from 0 to $t_{12} \gg \tau_c^{12}$, both "distributions" become wider and lower, and the relation $n_{0,\min}(t_{12}) > n_{0,\max}(t_{12})$ is satisfied for any t_{12} [see Fig. 13(b)]. As a result, the signal of small order n is still determined by the "maxima" distribution $[W^{(3)}_n(t_{12}) \approx W^{(3)}_{n,\max}(t_{12})]$ and has positive asymmetry, while that of high order is determined by the "minima" distribution and has negative asymmetry. When the Doppler width is sufficiently large such that

$$\Delta_D \gg \left[\frac{\alpha}{t_p}\right]^{1/2},$$

condition (7.15) can be satisfied in the whole range of $\phi-\tilde{\phi}$ contributing to the signal, and the asymmetry becomes most visible.

In the opposite limiting case of noncorrelated pulses, the position as well as the amplitude of interference fringes varies in time [see Fig. 11(c)]. Therefore only the first type of the population correlations exists at $t_{12}=0$. Moreover, the additional detuning vanishs, and nothing changes for $t_{12} \neq 0$ as compared with the case of zero delay time. As a result, $W^{(3)}_0(t_{12}) \equiv W^{(3)}_0(0)$ and does not vary with t_{12}.

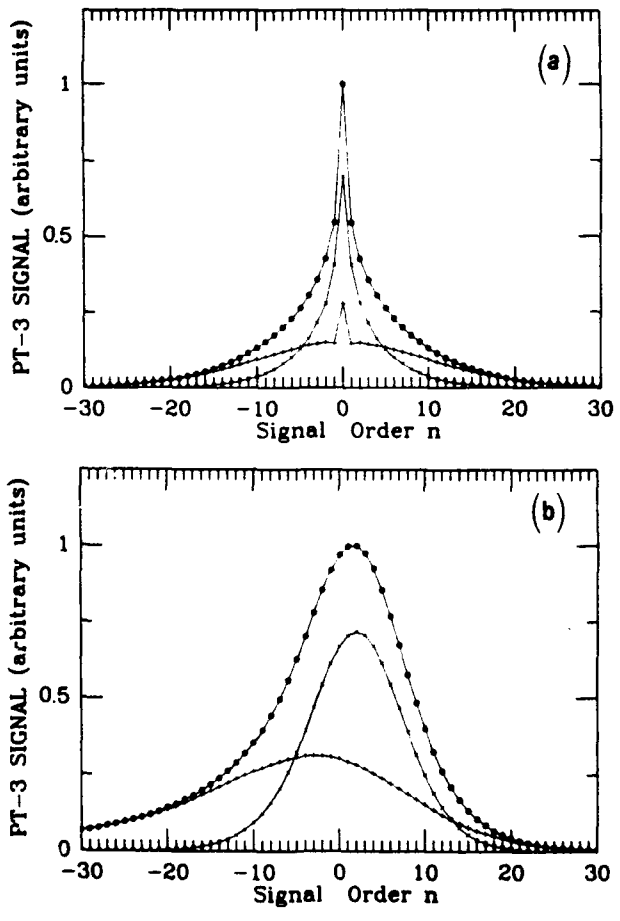

FIG. 13. Distribution of the signal intensity as a function of order n for different delay times: (a) $-t_{12}=0$; (b) $-t_{12}=2\tau_c^{12}$. The fully correlated pulses ($\Phi=1$) have nearly equal intensities ($\alpha_1 t_p=105$, $\alpha_2 t_p=100$), and $\Delta_D t_p=14$. All the notations are the same as in Fig. 12.

C. Dephasing of two Bloch vectors

Up to now, we have been concerned with the signal as a function of t_{12} for fixed t_p. One can also try to understand the qualitative behavior of the correlation function $T(t_p)=\langle \rho_3 \tilde{\rho}_3 \rangle$ as a function of t_p for fixed t_{12}. Explicitly, $T(t_p)=\exp\{\lambda_1 t_p\}/3$ [see Eqs. (6.9) and (6.10)] and leads to all the results for the PT-3 signal discussed in Sec. VI. This correlation function describes the relative dephasing of the components ρ_3 and $\tilde{\rho}_3$ of two Bloch vectors, $\mathbf{R}$ and $\tilde{\mathbf{R}}$, associated with two-level atoms having different velocities and spatial positions, $\mathbf{r}$ and $\tilde{\mathbf{r}}$, such that

$$\delta \neq \tilde{\delta} \quad \text{and} \quad \phi=\phi(\mathbf{r}) \neq \phi(\tilde{\mathbf{r}})=\tilde{\phi}\ . \tag{7.20}$$

To understand the origin of Eq. (6.9), we examine the rotation of $\mathbf{R}$ and $\tilde{\mathbf{R}}$ using the model discussed in Sec. III. We consider the excitation pulses to be fully overlapping and take into account a nonzero delay time by introducing an additional detuning $h_{\mathrm{ad},3}(t_{12},\phi)$ given by Eq. (3.10). It follows from condition (7.20) that, generally speaking, $h_{\mathrm{ad},3} \neq \tilde{h}_{\mathrm{ad},3}$. Hence, even if two atoms have equal velocities, their effective detunings differ if they are located at different spatial points. Moreover, these atoms see different field amplitudes at different spatial locations.

First we consider the Bloch vector $\mathbf{R}$. It rotates with the angular velocity $\mathbf{H}$ given by

$$\mathbf{H}=\begin{vmatrix} X \\ Y \\ -(\delta+h_{\mathrm{ad},3}) \end{vmatrix}, \tag{7.21}$$

[see Eq. (3.6)], where X and Y are the real and imaginary parts of the Rabi frequency $f(t)$ associated with a total electric field, $X+iY=-f(t)$, and the atom-field detuning δ is modified by the addition of $h_{\mathrm{ad},3}$. For the remainder of this section we assume that $\tau_c^{ij}=\tau_c; i,j=1,2$.

Owing to the fluctuating character of the angular ve-

locity components X and Y, the Bloch vector $\mathbf{R}$ rotates randomly and its tip undergoes a fast, random walk movement over the sphere having unit radius. This stochastic movement is superimposed on the free precession of the Bloch vector about the 3 axis with the constant angular velocity $-(\delta+h_{ad,3})$. By moving from the "absolute" reference frame, where the angular velocity is given by $\mathbf{H}$, into the reference frame that rotates about the 3 axis with angular velocity $-(\delta+h_{ad,3})$, one transforms away this regular rotation. In the new reference frame the component of the vector $\mathbf{H}$ along the 3 axis is zero and the X and Y components are modified. However, if

$$(\delta+h_{ad,3})\tau_c \ll 1 , \tag{7.22}$$

the modification of X and Y can be neglected. In the following discussion the analysis of the rotation of the vector $\mathbf{R}$ is carried out with respect to the rotating reference frame.

During time interval τ_c, X, and Y can be considered as constant, and the Bloch vector $\mathbf{R}$ deviates from its initial position $\mathbf{R}(t)$ by a small angle

$$\chi(\tau_c)\sim(X^2+Y^2)^{1/2}\tau_c \ll 1 . \tag{7.23}$$

The rotation occurring within the next interval of duration τ_c is independent of any previous one. According to the random walk model, after m such rotations, at time $t_1=m\tau_c$ the Bloch vector $\mathbf{R}(t+t_1)$ deviates from $\mathbf{R}(t)$ by an angle $\chi(t_1)$ whose mean square is

$$\langle\chi^2(t_1)\rangle=m\langle\chi^2(\tau_c)\rangle\sim 2\alpha(\phi)t_1 . \tag{7.24}$$

From Eq. (7.24) one can see that the Bloch vector loses memory of its initial conditions

$$\mathbf{R}(0)=(0,0,1) \tag{7.25}$$

in a time period of order $[\alpha(\phi)]^{-1}$, when it has rotated by an angle of order unity[44] (see Fig. 14). The criterion (7.23) of the random walk model at the same time justifies application of the decorrelation approximation in solving the Bloch equations (2.10), and leads to the exact solution (5.3) for $\langle\rho_3\rangle$. For $t>[\alpha(\phi)]^{-1}$, the position of the Bloch vector can be regarded as random. For such times, the mean square values of its components are equal, namely

$$\langle\rho_1^2\rangle=\langle\rho_2^2\rangle=\langle\rho_3^2\rangle=\tfrac{1}{3},\quad t>[\alpha(\phi)]^{-1} . \tag{7.26}$$

The second Bloch vector $\tilde{\mathbf{R}}$ has the same initial position (7.25) and undergoes a similar rotation that results in

$$\langle\tilde\rho_1^2\rangle=\langle\tilde\rho_2^2\rangle=\langle\tilde\rho_3^2\rangle=\tfrac{1}{3} \tag{7.27}$$

for times $t>[\alpha(\tilde\phi)]^{-1}$.

To start the analysis of the relative dephasing of $\mathbf{R}$ and $\tilde{\mathbf{R}}$, we first return to the "absolute" reference frame. Because $\mathbf{H}\neq\tilde{\mathbf{H}}$, the tip of the vector $\tilde{\mathbf{R}}$ follows a trajectory that differs from that of the vector $\mathbf{R}$. To find the relative dephasing of the Bloch vectors induced by fluctuations, one first has to eliminate any possible constant angle θ_0 between their projections on the plane defined by the axes 1 and 2. This angles does not affect the populations ρ_3 and $\tilde\rho_3$ and leads only to the constant phase shift between the coherences, $\rho_1+i\rho_2$ and $\tilde\rho_1+i\tilde\rho_2$, of two atoms. The angle θ_0 is given by

$$\theta_0=\langle\arg\tilde f(t)\rangle-\langle\arg f(t)\rangle$$

and can be obtained by the minimization of the expression $\langle|\mathbf{H}-\tilde{\mathbf{H}}_{\theta_0}|^2\rangle$, where $\tilde{\mathbf{H}}_{\theta_0}$ represents the vector $\tilde{\mathbf{H}}$ rotated by the angle θ_0 about the 3 axis. Solving the equation

$$\frac{d}{d\theta_0}\langle|\mathbf{H}-\tilde{\mathbf{H}}_{\theta_0}|^2\rangle=0 \tag{7.28}$$

yields

$$\tan\theta_0=\frac{\alpha_1\sin(\phi-\tilde\phi)+\alpha_{12}(\sin\phi-\sin\tilde\phi)}{\alpha_1\cos(\phi-\tilde\phi)+\alpha_2+\alpha_{12}(\cos\phi-\cos\tilde\phi)} . \tag{7.29}$$

Only after the Bloch vector $\tilde{\mathbf{R}}$ and its angular velocity vector $\tilde{\mathbf{H}}$ are rotated by the angle θ_0, given by Eq. (7.29), about the 3 axis, which is when the rotations

$$\tilde{\mathbf{R}}\rightarrow\tilde{\mathbf{R}}_{\theta_0};\tilde{\mathbf{H}}\rightarrow\tilde{\mathbf{H}}_{\theta_0}$$

are fulfilled, can one say that the remaining divergence of the trajectories of the Bloch vectors represents the process of their relative dephasing.

We need only consider Bloch vectors $\mathbf{R}$ and $\tilde{\mathbf{R}}_{\theta_0}$ whose tips follow close trajectories, since it is only these atoms for which the relative dephasing is sufficiently small for time $t=t_p$ to contribute appreciably to the signal. In the strong-field regime the necessary condition for a slow relative dephasing of the Bloch vector is

$$\alpha(\phi)\approx\alpha(\tilde\phi) . \tag{7.30}$$

Condition (7.30) implies that the two considered atoms are at positions where the intensities of the interference fringes are nearly equal. At time $t\sim[\alpha(\phi)]^{-1}\approx[\alpha(\tilde\phi)]^{-1}\ll t_p$ when conditions (7.26) and (7.27) are already satisfied, but the relative dephasing is still very small, the correlation function $T(t)$ takes the form

$$T(\alpha^{-1})=\langle\rho_3\tilde\rho_3\rangle=\langle\rho_3^2\rangle=\langle\tilde\rho_3^2\rangle=\tfrac{1}{3} . \tag{7.31}$$

For $\alpha^{-1}<t\le t_p$, however, the rotation and, consequently, the process of dephasing of the Bloch vectors continues. As a result, $T(t)$ slowly decreases from $\frac{1}{3}$ and tends towards 0. The question we address is as follows: What is the speed of this process and what is its origin?

By simple geometrical consideration one can show that in the strong-field regime the correlation function $T(t_p)$ is expressed in terms of an internal product of the Bloch vectors $(\mathbf{R}\cdot\tilde{\mathbf{R}})$ as

$$T(t_p)=\tfrac{1}{3}\langle(\mathbf{R}\cdot\tilde{\mathbf{R}})\rangle . \tag{7.32}$$

Equation (7.32) implies that it is convenient to analyze the relative dephasing of the Bloch vectors in a reference frame which we call the "R" frame, tied to the vector $\mathbf{R}$, rather than in the "absolute" frame where both of the vectors are rotating. In the absolute frame each of the three axes of the R frame rotates with the angular velocity $\mathbf{H}$ and at $t=0$ coincides with a corresponding axis of

the absolute frame, that is,

$$\dot{\mathbf{M}}_i=[\mathbf{H}\mathbf{M}_i];\ |\mathbf{M}_i|^2=1\ ,\qquad m_{ji}(0)=\delta_{ji},\ \ j,i=1,2,3\ , \tag{7.33}$$

where the unit vector $\mathbf{M}_i$ with coordinates (m_{1i},m_{2i},m_{3i}) determines direction of the i axis of the R frame at time t. All three vectors $\mathbf{M}_{1,2,3}$ undergo random rotation, remaining perpendicular to each other (see Fig. 14). It has been shown[44] that for $t\gg[\alpha(\phi)]^{-1}$ their coordinates have the following correlations:

$$\langle m_{ji}(t)m_{j'i'}(t-\tau)\rangle=\tfrac{1}{3}\delta_{jj'}\delta_{ii'}\times\begin{cases}e^{-\alpha(\phi)|\tau|} & \text{if } j=1,2\\ e^{-2\alpha(\phi)|\tau|} & \text{if } j=3\ ,\end{cases} \tag{7.34}$$

where the quantity $[\alpha(\phi)]^{-1}$ plays the role of a correlation time.

The vector $\mathbf{R}$ coincides with the 3 axis $\mathbf{M}_3$ of the R frame and, in this frame, is given by $\mathbf{R}_R=(0,0,1)$ at any time, where the script R means that a vector is considered in the R frame. Then, $T(t_p)$ given by Eq. (7.32) transforms into

$$T(t_p)=\tfrac{1}{3}\langle\tilde{\rho}_{R3}\rangle\ , \tag{7.35}$$

where $\langle\tilde{\rho}_{R3}\rangle$ is the average third component of $\tilde{\mathbf{R}}_R$. Thus, the two-atom correlation function in the absolute frame is now expressed in terms of the averaged component of the single Bloch vector in the R frame. Rotation of this vector takes the form

$$\dot{\tilde{\mathbf{R}}}_R=[\delta\mathbf{H}_R\tilde{\mathbf{R}}_R];\delta\mathbf{H}_R=(\tilde{\mathbf{H}}_{\theta_0}-\mathbf{H})_R\ . \tag{7.36}$$

According to Eq. (7.33), the components δh_{Ri} of the vector $\delta\mathbf{H}_R$ are given by

$$\delta h_{Ri}=\sum_{j=1}^{3}m_{ji}(\tilde{\mathbf{H}}_{\theta_0}-\mathbf{H})_j \tag{7.37}$$

and $\delta\mathbf{H}_R$ represents the vector $(\tilde{\mathbf{H}}_{\theta_0}-\mathbf{H})$ that undergoes some additional random rotation. This rotation is inverse to that of the Bloch vector $\mathbf{R}$ in the absolute frame and is described by characteristic time $\sim[\alpha(\phi)]^{-1}$ [see Eq. (7.34)]. All the components of the vector $\delta\mathbf{H}_R$ are fluctuating quantities, and using Eqs. (7.37) and (7.34) one obtains their correlation functions:

$$\langle\delta h_{Ri}(t)\delta h_{Rj}(t-\tau)\rangle=\tfrac{1}{3}\delta_{ij}\{\langle[f(t)-f_{\theta_0}(t)][f^*(t-\tau)-f^*_{\theta_0}(t-\tau)]\rangle+(\delta_-+h_{\mathrm{ad},3}-\tilde{h}_{\mathrm{ad},3})^2e^{-2\alpha(\phi)|\tau|}\},t\gg\alpha(\phi)\ . \tag{7.38}$$

One can see from Eq. (7.38) that fluctuations of the angular velocity vector in the "R" frame are characterized by two correlation times: the time τ_c of the Rabi frequency fluctuations and the time $[2\alpha(\phi)]^{-1}$ associated with random rotation of the component $-(\delta_-+h_{\mathrm{ad},3}-\tilde{h}_{\mathrm{ad},3})_R$ of the vector $\delta\mathbf{H}_R$, the latter time being much larger than τ_c.

Since the dephasing of the Bloch vectors is assumed to be slow relative to their random rotation, $\tilde{\mathbf{R}}_R$ varies only slightly in time $[2\alpha(\phi)]^{-1}$. As $[2\alpha(\phi)]^{-1}$ is the largest correlation time of the fluctuating vector $\delta\mathbf{H}_R$, under this condition the random rotation of the vector $\tilde{\mathbf{R}}_R$ can be considered to be of the random walk character, and the decorrelation approximation can be used in solving Eq. (7.36) [see discussion of Eq. (7.23)]. The third component of the vector $\langle\tilde{\mathbf{R}}_R\rangle$ is then given by

$$\langle\tilde{\rho}_{R3}(t_p)\rangle=e^{-\mu t_p}\ , \tag{7.39}$$

where

$$\mu=2\int_0^\infty\sum_{i=1}^{2}\langle\delta h_{Ri}(t)\delta h_{Ri}(t-\tau)\rangle d\tau\ . \tag{7.40}$$

The speed of dephasing μ can be represented as

$$\mu=\mu_f+\mu_\delta\ , \tag{7.41}$$

where μ_f describes the dephasing induced by fast fluctuations of $\delta\mathbf{H}_R$ (correlation time τ_c), while μ_δ originates from relatively slow fluctuations with correlation time $[2\alpha(\phi)]^{-1}$. Using Eq. (7.38), for μ_f one obtains

$$\mu_f=\tfrac{2}{3}\int_0^\infty\langle[f(t)-f_{\theta_0}(t)][f^*(t-\tau)-f^*_{\theta_0}(t-\tau)]\rangle d\tau\ . \tag{7.42}$$

Carrying out the averaging in Eq. (7.42) and using the expression (7.20) for θ_0 yields

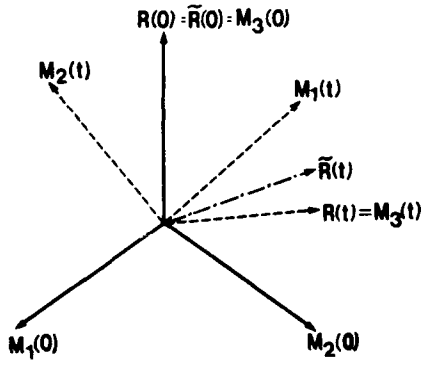

FIG. 14. The positions of the axes $\mathbf{M}_{1,2,3}$ of the "R" frame, tied to the Bloch vector $\mathbf{R}$ ($\mathbf{R}\equiv\mathbf{M}_3$), for time $t=0$ (the solid arrows), and after random rotation, for $t\neq0$ (the dashed arrows). The initial position of the Bloch vector $\tilde{\mathbf{R}}$ coincides with $\mathbf{R}(0)$. However, for time $t\neq0$, owing to difference in angular velocities, $\dot{\tilde{\mathbf{R}}}(t)$ depicted by the dot-dashed arrow is not equal to $\dot{\mathbf{R}}(t)$.

$$\mu_f=\frac{2\{2\alpha_1\alpha_2[1-\cos(\phi-\tilde{\phi})]-\alpha_{12}^2(\sin\phi-\sin\tilde{\phi})^2\}}{3[\alpha_1+\alpha_2+\alpha_{12}(\cos\phi+\cos\tilde{\phi})]} . \tag{7.43}$$

The second part of μ,μ_δ, is given by

$$\mu_\delta=\tfrac{2}{3}(\delta_-+h_{\mathrm{ad},3}-\bar{h}_{\mathrm{ad},3})^2\int_0^\infty e^{-2\alpha(\phi)\tau}d\tau$$
$$=\frac{2[\delta_-+G(t_{12})\alpha_{12}(\sin\phi-\sin\tilde{\phi})]^2}{3[\alpha_1+\alpha_2+\alpha_{12}(\cos\phi+\cos\tilde{\phi})]} , \tag{7.44}$$

where we take into account condition (7.30).

From Eqs. (7.35), (7.39), and (7.41) one finally obtains the correlation function $T(t_p)$ in the form

$$T(t_p)=\tfrac{1}{3}\exp[-(\mu_f+\mu_\delta)t_p] . \tag{7.45}$$

Expression (7.45) coincides with (6.9), since $(\mu_f+\mu_\delta)$ given by Eqs. (7.43) and (7.44) is equal to $-\lambda_1$ given by Eq. (6.10). The part of λ_1 which is independent of δ_- and $G(t_{12})$ coincides with μ_f, while the terms that depend on these parameters are contained in μ_δ.

Since we consider the limiting case where the relative dephasing of the Bloch vectors is a slow process compared with their random rotation, inequality

$$\mu_f,\mu_\delta \ll 2\alpha(\phi)t_p, 2\alpha(\tilde{\phi})t_p \tag{7.46}$$

must be satisfied, a condition equivalent to Eq. (C5).

VIII. QUANTITATIVE RESULTS IN A STRONG-RELAXATION LIMIT $\gamma_T T_p \gg 1$

In this section we calculate the PT-3 signal under conditions when relaxation plays an essential role in signal formation. It is assumed that

$$\gamma_t \gg t_p^{-1},(t_{13}-t_{12}-t_p)^{-1}\gg\gamma_l . \tag{8.1}$$

The condition $\gamma_l(t_{13}-t_{12}-t_p)\ll 1$ insures that the signal is not seriously attenuated in a time period between the second and the third pulses. At the same time, the condition $\gamma_t t_p \gg 1$ guarantees that relaxation of atomic coherence plays an essential role during the excitation pulses. The latter condition can result from pressure broadening produced by a buffer gas.

A. Weak-field regime

In a weak-field regime (6.2) and under condition (8.1) the strongest signal is of order $n=\pm 1$. One can use Eq. (2) to obtain the needed Fourier component in the form

$$T^{(1,-1)}(t_p)=\alpha_{12}^2 t_p^2+\frac{2\alpha_1\alpha_2\gamma_t t_p}{4\gamma_t^2+\delta_-^2} . \tag{8.2}$$

In the strong-relaxation limit, Eq. (2.23) is no longer valid, and the PT-3 signal must be obtained directly from Eqs. (2.14) and (8.2). Integrating over $\delta_\pm$ in Eq. (2.14), one arrives at the signal

$$W_n^{(3)}=K_0\alpha_{12}^2 t_p^2+\frac{K_1\alpha_1\alpha_2 t_p}{2\gamma_t} , \tag{8.3}$$

where

$$K_0=\exp\left[\frac{2\gamma_t^2}{\Delta_D^2}\right]\left[1-\mathrm{erf}\left[\frac{\gamma_t\sqrt{2}}{\Delta_D}\right]\right] ,$$
$$K_1=\frac{1}{2}\left[1-\frac{4\gamma_t^2}{\Delta_D^2}\right]K_0+\frac{\gamma_t}{\Delta_D}\sqrt{2/\pi} . \tag{8.4}$$

Similar to the signal in the weak-relaxation limit [see Eq. (6.7)], the signal (8.3) does not depend on the delay time. However, in contrast to that case, the first term in Eq. (8.3), which depends on the correlation of the pulses and is proportional to the square of the mean amplitude $\rho^{(1)}(t_p)$ of the population difference grating, can be much larger than the second term proportional to $\alpha_1\alpha_2$, which is independent of this correlation and originates from the stochastic part of the grating.

B. Moderate and strong-field regimes

If the intensity of the pulses increases so that $\alpha_{\max}t_p \geq 1$, the correlation function $T(t_p)$ is given by

$$T(t_p)=e^{-2xt_p}\left[1+\frac{8|Q|^2\gamma_t t_p}{4\gamma_t^2+\delta_-^2}\right]+T_0 , \tag{8.5}$$

where x and Q are defined in Eqs. (4.5) and (4.6) and we neglect all the terms leading to minor contributions to the PT-3 signal. Using Eqs. (2.19), (2.14), and (8.5) one obtains the PT-3 signal

$$W_n^{(3)}=e^{-2(\alpha_1+\alpha_2)t_p}\left[K_0 I_n^2(\zeta)+\frac{K_1 t_p}{2\gamma_t}\{\alpha_1\alpha_2[I_{n+1}^2(\zeta)+I_{n-1}^2(\zeta)]+(\alpha_1^2+\alpha_2^2+2\alpha_{12}^2)I_n^2(\zeta)\right.$$
$$\left.+2\alpha_{12}^2 I_{n-1}(\zeta)I_{n+1}(\zeta)-2\alpha_{12}(\alpha_1+\alpha_2)I_n(\zeta)[I_{n-1}(\zeta)+I_{n+1}(\zeta)]\}\right]+O\left[\frac{\gamma_t^2}{\alpha_{\max}\gamma_t}\right] , \tag{8.6}$$

where I_n is a modified Bessel function and $\zeta=2\alpha_{12}t_p$. The last term in Eq. (8.6), proportional to γ_l^2, is contributed by the steady-state solution T_0, and should be taken into account only when the rest of the signal vanishes.

When the intensity of the pulses increases, so that a strong-field regime (6.8) is realized, two very different situations may occur, depending on the degree of the mutual correlation of the pulses and their intensities.

If the pulses are almost fully correlated and have almost equal intensities ($\alpha_1\approx\alpha_2\approx\alpha_{12}=\alpha$), so that condition (6.52) is satisfied, the first term in Eq. (8.6) dominates, and the PT-3 signal is given by

$$W_n^{(3)}=K_0\frac{\exp(-n^2/2\alpha t_p)}{4\pi\alpha t_p}e^{-2(\alpha_1+\alpha_2-2\alpha_{12})t_p} . \quad (8.7)$$

The signal (8.7) does not exhibit any dependence on delay time t_{12} and for $n\ll\sqrt{\alpha t_p}$ it represents a plateau of height $(4\pi\alpha t_p)^{-1}$, provided $\alpha t_{12}\ll 1$. The PT-3 signal (8.7) is completely determined by the mean amplitude of the population grating, since

$$W_n^{(3)}=K_0\rho^2(n) . \quad (8.8)$$

In contrast with the results in a weak-relaxation limit (see discussion at the end of Sec. VI), when $\gamma_t t_p\gg 1$, the stochastic contribution to the population grating is effectively suppressed, while the mean amplitude is not effected by the relaxation of atomic coherence. Transition from the weak-relaxation limit to the strong-relaxation one is shown in Fig. 15.

For noncorrelated pulses or correlated pulses with very different intensities, condition

$$\alpha_1+\alpha_2\gg 2\alpha_{12}, t_p^{-1} \quad (8.9)$$

is satisfied, and the terms which are proportional to K_0 and K_1 in Eq. (8.6) become exponentially small. In the limit (8.9), which we examine for the remainder of this section, the signal is solely determined by the contribution from the steady-state solution T_0.

For moderate field intensities

$$t_p^{-1}\ll\alpha_{\max}\ll\gamma_t \quad (8.10)$$

one can approximate

$$T(t_p)\approx T_0=\frac{\gamma_l^2}{(\alpha_1+\alpha_2)^2}\left[1-\frac{2\alpha_{12}}{\alpha_1+\alpha_2}(\cos\phi+\cos\tilde{\phi})+\frac{4\alpha_{12}^2}{(\alpha_1+\alpha_2)^2}\cos\phi\cos\tilde{\phi}+\frac{8|Q|^2\gamma_t}{(\alpha_1+\alpha_2)(4\gamma_t^2+\delta_-^2)}\right] . \quad (8.11)$$

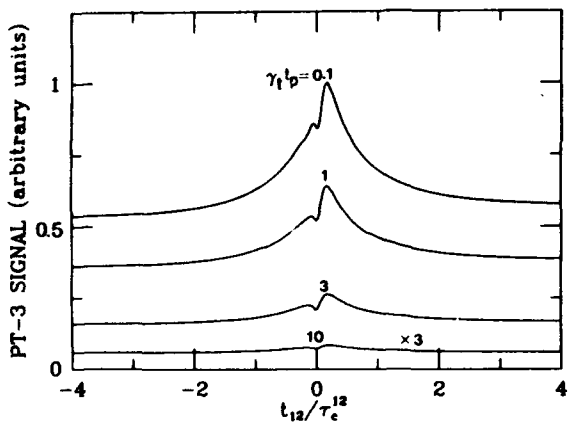

FIG. 15. Signals of order $n=1$ vs t_{12}/τ_c^{12} for different transverse relaxation parameter $\gamma_t t_p$ in the case of weak longitudinal relaxation: $\gamma_t t_p=0.2$. The fully correlated ($\Phi=1$) pulses have nearly equal intensities $\alpha_1 t_p=100$, $\alpha_2 t_p=105$, and $\Delta_D t_p=14$.

The strongest signal occurs for orders $n=\pm 1$. Picking up the terms proportional to $\exp[i(\phi-\tilde{\phi})]$ and integrating over $\delta_\pm$ in Eq. (2.14), one finds the PT-3 signal

$$W_{\pm 1}^{(3)}=\frac{\gamma_l^2}{(\alpha_1+\alpha_2)^2}\left[\frac{K_0\alpha_{12}^2}{(\alpha_1+\alpha_2)^2}+\frac{2K_1\alpha_1\alpha_2}{(\alpha_1+\alpha_2)\gamma_t}\right] , \quad (8.12)$$

which exhibits no dependence on delay time.

However, when the pulses become very strong,

$$\alpha_1+\alpha_2\gg\alpha_{12},\gamma_1 , \quad (8.13)$$

one has

$$T(t_p)=T_0=\frac{\gamma_l^2}{y+\delta_f^2+x\gamma_t} . \quad (8.14)$$

It is shown below that in the regime (8.13), which can be interpreted as a strong-field regime in a strong-relaxation limit, the correlation function (8.14) leads to the PT-3 signal whose dependence on delay time resembles very much that in a strong-field regime in a weak-relaxation limit. Integrating over ϕ_- in Eq. (2.19) and over $\delta_\pm$ in Eq. (2.14) yields

$$W_n^{(3)}=\frac{2K_0\gamma_l^2}{\pi\gamma_t(\alpha_1+\alpha_2)}\times\int_0^{\pi/2}\frac{\{1+Y^{-1}-[(1+Y^{-1})^2-1]^{1/2}\}^n}{\sqrt{1+2Y}}d\phi_+ , \quad (8.15)$$

where

$$Y=2\eta_\gamma^2[1-\Phi(1-G^2)\cos^2\phi_+] ,$$
$$\eta_\gamma=\left[\frac{\alpha_1\alpha_2}{(\alpha_1+\alpha_2)\gamma_t}\right]^{1/2} . \quad (8.16)$$

For one strong and one weak pulse,

$$\alpha_{\min}\ll\gamma_t\ll\alpha_{\max} ,$$

it follows that $Y\ll 1$ in Eq. (8.15), so that the signal can be approximated as

$$W_n^{(3)}=\frac{2K_0\gamma_l^2\alpha_{\min}}{\gamma_t^2\alpha_{\max}}[2-\Phi(1-G^2)] . \quad (8.17)$$

The signal (8.17) has the same dependence on the correlation and delay times as the weak-relaxation limit signal (6.14), but it is much weaker.

If both pulses are strong, that is if

$$\alpha_1,\alpha_2\gg\gamma_t , \quad (8.18)$$

the main contribution to the integral in Eq. (8.15) comes from the regions where $Y\gg 1$, and for $n\neq 0$, Eq. (8.15) can be transformed into

$$W_n^{(3)}=\frac{2K_0\gamma_l^2}{\pi\gamma_t(\alpha_1+\alpha_2)}\int_0^{\pi/2}\frac{\exp(-n\sqrt{2}/\sqrt{Y})}{\sqrt{2Y}}d\phi_+ . \quad (8.19)$$

The integral in Eq. (8.19) can be estimated by the same

method used to approximate the integral in Eq. (D7). The strongest signal, characterized by small n, $n \ll \eta_\gamma$, for strongly correlated pulses $(1-\Phi \ll 1)$ exhibits a symmetrical peak centered at $t_{12}=0$. The signal intensity for $t_{12} \leq \tau_c^{12}$ is given by

$$W_n^{(3)} = \frac{K_0 \gamma_l^2}{\pi(\alpha_1+\alpha_2)\gamma_t \eta_\gamma} \times \ln \frac{2\eta_\gamma}{n[\exp(-Z/2)+\sqrt{Z+\exp(-Z)}]} , \quad (8.20)$$

where

$$Z = \frac{[1-\Phi(1-G^2)]\eta_\gamma^2}{n^2} . \quad (8.21)$$

If one compares Eqs. (8.20) and (6.29), one finds that the signals in the strong-relaxation and in the weak-relaxation limits are similar, if $\alpha_{\max} \gg \alpha_{\min}$ (see Fig. 16). The peak has width $|t_{12}| \approx \tau_c^{12}$ and for fully correlated pulses ($\Phi=1$), is approximately $\ln(\eta_\gamma/n)$ times higher than the background signal

$$W_n^{(3)} = \frac{K_0 \gamma_l^2}{\pi(\alpha_1+\alpha_2)\gamma_t \eta_\gamma} , \quad (8.22)$$

which would be obtained for non-correlated pulses ($\Phi=0$).

The signal of higher order $n > \eta_\gamma \gg 1$, is given by

$$W_n^{(3)} = \frac{2K_0 \gamma_l^2}{\pi(\alpha_1+\alpha_2)\gamma_t \eta_\gamma} \exp\left[-\frac{n[4+\Phi(1-G^2)]}{4\eta_\gamma}\right] \times I_0\left[\frac{n\Phi(1-G^2)}{4\eta_\gamma}\right] . \quad (8.23)$$

For fully correlated pulses the signal (8.23) exhibits a profound dip centered at $t_{12}=0$, and for $|t_{12}| > \tau_c^{12}$ it coincides with the signal for noncorrelated pulses.

One can see from the results presented above, that under condition (8.13) the PT-3 signal in the strong-relaxation regime resembles that in the weak-relaxation time, attenuated approximately by a factor

$$\frac{3\sqrt{2\pi}K_0\gamma_l^2}{2\gamma_t(\alpha_1+\alpha_2)} \ll 1 ; \quad (8.24)$$

while the parameter $3(4\gamma_t)^{-1}$ plays the role of the effective pulse duration.

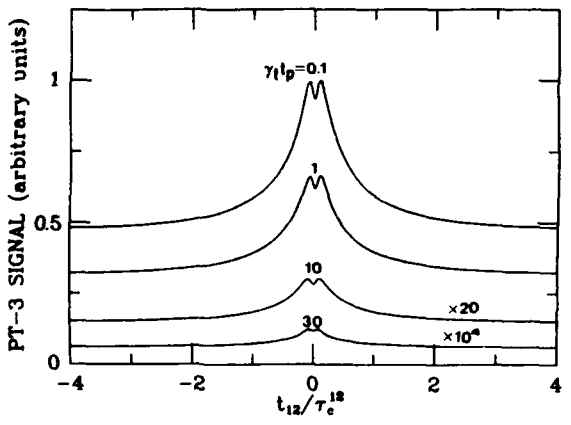

FIG. 16. Signals of order $n=1$ vs t_{12}/τ_c^{12} for different transverse relaxation parameter $\gamma_t t_p$ and a small longitudinal relaxation parameter: $\gamma_l t_p = 0.2$. The fully correlated ($\Phi=1$) pulses have very different intensities $\alpha_1 t_p = 100$, $\alpha_2 t_p = 10^4$, and $\Delta_D t_p = 14$.

IX. SUMMARY AND DISCUSSION

In this paper we have considered pulses with rectangular envelopes; that is, rise and fall times t_r and t_f of the pulses have been assumed to be negligible:

$$t_r = t_f = 0 . \quad (9.1)$$

If one takes into account nonzero values of t_r and t_f, one sees that, for the symmetrical part of the signal, W_S, generalization of the results obtained in Sec. VI is straightforward. Since W_S is proportional to $T^{(n,-n)}(t_p,\delta,\delta)$, one can show that all the results for W_S remain valid provided that the substitution

$$\alpha_{ii} t_p \Rightarrow \int_{-\infty}^{+\infty} \alpha_{ii}(t)dt \quad (9.2)$$

is made. Thus, the results leading to nearly symmetrical signals can be still used. However, the asymmetrical part of the signal may undergo serious charge, if $t_r, t_f > \alpha^{-1}, \Delta_D^{-1}$. In this case the effective range of detunings that can contribute to the signal narrows from Δ_D to $\min(t_r^{-1}, t_f^{-1})$. As a result, the parameter D increases:

$$D = \frac{3(\alpha_1+\alpha_2)}{4\Delta_D^2 t_p} \Rightarrow D \sim \frac{(\alpha_1+\alpha_2)\max(t_r^2, t_f^2)}{t_p} , \quad (9.3)$$

and asymmetry of the signal up to order $n = \alpha \max(t_r, t_f)$ is suppressed [see Eqs. (36) and (38)]. If $\max(t_r, t_f) \sim t_p$, signals of all orders become symmetrical.

It has been shown in Sec. VI that in a weak-relaxation limit the PT-3 signal in many cases depends only weakly on correlation properties of the pulses when $|t_{12}| > \tau_c^{12}$. This effect, however, cannot be interpreted as a loss of memory of the pulse correlations by the two-level atoms. This memory is preserved, if $\alpha|t_{12}| \ll 1$, and can be revealed under certain conditions, as in the case of the signals of high orders induced by excitation pulses having equal intensities. The origin of the Φ independence of the PT-3 signal for $|t_{12}| > \tau_c^{12}$ can be related to the fact that the third pulse is weak and noncorrelated with the first two. As a result, in the weak-relaxation and the strong-field limit, different velocity groups of atoms contribute to the signal independently [$W_n^{(3)} \approx T(t_p,\delta,\delta)$]. It will be shown elsewhere that in the case of two-pulse transients, when the atoms with different velocities might contribute to the signal coherently, the difference in the signals for correlated and noncorrelated pulses for $|t_{12}| > \tau_c^{12}$ can be significant.

In summary, we have studied the three-pulse optical coherent transients induced by broad-bandwidth pulses. Within the approximation of a small delay time between

the first two excitation pulses, we have considered, analytically and numerically, different values for the pulse intensities, relaxation times, and Doppler width. It was shown that if the intensities of the excitation pulses are high enough, stochastic spatial gratings of many orders can be created in the population difference of two-level atoms and the signals with comparable energies might be emitted in many directions. These signals, as functions of the delay time, can vary significantly on the time scale of the cross-correlation time τ_c^{12} of the pulses, provided the relaxation processes in the atomic vapor are negligible on this time scale. We predict that the signal for order $n \ll (\alpha_{\min} t_p)^{1/2}$ as a function of delay time exhibits a peak having width $|t_{12}| \sim \tau_c^{12}$. When the pulses are strongly correlated and their intensities are not equal, this peak has a very narrow dip at $t_{12}=0$ whose width is much smaller than τ_c^{12}. The signals of higher order can exhibit either a dip or a considerable negative asymmetry depending on the Doppler width of the atomic ensemble and ratio of intensities of the excitation pulses. All these features occur for strongly correlated pulses, when $\alpha_{\min} t_p > 1$.

For a two-level atom driven by two arbitrary pulses with delay time t_{12} satisfying $|t_{12}| \ll \alpha_{\max}$, we have shown that the final position of its Bloch vector can be described as a result of rotation performed under the influence of two fully overlapping pulses that coincide with the original pulses. However, as a result of this transformation, an additional fluctuating detuning parameter appears in the Bloch equations, which is the only effect of the time delay of the pulses. We have interpreted the obtained results by using this model.

If the relaxation cannot be neglected and the signal is detectable ($T_2 < t_p < T_1$), the signal, induced by fully correlated pulses with equal intensities, is much stronger than in all other cases and does not show any dependence on delay time. If the intensities are different, the PT-3 signal exhibits a profile which resembles that in a weak-relaxation regime; however, the signal is much weaker.

The experiments performed on different atomic vapors indicate that the PT-3 signal is very sensitive to the atomic level structure, which is usually much more complicated than a two-level system. The only experiment,[15] of which we are aware, where the active atoms could be realistically approximated as a two-level system, revealed direct dependence of the signal on τ_c^{12} in the case when one of the pulses was strong. Extension of this work to the case of two strong pulses would allow for a more complete test of our results.

ACKNOWLEDGMENTS

We would like to thank J.-L. Le Gouët and J.-C. Keller for many useful discussions. This research is supported by the U.S. Office of Naval Research and the National Science Foundation under Grant No. INT88015036.

APPENDIX A: GENERAL EXPRESSION FOR THE PT-3 SIGNAL

The energy $\mathcal{W}_n^{(3)}$ of the PT-3 signal radiated in the direction $\mathbf{k}_3 + n\mathbf{k}_d$ under the influence of the third pulse that starts at time t_3, $t_3 = t_{12} + t_{23}$, and has duration t_{3p} can be defined as[12]

$$\mathcal{W}_n^{(3)} = C(\Delta_D^2 \pi)^{-1} \int\int \psi(\delta-\Delta)\psi(\bar{\delta}-\Delta) \left| \int_{t_3}^{\infty} \langle \rho_{ab}^{(n)}(t;\delta)\rho_{ab}^{(-n)}(t;\bar{\delta})\rangle dt \right| d\delta\, d\bar{\delta} , \tag{A1}$$

where C is a constant. The third pulse is weak, and therefore a component $\rho_{ab}^{(n)}$ of the atomic coherence ρ_{ab} satisfies the equation

$$\dot{\rho}_{ab}^{(n)} = -(\gamma_t + i\delta)\rho_{ab}^{(n)} + i f_3 \rho_3^{(n)}(t_p^0) e^{-\gamma_t (t - t_p^0)} , \tag{A2}$$

where

$$\rho_{ab}(\mathbf{r}) = \sum_n \rho_{ab}^{(n)} e^{i(\mathbf{k}_3 + n\mathbf{k}_d)\mathbf{r}}, \quad f_3 = \mu_{ab}\hbar^{-1}\mathcal{E}_3(t) . \tag{A3}$$

Substituting the solution of Eq. (A2) into Eq. (A1), one has

$$\begin{aligned} \mathcal{W}_n^{(3)} = C(\Delta_D^2 \pi)^{-1} \int\int \psi(\delta-\Delta)\psi(\bar{\delta}-\Delta) \\ \times \left| \int_0^{\infty} dt \int_0^t dt' \int_0^t dt'' \langle f_3(t'+t_3) f_3^*(t''+t_3) \right. \\ \times e^{-\gamma_t (t_{13} - t_p^0 + t' + t'') - (i\delta + \gamma_t)(t-t') - (-i\bar{\delta} + \gamma_t)(t-t'')} \\ \left. \times \rho_3^{(n)}(t_p^0;\delta)\rho_3^{(-n)}(t_p^0;\bar{\delta})\rangle \right| d\delta\, d\bar{\delta} . \end{aligned} \tag{A4}$$

Since the third pulse is not correlated with the first two excitation pulses, averaging in Eq. (A4) can be carried out separately for $f_3(t'+t_3)f_3^*(t''+t_3)$ and $\rho_3^{(n)}(t_p^0;\delta)\rho_3^{(-n)}(t_p^0;\bar{\delta})$. Using the approximation of δ-correlated fluctuations for the third pulse,

$$\langle f_3(t'+t_3) f_3^*(t''+t_3)\rangle = \alpha_3 \delta(t'-t'') , \tag{A5}$$

where $0<t', t''<t_{3p}$, and $\alpha_3=\langle|f_3|^2\rangle\tau_c^{33}$, and integrating over t'', t, and t' in Eq. (A4), one finally gets the expression

$$\mathcal{W}_n^{(3)}=C(2\gamma_l\Delta_D^2\pi)^{-1}\alpha_3(1-e^{-2\gamma_l t_{3p}})e^{-2\gamma_l(t_{13}-t_p^0)}\int\int\frac{\psi(\delta-\Delta)\psi(\bar{\delta}-\Delta)}{2\gamma_t+i\delta_-}\langle T_{33}^{(n,-n)}(t_p^0;\delta,\bar{\delta})\rangle d\delta\, d\bar{\delta}\ . \tag{A6}$$

Introducing $W_n^{(3)}$ by the relation

$$W_n^{(3)}=[C\sqrt{\pi}\alpha_3(1-e^{-2\gamma_l t_{3p}})]^{-1}2\gamma_l\Delta_D e^{2\gamma_l(t_{13}-t_p^0)}\mathcal{W}_n^{(3)}\ , \tag{A7}$$

one obtains Eq. (2.14).

APPENDIX B: EXPRESSION FOR $T^{(1,-1)}(t)$ IN A WEAK-FIELD REGIME

In a weak-field regime

$$\alpha_1,\alpha_2\ll\max[t_p^{-1},\min(\gamma_l,\gamma_t)] \tag{B1}$$

perturbation theory can be applied in Eqs. (4.1)–(4.3). This is more convenient than taking the weak-field limit of the general solution (5.4). The population gratings of order ±1 dominate the process and lead to the signals of equal intensity. Iterating Eqs. (4.1)–(4.3) twice yields

$$T(t;1,-1)=\frac{\alpha_{12}^2}{\gamma_l^2}(1-e^{-\gamma_l t})^2+2\alpha_1\alpha_2\int_0^t\int_0^{t'}e^{-2\gamma_l(t-t')-2\gamma_t(t'-t'')}\times\cos\delta_-(t'-t'')dt'dt''\ . \tag{B2}$$

In a weak-relaxation limit (6.1), one obtains Eq. (6.3). In the case of strong transverse relaxation (8.1), Eq. (B2) leads to Eq. (8.2).

APPENDIX C: EXPRESSION FOR $T(t_P)$ IN A WEAK-RELAXATION LIMIT IN A STRONG-FIELD REGIME

In a weak-relaxation limit (6.1) the solution (5.4) is given by

$$T(t_p)=\sum_{i=1}^{3}e^{\lambda_i t_p}T_i\ , \tag{C1}$$

where the exponents $\lambda_{1,2,3}$ are the roots of the equation

$$\lambda(\lambda+x)(\lambda+3x)=-2y(\lambda+x)-\delta_f^2(\lambda+2x)\ . \tag{C2}$$

At time t_p, only those atoms whose Bloch vectors have not dephased contribute to the signal. In the weak-relaxation limit, the main contributions to the integral (2.19) come from those regions $(\phi,\bar{\phi})$, where solution (C1) is not exponentially small, that is, where at least one of the indexes λ_i satisfies the condition

$$\lambda_i t_p\ll1\ . \tag{C3}$$

If the pulses are not fully correlated or their intensities are not very close to each other, i.e., if

$$(\alpha_1+\alpha_2-2\alpha_{12})t_p\gg1\ , \tag{C4}$$

the regions in the plane $(\phi,\bar{\phi})$ that satisfy requirement (C3) are defined by condition

$$\sqrt{y},\delta_f\ll x\ . \tag{C5}$$

Then the roots of Eq. (C2) are given by

$$\lambda_1=-\frac{2(y+\delta_f^2)}{3x}\ ,\qquad \lambda_2\approx-x,\quad \lambda_3\approx-3x \tag{C6}$$

with $T_{1,2,3}$ being being equal to

$$T_1\approx\tfrac{1}{3},|T_2|\ll1,T_3\approx\tfrac{2}{3}\ . \tag{C7}$$

The root λ_1 is much smaller than the other two; under condition (C4) it follows that $xt_p\gg1$, and only the term having index λ_1 on the right-hand side of Eq. (C1) can provide a contribution which is not exponentially small. Taking into account Eqs. (C6) and (C7) yields

$$T(t_p)=\tfrac{1}{3}\exp\left[-\frac{2(y+\delta_f^2)t_p}{3x}\right]\ . \tag{C8}$$

If condition (C5) is violated, the difference between the exact solution (C1) and the approximate solution $T(t_p)$ given by Eq. (C8) is exponentially small. Thus, one can use Eq. (C8) for any y, δ_f, and x.

If the pulses are fully correlated and have almost equal intensities, i.e.,

$$(\alpha_1+\alpha_2-2\alpha_{12})t_p<1\ , \tag{C9}$$

condition (C5) is violated for the atoms situated close to the minima of the interference fringes, the regions for which the field is weak. Consequently, for

$$|\phi\pm\pi|,|\bar{\phi}\pm\pi|\ll\frac{1}{[(\alpha_1+\alpha_2)t_p]^{1/2}}\ll1\ . \tag{C10}$$

Equation (C8) is not valid. Despite this fact we are still be able to use Eq. (C8) since the contribution to the PT-3 signal from these regions is of order of $[(\alpha_1+\alpha_2)t_p]^{-1}$ and can be neglected.

Hence we may conclude that in a strong-field regime the signal is governed by the term (C8) alone. Taking into account expressions (4.5), (4.7), and (5.7), one gets Eqs. (6.9)–(6.10) of the text.

APPENDIX D: CALCULATION OF $W_N^{(3)}$ IN A STRONG-FIELD REGIME

Using the symmetry of Eq. (6.10) under the permutations

$$\phi \leftrightarrow -\tilde{\phi}+2\pi m\,;\ m=0,\pm 1,\ldots$$

we can rewrite Eq. (2.19) as

$$T^{(n,-n)}(t_p;\delta_-)=\frac{1}{\pi^2}\int_0^{\pi}d\phi_+\int_{-\pi/2}^{\pi/2}T(t_p)e^{-2in\phi_-}d\phi_-\ , \tag{D1}$$

with

$$T(t_p;\delta_-)=\tfrac{1}{3}\exp[-2t_p(4\sin^2\phi_-\{\alpha_1\alpha_2-[1-G^2(t_{12})]\alpha_{12}^2\cos^2\phi_+\}$$
$$+\delta_-^2+4\delta_-G(t_{12})\alpha_{12}\sin\phi_-\cos\phi_+)[3(\alpha_1+\alpha_2+2\alpha_{12}\cos\phi_-\cos\phi_+)]^{-1}]\ . \tag{D2}$$

In order to obtain the analytical expressions for the PT-3 signal with two strong pulses, one substitutes (D1) in Eq. (2.23) and carries out the δ_- integration to obtain

$$W_n^{(3)}=W_S+W_{AS}\ , \tag{D3}$$

with symmetrical, W_S, and asymmetrical, W_{AS}, parts of the signal given by

$$W_S=\frac{2}{3\pi^2}\int_0^{\pi}d\phi_+\int_0^{\pi/2}d\phi_-e^{-b}\cos 2n\phi_-\ , \tag{D4}$$

$$W_{AS}=\frac{2i}{3\pi^2}\int_0^{\pi}d\phi_+\int_0^{\pi/2}d\phi_-e^{-b}\sin(2n\phi_-)\mathrm{erf}(ia)\ , \tag{D5}$$

where erf is an error function and

$$a=\frac{\sqrt{2\Phi}G\eta\sin\phi_-\cos\phi_+}{\{(1+\sqrt{\Phi}\beta\cos\phi_-\cos\phi_+)[1+D(1+\sqrt{\Phi}\beta\cos\phi_-\cos\phi_+)]\}^{0.5}}\ ,$$
$$b=\frac{2\eta^2\sin^2\phi_-(1-\Phi_0\cos^2\phi_-)}{1+\sqrt{\Phi}\beta\cos\phi_-\cos\phi_+}\ , \tag{D6}$$
$$\eta=\left[\frac{4\alpha_1\alpha_2t_p}{3(\alpha_1+\alpha_2)}\right]^{1/2}\gg 1,\quad \Phi_0=\Phi(1-G^2)\le 1,\quad \beta=\frac{2(\alpha_1\alpha_2)^{1/2}}{\alpha_1+\alpha_2}\le 1,\quad D=\frac{3(\alpha_1+\alpha_2)}{4\Delta_D^2t_p}\ .$$

Using the fact that $\eta\gg 1$, one can analytically carry out the ϕ_- integration in Eq. (D4) provided $n\neq 0$. Using these conditions, the approximation $\sin\phi_-\approx\phi_-,\cos\phi_-\approx 1$ in expressions (D6) for a and b, and setting the upper integration limit equal to ∞, we carry out the integration over ϕ_- in Eq. (D4) to obtain

$$W_S=\frac{1}{3\eta\pi\sqrt{2\pi}}\int_0^{\infty}\left[\frac{1+\sqrt{\Phi}\beta\cos\phi_+}{1-\Phi_0\cos^2\phi_+}\right]^{1/2}\exp\left[-\frac{n^2(1+\sqrt{\Phi}\beta\cos\phi_+)}{2\eta^2(1-\Phi_0\cos^2\phi_+)}\right]d\phi_+\ . \tag{D7}$$

If, in addition, the inequality

$$(1-\Phi_0)\eta^2>1 \tag{D8}$$

is satisfied, it is also possible to carry out similar integration in Eq. (D5) that yields

$$W_{AS}=\frac{1}{3\eta\pi\sqrt{2\pi}}\int_0^{\pi}\left[\frac{1+\sqrt{\Phi}\beta\cos\phi_+}{1-\Phi_0\cos^2\phi_+}\right]^{1/2}\exp\left[-\frac{n^2(1+\sqrt{\Phi}\beta\cos\phi_+)}{2\eta^2(1-\Phi_0\cos^2\phi_+)}\right]\mathrm{erf}(\chi)d\phi_+\ , \tag{D9}$$

where

$$\chi=-\frac{Gn\sqrt{\Phi}\cos\phi_+}{\sqrt{2}\eta(1-\Phi_0\cos^2\phi_+)}\left[D+\frac{(1-\Phi\cos^2\phi_+)}{(1-\Phi_0\cos^2\phi_+)(1+\sqrt{\Phi}\beta\cos\phi_+)}\right]^{-0.5}\ . \tag{D10}$$

1. Weak mutual correlation of the pulses

Assuming that

$$\frac{\Phi}{4}\left[1+\frac{n^2}{\eta^2}\left[1+\frac{n^2}{(\alpha_1+\alpha_2)t_p}\right]\right]\ll 1\ , \tag{D11}$$

it follows that

$$\beta,\Phi_0 \ll \left[1+\frac{n^2}{\eta^2}\right]^{-1};\chi \ll 1 ,$$

and that inequality (D8) is valid. Extracting the terms of zero, first, and second orders in $\sqrt{\Phi}$ in the integrals (D7) and (D9) one finds

$$W_n^{(3)}=\frac{e^{-n^2/2\eta^2}}{3\eta\pi\sqrt{2\pi}}\int_0^{\pi}\left\{1+\sqrt{\Phi}\cos\phi_+\left[\frac{\beta}{2}\left[1-\frac{n^2}{\eta^2}\right]+\frac{Gn}{\eta\sqrt{D+2}}\right]\right.$$
$$\left.+\cos^2\phi_+\left[\frac{\Phi_0}{2}\left[1-\frac{n^2}{\eta^2}\right]-\frac{\Phi\beta^2}{8}\left[1+\frac{2n^2}{\eta^2}-\frac{n^4}{\eta^4}\right]+\frac{\Phi\beta Gn}{\eta\sqrt{2\pi(1+D)}}\left[\frac{2+D}{1+D}-\frac{n^2}{\eta^2}\right]\right]\right\}d\phi_+ . \tag{D12}$$

Carrying out the integration in (D12), one recovers Eq. (6.19).

2. Strongly correlated pulses

In this case $1-\Phi \ll 1$, and $(1-\Phi)$ is treated as a small parameter. The remainder of this Appendix is devoted to a consideration of this limit.

a. Signals of order $n \ll \eta$. First we consider signals, characterized by small n, $n \ll \eta$. To estimate the symmetrical part of the signal, W_S, from Eq. (D7), we observe that the expression under the integral sign is not exponentially small only if $y_+ \le \phi_+ \le \pi - y_-$, where $y_\pm$ can be expressed as

$$y_\pm=\frac{n\sqrt{1\pm\beta\sqrt{\Phi}}}{\eta}\exp\left[-\frac{(1-\Phi_0)\eta^2}{(1\pm\beta\sqrt{\Phi})n^2}\right]\ll 1 . \tag{D13}$$

Taking into account only the contributions which are not exponentially small, one has

$$W_S=\frac{1}{3\eta\pi\sqrt{2\pi}}\left[\int_0^{\pi}\left[\frac{1+\sqrt{\Phi}\beta\cos\phi_+}{1-\Phi_0\cos^2\phi_+}\right]^{1/2}d\phi_+-\int_0^{y_+}\left[\frac{1+\sqrt{\Phi}\beta}{1-\Phi_0(1-\phi_+^2)}\right]^{1/2}d\phi_+\right.$$
$$\left.-\int_0^{y_-}\left[\frac{1-\sqrt{\Phi}\beta}{1-\Phi_0(1-\phi_+^2)}\right]^{1/2}d\phi_+\right] . \tag{D14}$$

Expanding $(1+\beta\sqrt{\Phi}\cos\phi_+)^{1/2}$ in terms of $\beta\sqrt{\Phi}$ up to the fifth order in the first term of Eq. (D14) gives good accuracy even for $\beta=1$. In this limit the integrals reduce to

$$W_S=\frac{1}{3\eta\pi\sqrt{2\pi}}\left\{\left[2-\frac{\Phi\beta^2}{4\Phi_0}-\frac{5(2+\Phi_0)\Phi^2\beta^4}{192\Phi_0^2}\right]F(\Phi_0)+\frac{\Phi\beta^2}{4\Phi_0}\left[1+\frac{5(1+\Phi_0)\Phi\beta^2}{96\Phi_0}\right]E(\Phi_0)\right.$$
$$\left.-\sum_{\pm}\left[\frac{1\pm\sqrt{\Phi}\beta}{\Phi_0}\right]^{1/2}\ln\left[\frac{(\Phi_0)^{1/2}y_\pm}{(1-\Phi_0)^{1/2}}+\left[1+\frac{\Phi_0 y_\pm^2}{1-\Phi_0}\right]^{1/2}\right]\right\} , \tag{D15}$$

where F and E are elliptic integrals of the first and second kind,[43] respectively.

Under the assumption that $(1-\Phi_0) \ll 1$, one can use asymptotic expressions for the elliptical functions, and, taking into account the fact that

$$2-\frac{\Phi\beta^2}{4\Phi_0}-\frac{5(2+\Phi_0)\Phi^2\beta^4}{192\Phi_0^2}\approx(1+\sqrt{\Phi}\beta)^{1/2}+(1-\sqrt{\Phi}\beta)^{1/2} , \tag{D16}$$

one can arrive at Eq. (6.30) of the text.

For $t_{12} \gg \tau_c^{12}$ it follows that $G=1$ and $\Phi_0=0$, and thus $y_\pm=0$. Although the accuracy of Eq. (D15) is reasonably good, one can use the more accurate expression (D14) to obtain the background value of W_S:

$$W_S(t_{12} \gg \tau_c)=\frac{\sqrt{2}}{3\pi\eta\sqrt{\pi}}\left[1+\frac{2\alpha_{12}}{\alpha_1+\alpha_2}\right]^{1/2}E\left[\frac{4\alpha_{12}}{\alpha_1+\alpha_2+2\alpha_{12}}\right] . \tag{D17}$$

The background signal depends only weakly on the correlation parameter Φ, and, independent of Φ, differs by at most 10% from the value

$$W_n^{(3)}=\frac{1}{3\eta\sqrt{2\pi}} ,$$

which would be obtained for noncorrelated pulses ($\Phi=0$). For $\alpha_{\min}\ll\alpha_{\max}$ one obtains Eq. (6.37), while for $\alpha_1=\alpha_2;\Phi=1$, Eq. (D17) leads to the symmetrical part of Eq. (6.42).

To estimate the asymmetrical part of the signal, W_{AS}, we represent it in the form

$$W_{AS}=A_+-A_- , \tag{D18}$$

where, according to Eq. (D5), $A_\pm$ is given by

$$A_\pm=\frac{2i}{3\pi^2}\int_0^{\pi/2}d\phi_+\int_0^{\pi/2}d\phi_- e^{-b_\pm}\sin(2n\phi_-)\mathrm{erf}(ia_\pm) , \tag{D19}$$

and $a_\pm=a(\pm\beta),b_\pm=b(\pm\beta)$. It is not difficult to show that $A_\pm>0$, and thus the signal has a positive asymmetry, when $A_+>A_-$, and a negative one in the opposite case.

If $(1-\Phi_0)\eta<1$, one has to evaluate this exact expression. However, if $(1-\Phi_0)\eta>1$, one can use Eq. (D9) to approximate it as

$$A_\pm=\frac{1}{3\eta\pi\sqrt{2\pi}}\int_{y_\pm}^{\pi/2}\left[\frac{1\pm\sqrt{\Phi}\beta\cos\phi_+}{1-\Phi_0\cos^2\phi_+}\right]^{1/2}\mathrm{erf}(\chi_\pm)d\phi_+ , \tag{D20}$$

where $\chi_\pm=\chi(\pm\beta)$.

In the case of small order $n,n\ll\eta$, which is considered now, it is shown below that $W_{AS}<W_S$; however, there are certain cases where W_{AS} qualitatively modifies the signal. Such a modification can occur for $\beta=1$, corresponding to equal intensities of the pulses.

First we estimate W_{AS} for

$$(1-\Phi_0)\eta^2<1 , \tag{D21}$$

using the exact equation (D19). In the limit (D21),

$$\mathrm{erf}(ia)=\frac{-2i}{\sqrt{\pi}}(a+\tfrac{1}{3}a^3) ,$$

and, expanding $\exp(-b)$ up to the first order in the parameter $(1-\Phi_0)\eta^2$, one finds

$$\begin{aligned}A_\pm=\frac{4}{3\pi^2\sqrt{\pi}}\int_0^{\pi/2}d\phi_+\int_0^{\pi/2}d\phi_-\exp\left[-\frac{2\eta^2\sin^2\phi_-\sin^2\phi_+}{1\pm\sqrt{\Phi}\cos\phi_-\cos\phi_+}\right]\sin(2n\phi_-)\\ \times\left[\frac{\sqrt{2}G\eta\sin\phi_-\cos\phi_+}{\{(1\pm\sqrt{\Phi}\cos\phi_-\cos\phi_+)[1+D(1\pm\sqrt{\Phi}\cos\phi_-\cos\phi_+)]\}^{0.5}}\right.\\ +\frac{2\sqrt{2}G\eta^3\sin^3\phi_-\cos^3\phi_+}{\{(1\pm\sqrt{\Phi}\cos\phi_-\cos\phi_+)^3[1+D(1\pm\sqrt{\Phi}\cos\phi_-\cos\phi_+)]\}^{0.5}}\\ \left.\times\left[\frac{G^2}{3[1+D(1\pm\sqrt{\Phi}\cos\phi_-\cos\phi_+)]}-1+\Phi_0\right]\right] .\end{aligned} \tag{D22}$$

Taking into account the fact that the main contribution to the integral (D22) comes from the region $0\le\phi_+\ll1$, we first integrate Eq. (D22) over ϕ_+, putting $\sin\phi_+=\phi_+$ and $\cos\phi_+=1$ to obtain

$$\begin{aligned}A_\pm=\frac{2G}{3\pi^2}\int_0^{\pi/2}d\phi_-\frac{\sin(2n\phi_-)}{[1+D(1\pm\sqrt{\Phi}\cos\phi_-)]^{1/2}}\\ \times\left[1+\frac{2\eta^2\sin^2\phi_-}{1\pm\sqrt{\Phi}\cos\phi_0}\left[\frac{G^2}{3[1+D(1\pm\sqrt{\Phi}\cos\phi_0)]}-1+\Phi_0\right]\right] .\end{aligned} \tag{D23}$$

When $D\gg1$, $A_\pm\sim[\max(n,\sqrt{D})]^{-1}$ and leads to a negligibly small asymmetrical signal. Evaluating the integral (D23) under the assumption that $D\ll1$ and subtracting A_- from A_+, one obtains

$$W_{AS}=\frac{2nG}{3\pi^2(4n^2-1)}\left[-D+4\eta^2\left[1-\Phi_0-\frac{G^2}{3}\right]\right] ; \tag{D24}$$

for $(1-\Phi)\ll n^2/\eta^2$, one recovers Eq. (6.39).

To estimate W_{AS} when $(1-\Phi_0)\eta^2 > 1$, one can use Eq. (D20) and calculate only A_+, as $A_+ \gg A_-$. If

$$1 \ll (1-\Phi_0)\eta^2 \ll n^2 , \tag{D25}$$

then $y_+ = n/\eta \ll 1$, and for the integration range $y_+ \le \phi_+ \le \pi/2$ in Eq. (D20), it follows that $\chi \ll 1$, and $\sin^2\phi_+ \gg (1-\Phi_0)$. Consequently, A_+ takes the form

$$A_+ = \frac{1}{3\pi\eta^2\sqrt{\pi}} \int_{y_+}^{\pi/2} \frac{Gn\cos\phi_+}{\sin^3\phi_+\sqrt{2D+1}} d\phi_+$$

$$= \frac{G}{6\pi n\sqrt{\pi(2D+1)}} , \tag{D26}$$

which leads to Eq. (6.40) for $D \ll 1$.

If $(1-\Phi_0)\eta^2 \gg n^2$, then $y_+ = 0$; and $\chi < 1$ for $y_0 \le \phi_+$, where

$$y_0 = \frac{Gn}{\eta[(1-\Phi_0)(1+2D\Phi_0)]^{1/2}} \exp\left[-\frac{\eta^2(1-\Phi_0)[(1-\sqrt{\Phi})+D(1-\Phi_0)]}{n^2G^2} \right] \ll \left[\frac{1-\Phi_0}{\Phi_0} \right]^{1/2} . \tag{D27}$$

The main contribution to the integral (D20) comes from the region $\phi_+ < 1$. Then one finds

$$A_+ = \frac{1}{3\pi\eta\sqrt{2\pi}} \left[\int_0^{y_0} \left[\frac{2}{1-\Phi_0+\Phi_0\phi_+^2} \right]^{1/2} d\phi_+ \right.$$

$$\left. + \frac{2Gn}{\eta\sqrt{\pi}} \int_{y_0}^{1} \frac{d\phi_+}{(1-\Phi_0+\Phi_0\phi_+^2)[D(1-\Phi_0)+(1-\sqrt{\Phi})+\phi_+^2(0.5+D\Phi_0)]^{1/2}} \right] , \tag{D28}$$

which can be integrated exactly. We present here the results in the most important cases. If $D > 1$,

$$W_{AS} = A_+ = \frac{2Gn}{3\pi^2\eta^2(1-\Phi_0)\sqrt{2D}} , \tag{D29}$$

which is negligibly small. If $D \ll 1$, one arrives at

$$W_{AS} = \frac{1}{3\pi\eta\sqrt{\pi}} \left[\frac{y_0}{(1-\Phi_0)^{1/2}} + \frac{2Gn}{\eta\sqrt{\pi}(1-\Phi_0)} \ln\left[\frac{2(1-\Phi_0)^{1/2}}{y_0+[y_0^2+(1-\sqrt{\Phi})+2D(1-\Phi_0)]^{1/2}} \right] \right] ; \tag{D30}$$

for $\Phi = 1$ Eq. (D30) reduces to Eq. (6.41).

b. Signals of higher order: $n \gg \eta \gg 1$. In this case to estimate the signal one can use Eq. (D9) to obtain W_{AS}, as the inequality (D8) is only violated for very small t_{12}, where the variation of the signal is negligible.

For pulses with very different intensities,

$$\alpha_{max} \gg \alpha_{min} \gg t_p^{-1} , \tag{D31}$$

one has

$$\beta \ll 1 . \tag{D32}$$

If β is so small, that

$$\beta\frac{n^2}{\eta^2} \ll 1 , \tag{D33}$$

the asymmetrical part of the signal is negligible. For its symmetrical part, W_S, the main contribution to the integral (7) is from the region defined by $(1-\Phi_0\cos^2\phi_+) \approx 1$, leading to the result

$$W_n^{(3)} = \frac{1}{3\eta\pi\sqrt{2\pi}} \int_0^{\pi} \exp\left[-\frac{n^2}{2\eta^2}(1+\Phi_0\cos^2\phi_+) \right] d\phi_+$$

$$= \frac{1}{3\eta\sqrt{2\pi}} \exp\left[-\frac{(2+\Phi_0)n^2}{4\eta^2} \right] I_0\left[\frac{\Phi_0 n^2}{4\eta^2} \right] , \tag{D34}$$

where I_0 is a modified Bessel function, which is Eq. (6.45).

If

$$\Phi_0 \gg \beta \gg \frac{\eta^2}{n^2} , \tag{D35}$$

the result (34) is still valid. However, if

$$1 \gg \beta \gg \Phi_0, \frac{\eta^2}{n^2},$$

the major contribution to the integrals (D7) and (D9), which can be used in this case, comes from the region $y = \pi - \phi_+ \ll 1$, and the PT-3 signal is given by

$$W_n^{(3)} = \frac{1}{3\eta\pi\sqrt{2\pi}} \left[1 - s \operatorname{erf} \left[\frac{n}{\eta\sqrt{2}} [D + (1-\Phi)]^{-1/2} \right] \right] \int_0^{\pi} \exp \left\{ -\frac{n^2}{2\eta^2} \left[1 - \beta \left[1 - \frac{y^2}{2} \right] \right] \right\} dy$$

$$= \frac{e^{-n^2(1-\beta)/2\eta^2}}{3\pi n\sqrt{2\beta}} \left[1 - s \operatorname{erf} \left[\frac{n}{\eta\sqrt{2}} [D + (1-\Phi)]^{-1/2} \right] \right], \tag{D36}$$

where s is defined by Eq. (2.21).

The signal has a negative asymmetry ($A_- > A_+$), which can be large, when $D\eta^2/n^2 < 1$.

In the limiting case of equal pulse intensities, $\alpha_1 = \alpha_2$ or $\beta = 1$, the region $y = \pi - \phi_+ \ll 1$ provides the main contribution to the integrals (D7) and (D9) for any G. Then for $G = 0$ one has

$$W_n^{(3)} = \frac{1}{3\eta\pi\sqrt{2\pi}} \int_0^{\pi} \exp \left[-\frac{n^2(1 + y^2/4)}{4\eta^2} \right] dy$$

$$= \frac{\sqrt{2}}{3n\pi} e^{-n^2/4\eta^2}. \tag{D37}$$

For $(1-\Phi_0)n^2/\eta^2 > 1$, the signal is given by

$$W_n^{(3)} = \frac{1}{6\eta\pi\sqrt{\pi}} \int_0^{\min\{\pi, (\Phi_0^{-1}-1)^{1/2}\}} \frac{y}{(1-\Phi_0)^{1/2}} \exp \left[-\frac{n^2 y^2}{4\eta^2(1-\Phi_0)} \right] \times \left[1 - \operatorname{erf} \left[\frac{Gn}{\eta\{2(1-\Phi_0)[D(1-\Phi_0)+2]\}^{1/2}} \right] \right] dy$$

$$= \frac{\eta(1-\Phi_0)^{1/2}}{3n^2\pi\sqrt{\pi}} \left[1 - \operatorname{erf} \left[\frac{Gn}{\eta\{2(1-\Phi_0)[D(1-\Phi_0)+2]\}^{1/2}} \right] \right]; \tag{D38}$$

for $\Phi = 1$, Eq. (D38) reduces to Eq. (6.47).

[1] S. Asaka, H. Nakatsuka, M. Fujiwara, and M. Matsuoka, Phys. Rev. A **29**, 2286 (1984).

[2] H. Nakatsuka, M. Tomita, M. Fujiwara, and S. Asaka, Opt. Commun. **52**, 150 (1984).

[3] N. Morita and T. Yajima, Phys. Rev. A **30**, 2525 (1984).

[4] M. Fujiwara, R. Kuroda, and H. Nakatsuka, J. Opt. Soc. Am. B **2**, 1634 (1985).

[5] J. E. Golub and T. W. Mossberg, J. Opt. Soc. Am. B **3**, 554 (1986).

[6] J. E. Golub and T. W. Mossberg, Opt. Lett. **11**, 431 (1986).

[7] M. Tomita and M. Matsuoka, J. Opt. Soc. Am. B **3**, 560 (1986).

[8] M. Defour, J.-C. Keller, and J.-L. Le Gouët, J. Opt. Soc. Am. B **3**, 544 (1986).

[9] T. Hattori, A. Terazaki, and T. Kobayashi, Phys. Rev. A **35**, 715 (1987).

[10] K. Kurokawa, T. Hattori, and T. Kobayashi, Phys. Rev. A **36**, 1298 (1987).

[11] R. Beach, D. De Beer, and S. R. Hartmann, Phys. Rev. A **32**, 3467 (1985).

[12] M. Defour, J.-C. Keller, and J.-L. Le Gouët, Phys. Rev. A **36**, 5226 (1987).

[13] P. Tchénio, A. Debarre, J.-C. Keller, and J.-L. Le Gouët, Phys. Rev. A **38**, 5235 (1988).

[14] P. Tchénio, A. Debarre, J.-C. Keller, and J.-L. Le Gouët, Phys. Rev. A **39**, 1970 (1989).

[15] P. Tchénio, A. Debarre, J.-C. Keller, and J.-L. Le Gouët, Phys. Rev. Lett. **62**, 415 (1989).

[16] K. Wynne, M. Müller, and J. D. W. Van Voorst, Phys. Rev. Lett. **62**, 3031 (1989).

[17] X. Mi, H. T. Zhou, R. H. Zhang, and P. X. Ye, J. Opt. Soc. Am. B **6**, P184 (1989).

[18] J. Cooper, A. Charlton, D. R. Meacher, P. Ewart, and G. Alber, Phys. Rev. A **40**, 5705 (1989).

[19] For the references prior to 1984 see the reasonably complete list in B. W. Shore, J. Opt. Soc. Am. B **1**, 176 (1984).

[20] V. Finkelstein, Phys. Rev. A **27**, 961 (1984).

[21] S. N. Dixit and A. T. Georges, Phys. Rev. A **29**, 200 (1984).

[22] P. T. Greenland, J. Phys. B **17**, 1919 (1984).

[23] J. H. Eberly, K. Wodkiewicz, and B. W. Shore, Phys. Rev. A **30**, 2381 (1984).

[24] K. Wodkiewicz, B. W. Shore, and J. H. Eberly, Phys. Rev. A **30**, 2390 (1984).

[25] G. Hazak, M. Strauss, and J. Oreg, Phys. Rev. A **32**, 3475 (1985).

[26] I. Schek and J. Jortner, Chem. Phys. **97**, 1 (1985).

[27] Y. Prior, I. Schek, and J. Jortner, Phys. Rev. A **31**, 3775

(1985).
[28]S. Swain, J. Opt. Soc. Am. B **2**, 1666 (1985).
[29]K. Wodkiewicz and J. H. Eberly, J. Opt. Soc. Am. B **3**, 628 (1986).
[30]F. Rohart, J. Opt. Soc. Am. B **3**, 622 (1986).
[31]P. Franken and C. H. Joachain, Phys. Rev. A **36**, 1663 (1987).
[32]R. Boscaino and R. N. Mantegna, Phys. Rev. A **36**, 5482 (1987).
[33]M. W. Hamilton, K. Arnett, S. J. Smith, D. S. Elliot, M. Dziemballa, and P. Zoller, Phys. Rev. A **36**, 178 (1987).
[34]V. Finkelstein and V. Namiot, Moscow Univ. Phys. Bull. **42**, 81 (1987).
[35]G. S. Agarwal, C. V. Kunasz, and J. Copper, Phys. Rev. A **36**, 143 (1987).
[36]B. H. W. Hendriks and G. Nienhuis, Phys. Rev. A **36**, 5615 (1987).
[37]T. A. B. Kennedy and S. Swain, Phys. Rev. A **36**, 1747 (1987).
[38]Th. Haslwanter, H. Ritsch, J. Cooper, and P. Zoller, Phys. Rev. A **38**, 5652 (1988).
[39]A. I. Burshtein, A. A. Zharikov, and S. I. Temkin, J. Phys. B **21**, 1907 (1988).
[40]A. G. Kofman, R. Zaibel, A. M. Levine, and Y. Prior, Phys. Rev. Lett. **61**, 251 (1988).
[41]R. G. Friedberg and S. R. Hartmann, J. Phys. B **21**, 683 (1988).
[42]W. G. Van Kampen, *Stochastic Processes in Physics and Chemistry* (North-Holland, Amsterdam, 1981), Chap. XIV.
[43]*Handbook of Mathematical Functions*, edited by M. Abramowitz and I. A. Stegun (Dover, New York, 1980).
[44]V. Finkelstein, Zh. Eksp. Teor. Fiz. **78**, 2138 (1980) [Sov. Phys.—JETP **51**, 1072 (1980)].

Macroscopic quantum jumps from a two-atom system

K. Yamada and P. R. Berman
Department of Physics, New York University, 4 Washington Place, New York, New York 10003
(Received 25 August 1989)

We analyze the macroscopic quantum jumps (sudden interruptions in the fluorescence on a macroscopic time scale) that are produced when a pair of two-level atoms separated by a distance d is irradiated by a strong laser having wavelength λ_0, with $\lambda_0 \gg d$. Included in the analysis is the dipole-dipole coupling of the atoms, the ac Stark effect, and the role played by a term that is present in the atom-laser field interaction Hamiltonian when $\mathbf{k}\cdot\mathbf{d}\neq 0$ ($\mathbf{k}$ is the wave vector of the laser field and $\mathbf{d}$ is the vector connecting the two atoms). Our treatment is based on frequency-resolved delay functions, an extension of a concept developed by Reynaud, Dalibard, and Cohen-Tannoudji [IEEE J. Quantum Electron. **24**, 1395 (1988)], which is shown to be useful to study frequency-resolved photon statistics. As examples, we study the statistics of the fluorescence produced by the two-atom system as well as those in the components of the fluorescent triplet produced by a single two-level atom.

I. INTRODUCTION

When identical two-level atoms are separated by a distance d that is smaller than their resonant wavelength λ_0, cooperative decay phenomena can occur. Dicke[1] and others[2,3] found that the exchange of photons between the two atoms produces new eigenstates with new decay rates. Denoting the ground and excited states of atom i by $|e_i\rangle$ and $|g_i\rangle$ ($i=1,2$), these states are a triplet of symmetric states $[|E\rangle=|e_1e_2\rangle, |S\rangle=(1/\sqrt{2})(|e_1g_2\rangle+|g_1e_2\rangle, |G\rangle=|g_1g_2\rangle)$, and one antisymmetric state $(|A\rangle=(1/\sqrt{2})(|e_1g_2\rangle-|g_1e_2\rangle)]$. These states are shown in Fig. 1. When $\lambda_0 \gg d$, the system, initially excited by an incoherent or a weak coherent field to state $|E\rangle$, can decay to state $|G\rangle$ via state $|S\rangle$ with a rate $\Gamma_S \cong 2\Gamma$ (Γ is the decay rate of a single atom). As can be seen from Fig. 1, a two-peaked fluorescence spectrum centered at $\omega_0 \pm V$ is produced when the system undergoes the $|E\rangle \rightarrow |S\rangle \rightarrow |G\rangle$ cascade.

Cooperative effects in resonance fluorescence produced by the two-atom system when it is continuously excited by a strong coherent laser was studied by Senitzky[4] and others.[5] They searched for the existence of extra sidebands not present in the single-atom fluorescence spectrum (Mollow triplet).[6] An interpretation of the spectrum was provided by Freedhoff.[7] She calculated the fluorescence as arising from transitions between dressed states of the two-atom plus laser-field system and obtained a spectrum containing seven peaks.

In most treatments of the problem, the atoms have been considered to be so close as to render the antisymmetric state optically inactive in the sense that the decay rate Γ_A for the $|E\rangle \rightarrow |A\rangle$ and $|A\rangle \rightarrow |G\rangle$ transitions is set identically equal to zero. The decay rate Γ_A is approximately given by $\Gamma_A \cong (2\pi d/\lambda_0)^2\Gamma/5 (\ll \Gamma)$.[2] As will be seen below, this small but finite decay rate can lead to macroscopic quantum jumps (MQJ).[8-14] The origin of the MQJ is the metastability of the antisymmetric state $|A\rangle$; once the system is shelved in this state the fluorescence produced by the $|E\rangle \rightarrow |S\rangle \rightarrow |G\rangle$ cascade is interrupted for a time interval on the order of Γ_A^{-1}.

In this paper, we analyze the MQJ produced by this cooperative atomic effect. Recently, this effect was partially incorporated into the problem "MQJ due to two three-level atoms" by Javanainen and Lewenstein.[15] We extend their work by including effects relating to the energy shifts of states $|S\rangle$ and $|A\rangle$ resulting from the atomic dipole-dipole interaction. Moreover, we allow for an additional mixing of the symmetric and antisymmetric states produced by a term in the laser-field–atom interaction Hamiltonian that is present when $\mathbf{k}\cdot\mathbf{d}\neq 0$ ($\mathbf{k}$ is the wave vector of the laser field and $\mathbf{d}$ is the vector connecting the two atoms). The former effect is important because the $|E\rangle \leftrightarrow |S\rangle$ and $|S\rangle \leftrightarrow |G\rangle$ transitions are no longer resonant with a laser tuned to ω_0; the energy shift

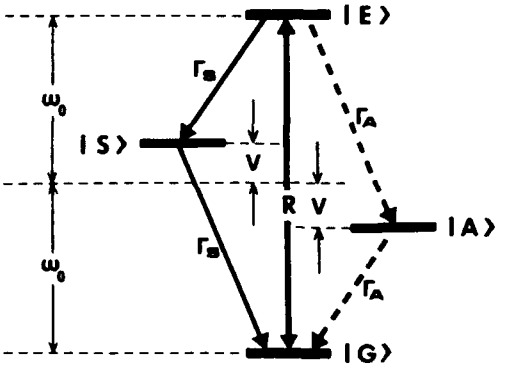

FIG. 1. Energy diagram for a two-atom composite system. When the atomic separation $d \ll \lambda_0 = 2\pi d/\omega_0$, $\Gamma_S \cong 2\Gamma$, $\Gamma_A \cong (2\pi d/\lambda_0)^2\Gamma/5$, and $V=(2\pi d/\lambda_0)\,3\Gamma/4$, where Γ is the decay rate and ω_0 is the resonant frequency of a single atom. Transitions between states $|E\rangle$ and $|G\rangle$ (at rate R) are produced by an incoherent pump field. State $|A\rangle$ acts as a shelving state in the problem of macroscopic quantum jumps.

$V=(2\pi d/\lambda_0)^{-3}3\Gamma/4$ is much larger than Γ, in the same limit where state $|A\rangle$ becomes metastable. The latter effect is also important because it drastically alters the duration of the bright and dark periods. Our analysis is based on so-called frequency-resolved delay functions (an extension of a concept introduced by Reynaud, Dalibard, Cohen-Tannoudji, and others),[11-13] which is shown to be very convenient in analyzing quantities such as frequency-resolved photon statistics (FRPS).

The paper is organized as follows. In Sec. II, we assume an incoherent pumping of the $|E\rangle \leftrightarrow |G\rangle$ transition and analyze the statistics of the bright and dark periods of the fluorescence. The FRPS in a bright period is calculated in Sec. III utilizing the method developed in Sec. II. In Sec. IV, we analyze the statistics of bright and dark periods for the case of strong coherent pumping when $\mathbf{k}\cdot\mathbf{d}=0$. In Sec. V, we consider the application of the method developed in Sec. IV to two problems in FRPS in a dressed-atom picture: fluorescence photons produced by a single two-level atom and by the two-atom system considered in this paper. Finally, in Sec. VI, we consider a coupling of the antisymmetric state to the symmetric states by the laser field when $\mathbf{k}\cdot\mathbf{d}\neq 0$ and show how this alters the statistics of the bright and dark periods considered in Sec. IV.

II. INCOHERENT PUMP

We first consider the two-atom system irradiated by a strong incoherent pump which couples states $|E\rangle$ and $|G\rangle$ directly with rate R (see Fig. 1). It can be shown that this is a good model when a reasonably strong broadband laser whose center is tuned to the transition frequency of each atom is used [see the argument below Eq. (28) in Sec. IV]. When $\Gamma_S, R \gg \Gamma_A$, this system exhibits two phases in its fluorescence: a bright period (BP), in which repeated cycling through the channel $|E\rangle \rightarrow |S\rangle \rightarrow |G\rangle$ produces many fluorescence photons, and a dark period (DP), in which the system is shelved in the metastable state $|A\rangle$. A bright period begins (ends) when the system jumps from state $|A\rangle$ to state $|G\rangle$ (state $|E\rangle$ to state $|A\rangle$). Therefore, to determine the probability distributions $P_B(\tau)$ or $P_D(\tau)$ of the duration τ of a single BP or DP, respectively, we must find the time delay between *successive* transitions. The distribution $P_B(\tau)$ is determined by the delay between an $|A\rangle \rightarrow |G\rangle$ transition and the *next* $|E\rangle \rightarrow |A\rangle$ transition, while $P_D(\tau)$ is determined by the delay between an $|E\rangle \rightarrow |A\rangle$ transition and the *next* $|A\rangle \rightarrow |G\rangle$ transition. The calculation starts with rate equations

$$\frac{d}{dt}\Pi_i(t) = -\Pi_i(t)\sum_j \Gamma_{ij} + \sum_j \Pi_j(t)\Gamma_{ji} , \tag{1}$$

where $\Pi_i(t)$ is the population of state $|i\rangle$ at time t and Γ_{ij} is the transition rate from state $|i\rangle$ to state $|j\rangle$ $(i,j=E,S,G,A)$, which can be written in matrix form as

$$\Gamma_{ij} = \begin{bmatrix} 0 & \Gamma_S & R & \Gamma_A \\ 0 & 0 & \Gamma_S & 0 \\ R & 0 & 0 & 0 \\ 0 & 0 & \Gamma_A & 0 \end{bmatrix} . \tag{2}$$

The solution for $\Pi_i(t)$ includes contributions from any number of possible pathways leading to a final state population Π_i at time t. For example, suppose that the system decays from state $|A\rangle$ to state $|G\rangle$ at time $t=0$ (a BP begins at time $t=0$). The population $\Pi_A(t)$ obtained by solving Eqs. (1) and (2) with the initial condition $\Pi_G(0)=1$ includes contributions from pathways such as $|G\rangle \xrightarrow{t_1} |E\rangle \xrightarrow{t_2} |A\rangle$, $|G\rangle \xrightarrow{t_1} |E\rangle \xrightarrow{t_2} |A\rangle \xrightarrow{t_3} |G\rangle \xrightarrow{t_4} |E\rangle \xrightarrow{t_5} |A\rangle$, etc. $(0\le t_1 < t_2 \cdots \le t)$. In the $|G\rangle \xrightarrow{t_1} |E\rangle \xrightarrow{t_2} |A\rangle$ pathway, the first BP ends and the first DP begins at time t_2, with no further transition between times t_2 and t. In the $|G\rangle \xrightarrow{t_1} |E\rangle \xrightarrow{t_2} |A\rangle \xrightarrow{t_3} |G\rangle \xrightarrow{t_4} |E\rangle \xrightarrow{t_5} |A\rangle$ pathway, the second BP ends and the second DP begins at time $t=t_5$, with no further transition between times t_5 and t. Note that in both pathways, any number of transitions $|E\rangle \rightarrow |S\rangle \rightarrow |G\rangle \rightarrow |E\rangle$ is allowed before each transition to state $|A\rangle$. In order to calculate the duration of a single BP we need to separate out the contribution of the first decay to $\Pi_A(t)$. To do this, we pretend that the system will never escape from state $|A\rangle$ after the first $|E\rangle \rightarrow |A\rangle$ decay. This corresponds to setting $\Gamma_{AG}=0$ in Eq. (2), and solving Eq. (1) for $\Pi_A(t)$ with the initial condition $\Pi_G(0)=0$. We designate this population with a prime, $\Pi'_A(t)$, to distinguish from the true population of state $|A\rangle$. The crucial point in setting $\Gamma_{AG}=0$ in Eq. (2) is that it in no way influences the dynamics of the system for times before the first $|E\rangle \rightarrow |A\rangle$ decay. A quantity $W(E\rightarrow A/G;t)$ defined as the probability per unit time that, starting from state $|G\rangle$, the system decays to state $|A\rangle$ for the first time at t, can be found through

$$W(E\rightarrow A/G;t) = \frac{d}{dt}\Pi'_A(t) . \tag{3}$$

When $\Gamma_S, R \gg \Gamma_A$, a simple calculation using Eqs. (1), (3), and (2) with $\Gamma_{AG}=0$ yields

$$\begin{aligned} W(E\rightarrow A/G;t) = {} & \frac{\Gamma_A R(R-B)}{2B(R+\Gamma_S-B)}\exp[-(R+\Gamma_S-B)t] \\ & - \frac{\Gamma_A R(R+B)}{2B(R+\Gamma_S+B)} \\ & \times \exp[-(R+\Gamma_S+B)t] \\ & + \frac{R\Gamma_A}{3R+\Gamma_S}\exp[-R\Gamma_A t/(3R+\Gamma_S)] , \end{aligned} \tag{4}$$

where

$$B=(R^2-R\Gamma_S)^{1/2} .$$

From Eq. (4), it follows that $W(E\rightarrow A/G;t)\cong 0$ in the transient regime $t \ll R^{-1}$, reflecting the fact that it takes a time $\sim R^{-1}$ for the system to be pumped from state $|G\rangle$ to state $|E\rangle$, from which it can then decay to state $|A\rangle$. In the third term of Eq. (4), the factor $R/(3R+\Gamma_S)$ can be interpreted as the quasi-steady-state population (Π_E^{qs}) that state $|E\rangle$ would have if a decay to state $|A\rangle$ were forbidden. The appearance of this factor is related to the fact that fast transitions among states

$|E\rangle$, $|S\rangle$, and $|G\rangle$ drive their populations to the quasi-steady-state values long before any $|E\rangle \rightarrow |A\rangle$ decay occurs.

The probability distribution function $P_B(\tau)$ for the duration τ of a single BP is equal to the probability that, starting from state $|G\rangle$, the system will not decay to state $|A\rangle$ until time τ. Thus we can write $P_B(\tau)$ in terms of $W(E \rightarrow A/G;t)$ as

$$P_B(\tau)=1-\int_0^{\tau} W(E \rightarrow A/G;t)dt \ . \tag{5}$$

By using Eqs. (4) and (5), one sees immediately that both the first and the second terms in Eq. (4) do not contribute in the limit $\Gamma_S, R \gg \Gamma_A$; in this limit, we find

$$P_B(\tau)=\exp(-\tau/\tau_B), \quad \tau_B=\frac{3R+\Gamma_S}{R\Gamma_A} \ , \tag{6}$$

where τ_B is the average duration of a single BP. The inverse of the average duration of a single BP, τ_B^{-1}, is simply equal to the quasi-steady-state population of state $|E\rangle$ [given by $\Pi_E^{qs}=R/(3R+\Gamma_S)$] multiplied by the rate Γ_A for the $|E\rangle \rightarrow |A\rangle$ decay. As R/Γ_S increases, τ_B decreases, and eventually saturates at a value equal to $3\Gamma_A^{-1}$.

In order to find the analogous probability function $P_D(\tau)$, we apply a similar method [setting $\Gamma_{GE}=0$ in Eq. (2) and solving Eq. (1) for $\Pi_G(t)$ with the initial condition $\Pi_A(0)=1$] to find

$$W(A \rightarrow G/A;t)=\Gamma_A \exp(-\Gamma_A t) \tag{7}$$

and

$$P_D(\tau)=1-\int_0^{\tau} W(A \rightarrow G/A;t)dt=\exp(-\tau/\tau_D) \ ,$$

$$\tau_D=\frac{1}{\Gamma_A} \ , \tag{8}$$

where τ_D is the average duration of a single dark period. Note that the ratio $\tau_B/\tau_D=(3R+\Gamma_S)/R \Longrightarrow 3$ when $R \gg \Gamma_S$. This result is larger than that obtained in a single three-level atom (MQJ)[8-13] because of the additional active level $|S\rangle$ which is present in our problem.

In this section, we found $W(E \rightarrow A/G;t)$ and $W(A \rightarrow G/A;t)$ in order to calculate $P_B(\tau)$ or $P_D(\tau)$. The beginning or ending of a BP or DP corresponds to a distinctive decay $|E\rangle \rightarrow |A\rangle$ or $|A\rangle \rightarrow |G\rangle$, respectively. Depending on the W function to be evaluated, we alter Eq. (2) by setting some of the Γ's equal to zero. It is a generalization of a method developed by others.[11-13] As is shown in Sec. III, this approach is useful for calculating the frequency-resolved photon statistics.

In this problem and related problems, the quasi-steady-state populations in each period determine the probability distributions for the durations of a single BP and DP. Specifically, it has the form $P_i(\tau)=\exp(-\tau/\tau_i)$, where τ_i is the average duration of the period i ($i=B$ or D). As a simple application of this, we consider the three-level system depicted in Fig. 2 which has been studied extensively.[8-13] In Fig. 2, R_1 and R_2 represent incoherent pumps and Γ_1 and Γ_2 represent spontaneous decay rates. When $R_1, \Gamma_1 \gg R_2, \Gamma_2$, this three-level system, with state $|2\rangle$ metastable, exhibits BP and DP in its fluorescence: the BP involves transitions between states $|1\rangle$ and $|3\rangle$, and the DP is triggered by the rare excitation $|3\rangle \rightarrow |2\rangle$. When the system is in a DP, the next BP will start following by the transition $|2\rangle \rightarrow |3\rangle$. A simple calculation yields the quasi-steady-state population of state $|3\rangle$ in a BP as $\Pi_3^{qs}=(R_1+\Gamma_1)/(2R_1+\Gamma_1)$. Since the next DP is triggered by the transition $|3\rangle \rightarrow |2\rangle$ with a rate $\Gamma_{32}=R_2$, one finds

$$\tau_B=(\Pi_3^{qs}\Gamma_{32})^{-1}=[(R_1+\Gamma_1)R_2/(2R_1+\Gamma_1)]^{-1} \ ,$$

which is equal to $(R_2/2)^{-1}$ when $R_1 \gg \Gamma_1$. A similar argument produces that $\tau_D=(R_2+\Gamma_2)^{-1}$, which reduces to R_2^{-1} when $R_2 \gg \Gamma_2$. These results agree with those that have been obtained previously.[10]

III. PHOTON STATISTICS IN A BRIGHT PERIOD

In this section, we study the FRPS in a BP by using the method developed in the previous section. We calculate the delay function $D(\omega_{ES},\tau)$, the probability distribution describing the delay time τ between *successive* emissions of ω_{ES} photons (produced by the $|E\rangle \rightarrow |S\rangle$ decays) in a BP. As is seen in Fig. 1, these photons contribute to the peak in the spectrum centered at $\omega_0 - V$ and can be distinguished from ω_{SG} photons (produced by the $|S\rangle \rightarrow |G\rangle$ transitions). In this section, we ignore the existence of state $|A\rangle$ [all Γ_A's in Eq. (2) are set equal to zero] because of the time scale involved ($\Gamma_S^{-1}, R^{-1} \ll \Gamma_A^{-1}$).

We assume that an emission of a ω_{ES} photon takes place at time $t=0$ leaving the system in state $|S\rangle$. In order to emit the next photon at time τ, the system decays from state $|S\rangle$ to state $|G\rangle$ at any instant t, is excited to state $|E\rangle$ at any instant after t, t', and then undergoes an $|E\rangle \rightarrow |S\rangle$ decay at time τ ($0 \le t \le t' \le \tau$). Therefore the delay function for the ω_{ES} photon should be written in

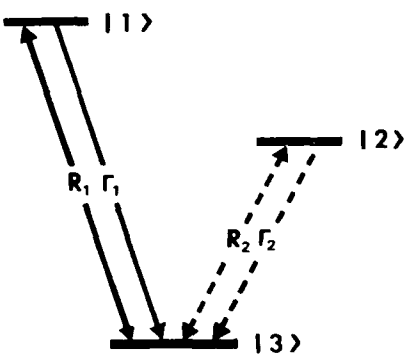

FIG. 2. Energy-level scheme for a single three-level atom producing macroscopic quantum jumps. The transition between states $|1\rangle$ and $|3\rangle$ is strongly driven at rate R_1, while that between states $|2\rangle$ and $|3\rangle$ is weakly driven at rate R_2. The decay rate from state $|1\rangle$ to state $|3\rangle$ is Γ_1 and the decay rate from state $|2\rangle$ to state $|3\rangle$ is Γ_2. These rates satisfy the condition $R_1, \Gamma_1 \gg R_2, \Gamma_2$. State $|2\rangle$ is the shelving state.

terms of two types of W functions [$W(S\rightarrow G/S;t)$ and $W(E\rightarrow S/G;t)$] as

$$D(\omega_{ES},\tau)=\int_0^\tau W(S\rightarrow G/S;t)W(E\rightarrow S/G;\tau-t)dt\ , \tag{9}$$

where the function $W(S\rightarrow G/S;t)$ is the probability per unit time that, starting from state $|S\rangle$, the system undergoes the *first* $|S\rangle\rightarrow|G\rangle$ transition at time t and the function $W(E\rightarrow S/G;t)$ is the probability per unit time that, starting from state $|G\rangle$, the system is pumped up to state $|E\rangle$ at any time $t'(0\leq t'\leq t)$ and makes the *first* $|E\rangle\rightarrow|S\rangle$ transition at time t. The way of finding these W functions from Eq. (1) and a modified form of Eq. (2) is the same as in Sec. I, and is not repeated here. A straightforward calculation yields

$$W(S\rightarrow G/S;t)=\Gamma_S\exp(-\Gamma_S t)\ ,$$

$$W(E\rightarrow S/G;t)=\frac{R\Gamma_S}{C}\exp\left[\left(-R-\frac{\Gamma_S}{2}+\frac{C}{2}\right)t\right]-\frac{R\Gamma_S}{C}\exp\left[\left(-R-\frac{\Gamma_S}{2}-\frac{C}{2}\right)t\right]\ , \tag{10}$$

where

$$C=(4R^2+\Gamma_S^2)^{1/2}\ .$$

Substitution of Eq. (10) into Eq. (9) yields

$$D(\omega_{ES},\tau)=\frac{\Gamma_S^2 R}{C}\left[\frac{\exp(-\Gamma_S\tau)-\exp[(-R-\Gamma_S/2-C/2)\tau]}{-R+\Gamma_S/2-C/2}\right]+(C\rightarrow -C)\ , \tag{11}$$

where $(C\rightarrow -C)$ represents a term substituting $-C$ for C. This function clearly manifests an antibunching effect[16] [$D(\omega_{ES},0)=0$]. (It is impossible to emit the second ω_{ES} photon right after the first emission of a ω_{ES} photon.) In the limit of strong pumping $R\gg\Gamma_S$ Eq. (11) reduces to a form

$$D(\omega_{ES},\tau)=\Gamma_S[\exp(-\Gamma_S\tau/2)-\exp(-\Gamma_S\tau)]\ , \tag{12}$$

which still exhibits antibunching. This can be expected from the cascade structure of the system.[17] In other words, the system still takes a time Γ_S^{-1} to decay out of state $|S\rangle$ even though the pumping R is so strong that the system can be rapidly pumped to state $|E\rangle$ from state $|G\rangle$.

A knowledge of the delay function $D(\omega_{ES},\tau)$ is enough to determine the complete photon statistics. The quantities $\bar{m}_T$ and Δm_T, defined as the average number and the dispersion of ω_{ES} photons emitted during a time period T, can be determined from[12]

$$\bar{m}_T=T/\bar{\tau},\quad \Delta m_T^2=\bar{m}_T\Delta\tau^2/\bar{\tau}^2\ , \tag{13}$$

where $\bar{\tau}$ and $\Delta\tau^2$ (the average and the dispersion of the delay time τ between successive photon emissions) can be calculated from Eq. (11) to be

$$\bar{\tau}=\frac{3R+\Gamma_S}{R\Gamma_S},\quad \Delta\tau^2=\frac{5R^2+2R\Gamma_S+\Gamma_S^2}{R^2\Gamma_S^2}\ . \tag{14}$$

It follows from Eqs. (13) and (14) that

$$\bar{m}_T=T\frac{R\Gamma_S}{\Gamma_S+3R},\quad \Delta m_T^2=\bar{m}_T\frac{5R^2+2R\Gamma_S+\Gamma_S^2}{(\Gamma_S+3R)^2}\ , \tag{15}$$

where the factor $R/(\Gamma_S+3R)$ can again be interpreted as the quasi-steady-state population of state $|E\rangle$. Here, we find that $\Delta m_T^2<\bar{m}_T$ and the photon statistics are sub-Poissonian. This reduced fluctuation (as compared to a coherent state where $\Delta m_T^2=\bar{m}_T$) can be explained by noting that $D(\omega_{ES},\tau)$ is a more sharply peaked function of τ than the corresponding D function for a coherent state [$D(\tau)=\Gamma\exp(-\Gamma\tau)$] so that the time delay between successive photon emissions is approximately constant. Thus we should detect roughly the same number of photons in each time interval T. Sub-Poissonian, Poissonian, or super-Poissonian statistics are usually characterized by Mandel's Q factor,[18] which is defined in terms of $\bar{m}_T$ and Δm_T^2 as

$$Q=\Delta m_T^2/\bar{m}_T-1\ , \tag{16}$$

where

$$Q\begin{cases}<0, & \text{sub-Poissonian}\\ =0, & \text{Poissonian}\\ >0, & \text{super-Poissonian}\ .\end{cases} \tag{17}$$

In our problem, we find, by using Eqs. (15) and (16), that

$$Q=-\frac{4R(\Gamma_S+R)}{(\Gamma_S+3R)^2}\cong-\frac{4}{9}\quad(\text{when } R\gg\Gamma_S)\ . \tag{18}$$

IV. COHERENT PUMP

The incoherent pump field is now replaced by a strong coherent pump (laser) field. The laser field is assumed to be resonant with the transition frequency of each atom and is strong enough to saturate the two-photon $|G\rangle\leftrightarrow|E\rangle$ transition. We use a dressed-atom approach,[19] not only because it can account for quantum-mechanical coherence effects such as the ac Stark splitting, but also because it can permit us to interpret the results in a relatively simple manner. In this picture, we first neglect the coupling of the two-atom system to the vacuum which is responsible for spontaneous emission. After the laser field is quantized, the dynamics of the to-

tal system (two-atom plus the laser field) is governed by the time-independent Hamiltonian[20]

$$H=\hbar\omega_0(\sigma_1^+\sigma_1^-+\sigma_2^+\sigma_2^-+a^\dagger a)+\hbar V(\sigma_1^+\sigma_2^-+\sigma_2^+\sigma_1^-)$$
$$+i\hbar g(e^{-i\mathbf{k}\cdot\mathbf{d}/2}\sigma_1^+ + e^{i\mathbf{k}\cdot\mathbf{d}/2}\sigma_2^+)a+\text{H.c.}\ , \tag{19}$$

where σ_i^+ (σ_i^-) is the atomic raising (lowering) operator of the ith atom ($i=1,2$) and $a^\dagger(a)$ is the creation (annihilation) operator of the laser photons. The first line in Eq. (19) represents the free energy of the atoms and the laser field. The second line represents the atom-atom interaction which is responsible for the energy shifts V shown in Fig. 1. The third line represents the atom-field dipole interaction, with coupling constant $g\exp(\mp i\mathbf{k}\cdot\mathbf{d}/2)$, where $\pm\mathbf{d}/2$ are the positions of the atoms and $\mathbf{k}$ is the wave vector of the laser field. The eigenstates for the Hamiltonian (19), called dressed states, are superpositions of products of atomic states and field states. In this section, we assume that $\mathbf{k}\cdot\mathbf{d}=0$, so that the atom-field coupling is identical for both atoms. When $\mathbf{k}\cdot\mathbf{d}=0$, the coupling in Eq. (19) involves only the symmetrical atomic states [i.e., only $i\hbar g(\sigma_1^+ +\sigma_2^+)a+\text{H.c.}$ appears]. In this case, the dressed states are found to be[7]

$$|1,n\rangle=\frac{\cos\theta}{\sqrt{2}}(|E,n-2\rangle-|G,n\rangle)-i\sin\theta|S,n-1\rangle\ ,$$
$$|2,n\rangle=\frac{1}{\sqrt{2}}(|E,n-2\rangle+|G,n\rangle)\ ,$$
$$|3,n\rangle=\frac{\sin\theta}{\sqrt{2}}(|E,n-2\rangle-|G,n\rangle)+i\cos\theta|S,n-1\rangle\ , \tag{20}$$
$$|4,n\rangle=|A,n-1\rangle\ ,$$

with the corresponding eigenenergies

$$E_{1,n}=\hbar\{n\omega_0+\tfrac{1}{2}[(V^2+\Omega_R^2)^{1/2}+V]\}\ ,$$
$$E_{2,n}=\hbar(n\omega_0)\ ,$$
$$E_{3,n}=\hbar\{n\omega_0-\tfrac{1}{2}[(V^2+\Omega_R^2)^{1/2}-V]\}\ , \tag{21}$$
$$E_{4,n}=\hbar(n\omega_0-V)\ ,$$

where n ($n=1,2,\ldots$) is the occupation number for the laser field state and Ω_R is the usual Rabi frequency which can be written in terms of g and $\bar{n}$ (the average number of laser photons) as

$$\Omega_R=4g\bar{n}^{1/2}\ . \tag{22}$$

Note that we exploited the quasiclassical character of the laser field by evaluating Ω_R at $\bar{n}$.[19] The factors $\cos\theta$ and $\sin\theta$ are functions of Ω_R and V

$$\cos\theta=\left[\frac{(V^2+\Omega_R^2)^{1/2}-V}{2(V^2+\Omega_R^2)^{1/2}}\right]^{1/2}\ ,$$
$$\sin\theta=\left[\frac{(V^2+\Omega_R^2)^{1/2}+V}{2(V^2+\Omega_R^2)^{1/2}}\right]^{1/2}\ . \tag{23}$$

Energy levels of these states are shown in Fig. 3 and form an infinite ladder of nearly degenerate four-state multiplets. Adjacent multiplets are separated by the laser frequency ω_0.

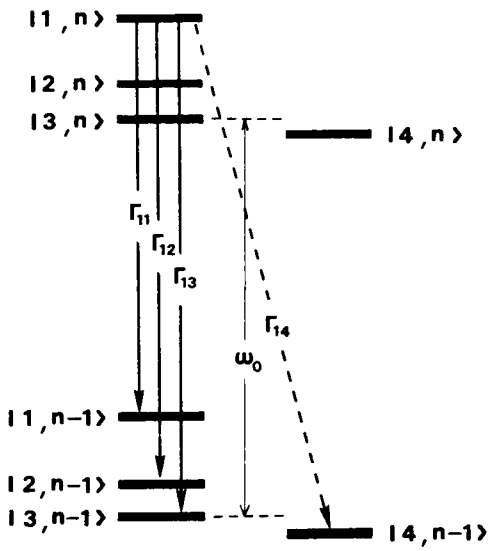

FIG. 3. Energy levels of the dressed states $|\alpha,n\rangle$ for the two-atom plus laser field system. Adjacent multiplets are separated by the laser frequency ω_0. Decay rates $\Gamma_{1\alpha}$ from state $|1,n\rangle$ to the lower lying states $|\alpha,n-1\rangle$ ($\alpha=1,2,3,4$) are indicated in the figure. When $d\ll\lambda_0$, the decay rate Γ_{14} to state $|4,n-1\rangle$ (represented by a dashed arrow) is much smaller than the decay rates to the other states (represented by solid arrows).

Coupling the states to the vacuum produces states having bandwidths on the order of Γ_S or Γ_A, and results in the system's cascade down the quantum ladder in which the decays between adjacent multiplets occur with rates Γ_S or Γ_A. Each of these decays corresponds to the creation of a fluorescence photon whose frequency is determined by the energy separation between the dressed states, within the uncertainty given by the bandwidths. It is assumed that the states in a given multiplet do not overlap (secular approximation),[19] i.e.,

$$(E_{\alpha,n}-E_{\beta,n})/\hbar\gg 2\Gamma(\cong\Gamma_S\gg\Gamma_A)\ \text{ for all } \alpha,\beta\ . \tag{24}$$

Under this condition, general relaxation theory dictates that the cascade of the system can be described as a rate process among the dressed states

$$\frac{d}{dt}\Pi_{\alpha,n}(t)=-\Pi_{\alpha,n}(t)\sum_{\beta=1}^{4}\Gamma_{\alpha\beta}^{(n)}+\sum_{\beta=1}^{4}\Pi_{\beta,n+1}(t)\Gamma_{\beta\alpha}^{(n+1)}\ , \tag{25}$$

where $\Pi_{\alpha,n}(t)$ is the time-dependent population of the state $|\alpha,n\rangle$ and $\Gamma_{\alpha\beta}^{(n)}$ is the decay rate for the $|\alpha,n\rangle\rightarrow|\beta,n-1\rangle$ ($\alpha,\beta=1,2,3,4$) transition calculated from[20]

$$\Gamma_{\alpha\beta}^{(n)}=\frac{\Gamma_S}{2}|\langle\alpha,n|(\sigma_1^+ +\sigma_2^+)|\beta,n-1\rangle|_{n=\bar{n}}^2+\frac{\Gamma_A}{2}|\langle\alpha,n|(\sigma_1^+ -\sigma_2^+)|\beta,n-1\rangle|_{n=\bar{n}}^2\ . \tag{26}$$

Using Eqs. (20) and (26), we find $\Gamma_{\alpha\beta}^{(n)}$ in matrix form as

$$\Gamma_{\alpha\beta}^{(n)}=\begin{bmatrix} \frac{1-D^2}{2}\Gamma_S & \frac{1-D}{4}\Gamma_S & \frac{D^2}{2}\Gamma_S & \frac{1+D}{4}\Gamma_A \\ \frac{1-D}{4}\Gamma_S & 0 & \frac{1+D}{4}\Gamma_S & \frac{1}{2}\Gamma_A \\ \frac{D^2}{2}\Gamma_S & \frac{1+D}{4}\Gamma_S & \frac{1-D^2}{2}\Gamma_S & \frac{1-D}{4}\Gamma_A \\ \frac{1+D}{4}\Gamma_A & \frac{1}{2}\Gamma_A & \frac{1-D}{4}\Gamma_A & 0 \end{bmatrix}, \tag{27}$$

where

$$D=\cos^2\theta-\sin^2\theta=-V/(V^2-\Omega_R^2)^{1/2},$$

and $\cos\theta$ and $\sin\theta$ are given in Eq. (23). The rows and columns in matrix (27) are labeled according to Eq. (26). Again, we evaluated $\Gamma_{\alpha\beta}^{(n)}$ at $n=\bar{n}$, so that $\Gamma_{\alpha\beta}^{(n)}$ is the same for any pair of adjacent multiplets. The first term in Eq. (26) represents decays among the atomic symmetrical states and constitutes the 3×3 subblock in matrix (27), while the second term represents decays between the atomic symmetrical and antisymmetrical states and constitutes the 1×3 and 3×1 subblocks in matrix (27).

As is seen from Eq. (27), there are 14 possible transitions corresponding to the creation of photons with at most 13 different frequencies (the $|1,n\rangle\rightarrow|1,n-1\rangle$ and $|3,n\rangle\rightarrow|3,n-1\rangle$ transitions create photons which have the same frequency ω_0). However, when the two atoms are very close ($d\ll\lambda_0$), six of the decays (those involving decays to or from states $|4,n\rangle$) are relatively improbable. Consequently, one expects bright and dark periods in the fluorescence owing to the metastable states $|4,n\rangle$. A BP corresponds to a fast cascade of the system among the short-lived states $|\alpha,n\rangle$ ($\alpha=1,2,3$). When a transition $|\alpha,n\rangle\rightarrow|4,n-1\rangle$ ($\alpha=1$, 2, or 3) occurs, this fast cascade is interrupted and the BP ends; once a $|4,n\rangle\rightarrow|\alpha,n-1\rangle$($\alpha=1$, 2, or 3) decay occurs, the next BP starts.

The steady-state and quasi-steady-state populations [obtained by setting $\Gamma_A=0$ in Eq. (27)] of the dressed states are found from Eq. (25) to be

$$\Pi_\alpha^{ss}=\left[\sum_{n=0}^{\infty}\Pi_{\alpha,n}\right]^{ss}=\frac{1}{4}\quad(\alpha=1,2,3,4),$$

$$\Pi_\alpha^{qs}=\left[\sum_{n=0}^{\infty}\Pi_{\alpha,n}\right]^{qs}=\frac{1}{3}\quad(\alpha=1,2,3)\text{ in a BP}. \tag{28}$$

In this limit, we also see from Eq. (20) that in a BP the quasi-steady-state populations of the bare atom states are equal $[\Pi_i^{qs}=(\sum_{n=0}^{\infty}\Pi_{i,n})^{qs}=\frac{1}{3}\ (i=E,S,G,)]$. The only approximation made leading to Eq. (28) is the secular approximation (24), which can be written in terms of Ω_R and V using Eq. (21) as $\sqrt{V\Gamma}\ll\Omega_R$ when $V\gg\Omega_R$. Therefore $\sqrt{V\Gamma}\ll\Omega_R\ll V$ is the condition under which the pumping scheme considered in Sec. II is valid. Note that when $\Omega_R\ll V$, the $|S\rangle\leftrightarrow|G\rangle$ transition is not appreciably driven by the laser field.

We now study the duration of a single BP and DP. Suppose that at time $t=0$ the system decays from state $|4,n+1\rangle$ to state $|\alpha,n\rangle$ and the state $|\alpha,n\rangle$ is populated with a probability p_α ($\alpha=1,2,3$) (the beginning of a BP). The probability p_α is the branching ratio

$$p_\alpha=\frac{\Gamma_{4\alpha}}{\sum_{\alpha'=1}^{3}\Gamma_{4\alpha'}}, \tag{29}$$

where the Γ's are given in Eq. (27). In order to obtain the probability describing the duration τ of a single BP, $P_B(\tau)$, we need to know when the *next* $|\beta,n'\rangle\rightarrow|4,n'-1\rangle$ ($\beta=1$, 2, or 3; $n'\le n$) transition occurs. Analogous to Eq. (5), we can write $P_B(\tau)$ as

$$P_B(\tau)=1-\int_0^\tau dt\left[\sum_{\alpha,\beta=1}^{3}p_\alpha W(\beta\rightarrow4/\alpha;t)\right]$$

$$=1-\int_0^\tau dt\left[\sum_{\alpha,\beta=1}^{3}p_\alpha\sum_{f=0}^{\infty}W^{(f)}(\beta\rightarrow4/\alpha;t)\right], \tag{30}$$

where the function $W^{(f)}(\beta\rightarrow4/\alpha;t)$ is the probability per unit time that, starting from state $|\alpha,n\rangle$, the system makes f successive decays *excluding* those of type $|\mu,n'\rangle\rightarrow|4,n'-1\rangle$ ($\mu=1,2,3$; $n\ge n'\ge n-f+1$) between times 0 and t, and then decays from state $|\beta,n-f\rangle$ to state $|4,n-f-1\rangle$ ($\beta=1$, 2, or 3) for the first time at t (see Fig. 4). It is tempting to try to calculate the function $W^{(f)}(\beta\rightarrow4/\alpha;t)$ by setting $\Gamma_{\mu4}^{(n')}$

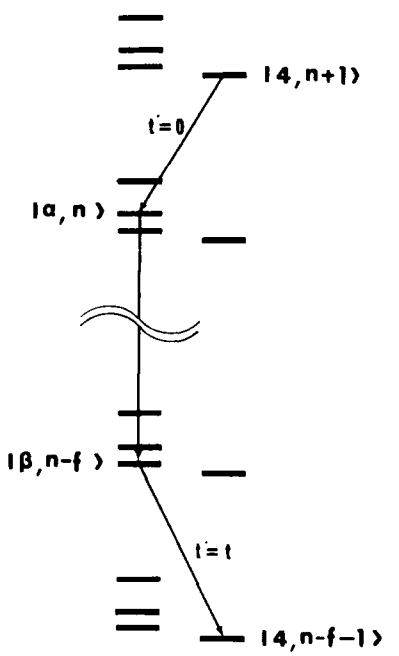

FIG. 4. The diagram shows a particular cascade which is characterized by the function $W^{(f)}(\beta\rightarrow4/\alpha;t)$, defined as a probability per unit time that, starting from state $|\alpha,n\rangle$, the system makes f successive decays *excluding* those of type $|\mu,n'\rangle\rightarrow|4,n'-1\rangle$ ($\mu=1,2,3$; $n\ge n'\ge n-f+1$) between times 0 and t, then decays from state $|\beta,n-f\rangle$ to state $|4,n-f-1\rangle$ ($\beta=1$, 2, or 3). The initial and final transitions in the cascade correspond to those out of and into metastable states.

($\mu=1,2,3$; $n\geq n'\geq n-f+1$) equal to zero in Eqs. (25) and (27). Tempting as it may be, this procedure leads to incorrect results since it modifies the dynamics of the system at times *before* the transition to the shelving level of interest. For this purpose, we introduce a more elementary branching function $w_{\mu\nu}(t)$, which is defined as the probability per unit time that, starting from state $|\mu,n'\rangle$, the system decays to state $|\nu,n'-1\rangle$ ($\mu,\nu=1,2,3,4$) at a time t. Since the branching function above involves only transitions between adjacent multiplets, it can be calculated by the same method used in Sec. II. Terms in Eqs. (25) and (27) corresponding to decays to states in the $(n'-2)$ multiplet are set equal to zero. Note that we still have a right to set these Γ's equal to zero because this does not alter the dynamics of the system *until* the system decays to states $|\nu,n'-1\rangle$. The branching function is found to be

$$w_{\mu\nu}(t)\left[=\frac{d}{dt}\Pi'_{\nu,n'-1}(t)\right]=\Gamma_{\mu\nu}\exp\left[-\sum_{\nu'=1}^{4}\Gamma_{\mu\nu'}t\right]. \tag{31}$$

In Eq. (31), the prime of the population denotes the modified population of state $|\nu,n-1\rangle$ as before. We now write $W^{(f)}(\beta\rightarrow 4/\alpha;t)$ using Eq. (31) by considering all possible paths during f successive decays as

$$W^{(f)}(\beta\rightarrow 4/\alpha;t)=\sum_{(\epsilon,\zeta,\ldots,\xi)=1}^{4}\int_0^t dt_f\int_0^{t_f}dt_{f-1}\cdots\int_0^{t_2}dt_1[w_{\alpha\epsilon}(t_1)w_{\epsilon\zeta}(t_2-t_1)\cdots w_{\xi\beta}(t_f-t_{f-1})w_{\beta 4}(t-t_f)], \tag{32}$$

where the summation $\sum$ excludes paths involving transitions $|\mu,n'\rangle\rightarrow|4,n'-1\rangle$ ($\mu=1,2,3$; $n\geq n'\geq n-f+1$). In order to proceed further, we first take the Laplace transform of Eq. (32). This yields a simple product of f functions of the form $w_{\mu\nu}(s)=\Gamma_{\mu\nu}/(s+\sum_{\nu'=1}^{4}\Gamma_{\mu\nu'})$; each being the Laplace transform of Eq. (31). Now, the summation over all possible intermediate states can be done easily by treating the $w_{\mu\nu}(s)$ function as the component of a matrix $\underline{W}(s)$. We see from Eqs. (27) and (31) that these matrices are identical so that the final result is the matrix $\underline{W}(s)$ raised to the fth power. However, the matrix must be modified to account for the fact that some of the paths are excluded from the summation. Thus we introduce a modified matrix, $\underline{W}_B(s)$ as

$$[\underline{W}_B(s)]_{\mu\nu}=\begin{cases}w_{\mu\nu}(s), & \text{when } (\mu,\nu)\neq(\mu',4),\ (\mu'=1,2,3)\\ 0, & \text{when } (\mu,\nu)=(\mu',4),\ (\mu'=1,2,3).\end{cases} \tag{33}$$

Note that we did not set $\Gamma_{\mu'4}$ ($\mu'=1,2,3$) equal to zero, which would alter matrix elements of $\underline{W}(s)$ corresponding to allowed transitions. Thus we write Eq. (32) as

$$W^{(f)}(\beta\rightarrow 4/\alpha;t)=\mathcal{L}_t^{-1}\{([\underline{W}_B(s)]^f)_{\alpha\beta}w_{\beta 4}(s)\}, \tag{34}$$

where the symbol $\mathcal{L}^{-1}$ represents the inverse Laplace transform. Then, substitution of Eqs. (29) and (34) into Eq. (30) yields

$$P_B(\tau)=1-\sum_{\alpha,\beta=1}^{3}\frac{\Gamma_{4\alpha}}{\sum_{\alpha'=1}^{3}\Gamma_{4\alpha'}}\int_0^\tau dt\,\mathcal{L}_t^{-1}\left[\sum_{f=0}^{\infty}([\underline{W}_B(s)]^f)_{\alpha\beta}w_{\beta 4}(s)\right]. \tag{35}$$

This formula is exact. However, in the limit $\Gamma_A\ll\Gamma_S$, this reduces to

$$P_B(\tau)=\exp\left[-\left[\sum_{\beta=1}^{3}\tfrac{1}{3}\Gamma_{\beta 4}\right]\tau\right]=\exp(-\tau/\tau_B),$$

$$\tau_B=\left[\sum_{\beta=1}^{3}\tfrac{1}{3}\Gamma_{\beta 4}\right]^{-1}=3\Gamma_A^{-1}. \tag{36}$$

The factor of $\frac{1}{3}$ in the exponential can be interpreted as the quasi-steady-state populations (28). The reason for the appearance of this factor is the same as before [see the argument below Eq. (4) in Sec. II].

A similar calculation yields

$$P_D(\tau)=1-\sum_{\beta=1}^{3}\int_0^\tau dt\,\mathcal{L}_t^{-1}\left[\sum_{f=0}^{\infty}([\underline{W}_D(s)]^f)_{44}w_{4\beta}(s)\right]$$

$$=\exp(-\tau/\tau_D).$$

$$\tau_D=\left[\sum_{\beta=1}^{3}\Gamma_{4\beta}\right]^{-1}=\Gamma_A^{-1}. \tag{37}$$

This time, matrix $\underline{W}_D(s)$ is defined as

$$[\underline{W}_D(s)]_{\mu\nu}=\begin{cases}w_{\mu\nu}(s),\\ \text{when } (\mu,\nu)\neq(4,\nu')\ (\nu'=1,2,3)\\ 0,\\ \text{when } (\mu,\nu)=(4,\nu')\ (\nu'=1,2,3).\end{cases} \tag{38}$$

We find that $P_B(\tau)$ and $P_D(\tau)$ are completely independent of the Rabi frequency Ω_R and the energy shift V.

This results in part from the secular approximation (24), and, in part, owing to the fact that state $|4,n\rangle$ is completely decoupled from the laser due to our choice of geometry ($\mathbf{k}\cdot\mathbf{d}=0$). Coupling of state $|4\rangle$ to the symmetrical states occurs via spontaneous decay only and does not involve the Rabi frequency Ω_R.

V. PHOTON STATISTICS IN A DRESSED-ATOM PICTURE

We have formulated the probability distributions of durations of a single BP and DP based on an elementary branching function $w_{\mu\nu}(t)$. However, the real power of this method will become apparent when frequency-resolved photon statistics are considered in a dressed-atom picture.

In this section, we consider a delay function $D(\omega_{\alpha\beta},\tau)$ defined as the probability distribution for the time delay τ between successive emissions of $\omega_{\alpha\beta}$ photons. For simplicity, let us suppose that the transition $|\alpha,n+1\rangle\rightarrow|\beta,n\rangle$ for fixed pairs of (α,β) and any n creates a photon with a definite frequency $\omega_{\alpha\beta}$. This assumption corresponds to the secular approximation, such as Eq. (24), and the quasiclassical character of the laser field. The first emission of a $\omega_{\alpha\beta}$ photon leaves the system in state $|\beta,n\rangle$ (n can be any integer) at time $t=0$. Therefore the function $D(\omega_{\alpha\beta},\tau)$ can be interpreted as a probability per unit time that from this initial state $|\beta,n\rangle$, the system makes any number (f) of successive decays while creating many types of photons *exclusive* of $\omega_{\alpha\beta}$ photons, and eventually reaches a state $|\alpha,n-f\rangle$, from which the system makes the final decay $|\alpha,n-f\rangle\rightarrow|\beta,n-f-1\rangle$ at time τ. Analogous to Eq. (34), we thus write $D(\omega_{\alpha\beta},\tau)$ as

$$D(\omega_{\alpha\beta},\tau)=\mathcal{L}_\tau^{-1}\left[\sum_{f=0}^{\infty}([\underline{W}_{(\alpha\beta)}(s)]^f)_{\beta\alpha}w_{\alpha\beta}(s)\right], \tag{39}$$

where matrix $\underline{W}_{(\alpha\beta)}(s)$ is defined as

$$[\underline{W}_{(\alpha\beta)}(s)]_{\mu\nu}=\begin{cases}w_{\mu\nu}(s), & \text{when } (\mu,\nu)\neq(\alpha,\beta)\\ 0, & \text{when } (\mu,\nu)=(\alpha,\beta)\ .\end{cases} \tag{40}$$

As a first example of an application of Eqs. (39) and (40), we consider the FRPS of the fluorescence photons produced by a single two-level atom irradiated by a strong coherent laser with Rabi frequency Ω_R and detuning δ.[21,22] The frequency spectrum of the fluorescence photons is the well-known Mollow triplet.[6] These photons are produced when the system cascades down the ladder consisting of states $|\alpha,n\rangle$, executing the four types of transitions $|\alpha,n\rangle\rightarrow|\beta,n-1\rangle$ ($\alpha,\beta=1,2$; $n=1,2,\ldots$). The decay rates $\Gamma_{\alpha\beta}$ between the adjacent multiplets were calculated to be[23]

$$\Gamma_{\alpha\beta}=\frac{\Gamma}{4(\Omega_R^2+\delta^2)}\begin{bmatrix}\Omega_R^2 & [(\Omega_R^2+\delta^2)^{1/2}-\delta]^2\\ [(\Omega_R^2+\delta^2)^{1/2}+\delta]^2 & \Omega_R^2\end{bmatrix}. \tag{41}$$

Let us calculate the delay function of the ω_{21} photons. The $\underline{W}_{(\alpha\beta)}(s)$ matrix in Eq. (40) takes the form

$$\underline{W}_{(21)}(s)=\begin{bmatrix}\dfrac{\Gamma_{11}}{s+\Gamma_{11}+\Gamma_{12}} & \dfrac{\Gamma_{12}}{s+\Gamma_{11}+\Gamma_{12}}\\ 0 & \dfrac{\Gamma_{22}}{s+\Gamma_{21}+\Gamma_{22}}\end{bmatrix}. \tag{42}$$

Substitution of Eqs. (42) and $w_{21}(s)=\Gamma_{21}/(s+\Gamma_{21}+\Gamma_{22})$ into Eq. (39) with the use of the formula

$$\begin{bmatrix}a & b\\ 0 & c\end{bmatrix}^f=\begin{bmatrix}a^f & b\dfrac{a^f-c^f}{a-c}\\ 0 & c^f\end{bmatrix}$$

yields

$$D(\omega_{21},\tau)=\frac{\Gamma_{12}\Gamma_{21}}{\Gamma_{12}-\Gamma_{21}}[\exp(-\Gamma_{21}\tau)-\exp(-\Gamma_{12}\tau)]\ . \tag{43}$$

This function clearly manifests the antibunching effect $D(\omega_{21},0)=0$, simply explained by the fact that the emission of a ω_{21} photon at time $t=0$ projects the wave function of the system to one of the dressed states $|1,n\rangle$ so that the system is unable to emit a photon created by the same type of transition $|2,n\rangle\rightarrow|1,n-1\rangle$ without any time delay. From Eq. (43), we find the average and the dispersion of the delay time τ to be

$$\bar{\tau}=\frac{\Gamma_{21}+\Gamma_{12}}{\Gamma_{21}\Gamma_{12}},\quad \Delta\tau^2=\frac{\Gamma_{21}^2+\Gamma_{12}^2}{\Gamma_{21}^2\Gamma_{12}^2}\ . \tag{44}$$

Substitution of Eq. (44) into Eq. (13) yields

$$\bar{m}_T=T\frac{\Gamma_{12}\Gamma_{21}}{\Gamma_{12}+\Gamma_{21}}=\frac{\Gamma T}{8}\frac{\Omega_R^4}{(\Omega_R^2+\delta^2)(\Omega_R^2+2\delta^2)}\ , \tag{45}$$

$$\Delta m_T=\left[\bar{m}_T\frac{\Gamma_{12}^2+\Gamma_{21}^2}{(\Gamma_{12}+\Gamma_{21})^2}\right]^{1/2}=\left[\bar{m}_T\frac{2(\Omega_R^2+2\delta^2)^2-\Omega_R^4}{2(\Omega_R^2+2\delta^2)^2}\right]^{1/2}, \tag{46}$$

where we used Eq. (41) to write Γ's in terms of Ω_R and δ. As can be seen from Eq. (46), the photon statistics are sub-Poissonian. Mandel's Q factor can be calculated from Eqs. (16), (45) and (46) to be

$$Q=-\frac{\Omega_R^4}{2(\Omega_R^2+2\delta^2)^2}\geq-\frac{1}{2}\ , \tag{47}$$

which is in complete agreement with previously obtained result.[22]

As a second example, we consider the FRPS in a BP of the fluorescence of two-atom system considered in Sec. IV, but now in a dressed-atom picture. This is more complicated owing to the level structure of the dressed states. For simplicity, we completely ignore the existence of state $|4,n\rangle$. In order to study the FRPS, we again need to know the delay function $D(\omega_{\alpha\beta},\tau)$ for a fixed pair of (α,β) $(\alpha,\beta=1,2,3)$. We must evaluate the fth power of a 3×3 $\underline{W}_{(\alpha\beta)}$ matrix, whose analytical expression is sometimes impossible to find. However, we can still find an approximate expression for $D(\omega_{\alpha\beta},\tau)$ by truncating the sum in Eq. (39), corresponding to the *minimum* delay time or *minimum* number of successive decays between the dressed states required for the emission of the *next* $\omega_{\alpha\beta}$ photon. As an example, let us consider ω_{12} photons. Since the first nonvanishing $([\underline{W}_{(12)}(s)]^f)_{21}$ occurs when $f=1$ in Eq. (39), we predict that

$$\begin{aligned}D(\omega_{12},\tau)&\cong\mathcal{L}_\tau^{-1}[w_{21}(s)w_{12}(s)]\\&=\left[\frac{(3-D)\Gamma_S}{4}\right]^2\tau\exp\left[-\frac{(3-D)\Gamma_S}{4}\tau\right],\end{aligned} \tag{48}$$

where $D(\omega_{12},\tau)$ is renormalized as $\int_0^\infty D(\omega_{12},\tau)d\tau=1$. Using Eqs. (13) and (48), we find that $\bar{m}_T=T\Gamma_S(3-D)/8$ and $\Delta m=(\bar{m}_T/2)^{1/2}$ (sub-Poissonian).

VI. COHERENT PUMPING WITH ARBITRARY GEOMETRY ($\mathbf{k}\cdot\mathbf{d}\neq0$)

In Sec. IV, we considered the special case when $\mathbf{k}\cdot\mathbf{d}=0$. We found that only the transitions $|E\rangle\leftrightarrow|S\rangle$ and $|S\rangle\leftrightarrow|G\rangle$ involving the symmetrical atomic states were excited by the laser field. This result is also implied by Eq. (20) where the state $|4,n\rangle$ is the direct product $|A\rangle|n-1\rangle$. However, when $\mathbf{k}\cdot\mathbf{d}\neq0$, the situation is modified because the interatomic separation d now results in an atom–laser-field interaction Hamiltonian that varies as $i\hbar g[\cos(\mathbf{k}\cdot\mathbf{d}/2)](\sigma_1^+ +\sigma_2^+)a+\hbar g[\sin(\mathbf{k}\cdot\mathbf{d}/2)](\sigma_1^+-\sigma_2^+)a+\text{H.c.}$ It is seen that the coupling now contains antisymmetric as well as symmetric components. When $\mathbf{k}\cdot\mathbf{d}\ll1$, we find the approximate dressed states to be

$$\begin{aligned}|1,n\rangle'&=|1,n\rangle-\frac{\Omega_R\Lambda\mathbf{k}\cdot\mathbf{d}}{2(\Lambda+3V)}|4,n\rangle\ ,\\|2,n\rangle'&=|2,n\rangle\ ,\\|3,n\rangle'&=|3,n\rangle+\frac{\Omega_R\Lambda\mathbf{k}\cdot\mathbf{d}}{2(\Lambda-3V)}|4,n\rangle\ ,\\|4,n\rangle'&=|4,n\rangle+\frac{\Omega_R\Lambda\mathbf{k}\cdot\mathbf{d}}{2(\Lambda+3V)}|1,n\rangle\\&\quad-\frac{\Omega_R\Lambda\mathbf{k}\cdot\mathbf{d}}{2(\Lambda-3V)}|3,n\rangle\ ,\end{aligned} \tag{49}$$

where

$$\Lambda=(V^2+\Omega_R^2)^{1/2}\ .$$

The shift of eigenenergies $\Delta E_{\alpha,n}$ $(\alpha=1,2,3,4)$ from the energies given in Eq. (21) are expected to be small and on the order of $\Omega_R(\mathbf{k}\cdot\mathbf{d})^2$.

Modified decay rates between adjacent multiplets can be found from Eqs. (26) and (49). It is easy to see that the decay rates $\Gamma'_{\alpha\beta}$ $(\alpha,\beta=1,2,3)$ involving the short-lived states $|\alpha,n\rangle'$ $(\alpha=1,2,3)$ are not changed significantly from the values given in the 3×3 subblock in matrix (27), leading to the same quasi-steady-state populations (28). The rates $\Gamma'_{\alpha4}$ or $\Gamma'_{4\alpha}$ involving decays to or from the metastable states $|4,n\rangle'$, are different from the values given in the 1×3 and 3×1 subblocks in matrix (27). In particular, we find the modified total decay rate Γ'_4 to or from state $|4,n\rangle$ to be

$$\begin{aligned}\Gamma'_4&\equiv\sum_{\beta=1}^{3}\Gamma'_{4\beta}=\sum_{\beta=1}^{3}\Gamma'_{\beta4}\\&=\Gamma_A+\frac{(\mathbf{k}\cdot\mathbf{d})^2}{4}\frac{\Omega_R^2(\Omega_R^2+8V^2)}{(\Omega_R^2-8V^2)^2}\Gamma_S\\&\cong\Gamma_A\left[1+\frac{5(\hat{\mathbf{k}}\cdot\hat{\mathbf{d}})^2}{2}\frac{\Omega_R^2(\Omega_R^2+8V^2)}{(\Omega_R^2-8V^2)^2}\right],\end{aligned} \tag{50}$$

where approximate values for Γ_A and Γ_S appropriate to the limit $d\ll\lambda_0$ were used (see Sec. I). Analogous to Eqs. (36) and (37), we find

$$\begin{aligned}\tau'_B&=\left[\sum_{\beta=1}^{3}\frac{\Gamma'_{\beta4}}{3}\right]^{-1}=3(\Gamma'_A)^{-1}\ ,\\\tau'_D&=\left[\sum_{\beta=1}^{3}\Gamma'_{4\beta}\right]^{-1}=(\Gamma'_A)^{-1}\ .\end{aligned} \tag{51}$$

The reason for these shortened periods (τ'_D,τ'_B) is understood as follows: the laser excites not only the transitions $|E\rangle\leftrightarrow|S\rangle$ and $|S\rangle\leftrightarrow|G\rangle$ but also the transitions $|E\rangle\leftrightarrow|A\rangle$ and $|A\rangle\leftrightarrow|G\rangle$. Consequently, transitions to or from the shelving state $|A\rangle$ can be caused by stimulated emission and absorption (of the laser photons) to the short-lived states $|E\rangle$, $|S\rangle$, or $|G\rangle$ as well as by spontaneous emission.

VII. CONCLUSION

We have shown that it is possible to observe MQJ in the fluorescence through a cooperative atomic interaction. The jumps or discontinuous changes of the fluorescent intensity occurs on a time scale $\Gamma_A^{-1}\sim\Gamma^{-1}(\lambda_0/d)^2$. A restriction is imposed on the interatomic separation needed to observe MQJ by the finite response time of the detector. In order to make Γ_A^{-1} larger than the response time of the detector, d must be $\sim\lambda_0/100$. Current technology has yet to surmount this difficulty. Ion traps cannot be used because the Coulomb repulsion is too strong. Using neutral atom traps or confining atoms in a solid host may be the best hope of observing the two-atom MQJ described in this paper.

The formalism developed in this paper can be applied

to any four-level or more complicated scheme in which one or more states is metastable. Additionally, our formalism can be used to study the FRPS of any multilevel atom in a simple way.

Note added in proof. After submitting this article, we learned of a recent calculation of the dynamics of a two-atom composite system interacting with a weak incident field.[24] In that work, the time evolution of the symmetric states was studied, including the level shift of the intermediate symmetric state, but neglecting the transitions between symmetric and the antisymmetric states.

ACKNOWLEDGMENTS

This research is supported by National Science Foundation Grants No. PHY8415781 and No. PHY8814423, and by the U.S. Office of Naval Research.

[1]R. H. Dicke, Phys. Rev. **93**, 99 (1954).
[2]M. J. Stephen, J. Chem. Phys. **40**, 669 (1964).
[3]D. A. Hutchinson and H. F. Hameka, J. Chem. Phys. **41**, 2006 (1964); R. H. Lehmberg, Phys. Rev. A **2**, 883 (1970); D. F. Smirnov, I. V. Sokolov, and E. D. Trifonov, Zh. Eksp. Teor. Fiz. **63**, 2105 (1972) [Soviet Phys.—JETP **36**, 1111 (1973)].
[4]I. R. Senitzky, Phys. Rev. Lett. **40**, 1334 (1978).
[5]H. J. . michael, Phys. Rev. Lett. **43**, 1106 (1979); G. S. Agarwal, R. Saxena, L. M. Narducci, D. H. Feng, and R. Gilmore, Phys. Rev. A **21**, 257 (1980); M. Kus and K. Wodkiewicz, *ibid.* **23**, 853 (1981); C. C. Sung and C. M. Bowden, Opt. Commun. **45**, 273 (1983).
[6]B. R. Mollow, Phys. Rev. **188**, 1969 (1969).
[7]H. S. Freedhoff, Phys. Rev. A **19**, 1132 (1979).
[8]H. Dehmelt, Bull. Am. Phys. Soc. **20**, 66 (1975); R. J. Cook and H. J. Kimble, Phys. Rev. Lett. **54**, 1023 (1985).
[9]J. Javanainen, Phys. Rev. A **33**, 2121 (1986); D. T. Pegg, R. Loudon, and P. L. Knight, *ibid.* **33**, 4085 (1986); H. J. Kimble, R. J. Cook, and A. L. Wells, *ibid.* **34**, 3190 (1986); A. Schenzle, R. G. DeVoe, and R. G. Brewer, *ibid.* **33**, 2127 (1986).
[10]A. Schenzle and R. G. Brewer, Phys. Rev. A **34**, 3127 (1986).
[11]C. Cohen-Tannoudji and J. Dalibard, Europhys. Lett. **1**, 441 (1986).
[12]S. Reynaud, J. Dalibard, and C. Cohen-Tannoudji, IEEE J. Quantum Electron. **24**, 1395 (1988).
[13]P. Zoller, M. Marte, and D. F. Walls, Phys. Rev. A **35**, 198 (1987); G. Nienhuis, *ibid.* **35**, 4639 (1987); M. Porrati and S. Putterman, *ibid.* **39**, 3010 (1989); M. S. Kim and P. L. Knight, *ibid.* **40**, 215 (1989).
[14]W. Nagourney, J. Sandberg, and H. Dehmelt, Phys. Rev. Lett. **56**, 2797 (1986); Th. Sauter, W. Neuhauser, R. Blatt, and P. E. Toschek, *ibid.* **57**, 1696 (1986); J. C. Bergquist, R. G. Hulet, W. M. Itano, and D. J. Wineland, *ibid.* **57**, 1699 (1986).
[15]M. Lewenstein and J. Javanainen, Phys. Rev. Lett. **59**, 1289 (1987); M. Lewenstein and J. Javanainen, IEEE J. Quantum Electron. **24**, 1403 (1988).
[16]D. F. Walls, Nature **280**, 451 (1979), and references therein.
[17]R. Loudon, *The Quantum Theory of Light* (Oxford, Oxford, 1983), p. 326.
[18]L. Mandel, Opt. Lett. **4**, 205 (1979); R. J. Cook, Opt. Commun. **35**, 347 (1980); R. Short and L. Mandel, Phys. Rev. Lett. **51**, 384 (1983).
[19]C. Cohen-Tannoudji and S. Reynaud, J. Phys. B **10**, 345 (1977).
[20]G. S. Agarwal, *Quantum Optics*, Vol. 70 of *Springer Tracts in Modern Physics*, edited by G. T. Höhler (Springer-Verlag, New York, 1974).
[21]C. Cohen-Tannoudji and S. Reynaud, Philos. Trans. R. Soc. London Ser. A **293**, 223 (1979); P. A. Apanasevich and S. J. Kilin, J. Phys. B **12**, L83 (1979); A. Aspect and G. Roger, Phys. Rev. Lett. **45**, 617 (1980); J. Dalibard and S. Reynaud, J. Phys. (Paris) **44**, 1337 (1983).
[22]H. F. Arnoldus and G. Nienhuis, Opt. Commun. **48**, 322 (1984).
[23]C. Cohen-Tannoudji, in *Frontiers in Laser Spectroscopy*, Proceedings of the Les Houches Summer School 1975 Session 27, Les Houches, 1975, edited by R. Balian, S. Haroche, and S. Liberman (North-Holland, Amsterdam, 1977).
[24]M. Kim, F. A. M. de Oliveira, and P. L. Knight, Opt. Commun. **70**, 473 (1989).

Quantized-field approach to pressure-induced resonances

P. R. Berman
Department of Physics, New York University, 4 Washington Place, New York, New York 10003

G. Grynberg
Laboratoire de Spectroscopie Hertzienne de l'Ecole Normale Supérieure, 4 Place Jussieu, 75252 Paris CEDEX 05, France
(Received 25 July 1989)

Using a fully quantized dressed-atom approach, we present a theory and interpretation of the pressure-induced resonances in four-wave mixing (PIER4) that may arise when three incident fields interact with an ensemble of two-level atoms. The PIER4 resonances are seen to arise from a collisionally created modulation of a dressed-state population when an operator approach is used to solve the problem and from a level crossing between collisionally populated dressed states when an occupation-number formalism is used.

I. INTRODUCTION

In two previous papers,[1,2] we presented a theory and interpretation of various pressure-induced resonant structures that can appear in nonlinear spectroscopic line shapes. The first of these papers[1] concentrated on the problem of the excitation of a "three-level" atom by four incident radiation fields. Both semiclassical and fully quantized treatments were given, and an interpretation of the pressure-induced resonances in terms of transitions between atom-field dressed states was developed. In the second paper,[2] a semiclassical dressed-atom approach was followed. In that approach, the pressure-induced resonances that appear in four-wave mixing signals on a two-level atomic transition were interpreted in terms of a collisionally-induced creation of a modulated dressed-state population.

It is the purpose of this paper to present a fully quantized dressed-atom approach which is used to calculate the four-wave-mixing signal produced when three fields are incident on an ensemble of two-level atoms. This is one of the problems originally examined both theoretically and experimentally by Bloembergen and coworkers in their systematic study of pressure-induced resonances.[3] A more complete list of references to this and other work is included in our previous papers.[1,2]

To be more specific, we consider incident fields having amplitudes E_μ ($\mu=1,2,3$), frequencies

$$\Omega_1=\Omega,\ \Omega_2=\Omega,\ \Omega_3=\Omega+\delta\ , \tag{1}$$

and propagation vectors $\mathbf{k}_\mu$ ($\mu=1,2,3$). We seek the four-wave-mixing signal generated with propagation vector

$$\mathbf{k}_s=\mathbf{k}_1+\mathbf{k}_2-\mathbf{k}_3 \tag{2}$$

and frequency

$$\Omega_s=\Omega_1+\Omega_2-\Omega_3 \tag{3}$$

when these fields are incident on an ensemble of two-level atoms whose levels 1 and 2 are separated by frequency ω (Fig. 1). To satisfy phase-matching conditions, it is necessary that $|k_s-\Omega_s/c|L\ll 1$, where L is the length of the sample.

As δ is varied, the four-wave-mixing signal exhibits a resonant structure centered at $\delta=0$ in the presence of collisions.[1-3] This structure is given two interpretations in this work. First, in terms of operators, it is described as resulting from a collision-induced creation of a modulated dressed-state population operator. Second, in terms of occupation-number states, it is described as arising from a level crossing between collisionally populated dressed states. As such, the current approach provides a link between our two previous calculations. Moreover, it provides what we believe to be an attractive physical explanation for these pressure-induced resonances.

Section II introduces the basic assumptions and approximations of the theory. Section III contains the calculation in terms of dressed-state operators while Sec. IV summarizes the analogous calculation in terms of occupation-number dressed states.

It might be noted that several other fully quantum-mechanical calculations of four-wave mixing have appeared.[4] Our approach differs considerably in spirit from those calculations.

II. BASIC EQUATIONS AND ASSUMPTIONS

We consider a two-level atom (upper level 2, lower level 1) interacting with a quantized radiation field. In the absence of collisions, the Hamiltonian for such a system is given by

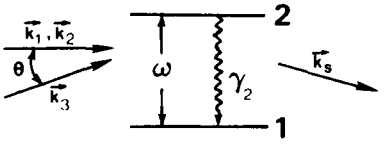

FIG. 1. The atom-field system considered in this work. The four-wave-mixing signal of interest is generated with propagation vector $\mathbf{k}_s=\mathbf{k}_1+\mathbf{k}_2-\mathbf{k}_3$ and frequency $\Omega_s=\Omega_1+\Omega_2-\Omega_3$.

$$H=\hbar\omega\sigma_{22}+\sum_{\mu}\hbar\Omega_{\mu}(a_{\mu}^{\dagger}a_{\mu}+\tfrac{1}{2})$$
$$-i\hbar\sum_{\mu}(f_{\mu}e^{i\mathbf{k}_{\mu}\cdot\mathbf{R}_0}\sigma_{21}a_{\mu}-f_{\mu}^{*}e^{-i\mathbf{k}_{\mu}\cdot\mathbf{R}_0}a_{\mu}^{\dagger}\sigma_{12}) , \quad (4)$$

where

$$\sigma_{ij}=|i\rangle\langle j| \quad (5)$$

is an atomic-state operator, ω is the frequency separation of levels 1 and 2, $a_{\mu}^{\dagger}$ and a_{μ} are creation and destruction operators, respectively, for field mode μ, Ω_{μ} is the frequency of field mode μ, and f_{μ} is a coupling constant to be specified below. For the present, the atom is assumed to be fixed at position $\mathbf{R}=\mathbf{R}_0$; a generalization to allow for atomic motion is included in the final results. A resonance or "rotating-wave" approximation is already implicit in the Hamiltonian (5); it is assumed that only modes with frequencies Ω_{μ} satisfying $|\Omega_{\mu}-\omega|/\omega\ll 1$ interact appreciably with the atoms.

We will work in the Heisenberg representation, in which any time-dependent operator $O(t)$ evolves as $\dot{O}=-(i/\hbar)[O,H]$. From the commutator relations

$$[\sigma_{ij}(t),\sigma_{kl}(t)]=\sigma_{il}(t)\delta_{jk}-\sigma_{kj}(t)\delta_{li} ,$$
$$[\sigma_{ij}(t),a_{\mu}(t)]=[\sigma_{ij}(t),a_{\mu}^{\dagger}(t)]=0 , \quad (6)$$
$$[a_{\mu}(t),a_{\mu'}(t)]=0, \quad [a_{\mu}(t),a_{\mu'}^{\dagger}(t)]=\delta_{\mu\mu'} ,$$

it follows directly that the time evolution of atomic and field operators is given by

$$\dot{\sigma}_{-}=-i\omega\sigma_{-}+\sum_{\mu}f_{\mu}e^{i\mathbf{k}_{\mu}\cdot\mathbf{R}_0}(\sigma_{22}-\sigma_{11})a_{\mu} , \quad (7a)$$

$$\dot{\sigma}_{22}=-\sum_{\mu}(f_{\mu}e^{i\mathbf{k}_{\mu}\cdot\mathbf{R}_0}\sigma_{+}a_{\mu}+f_{\mu}^{*}e^{-i\mathbf{k}_{\mu}\cdot\mathbf{R}_0}a_{\mu}^{\dagger}\sigma_{-}) , \quad (7b)$$

$$\dot{a}_{\mu}=-i\Omega_{\mu}a_{\mu}+f_{\mu}^{*}e^{-i\mathbf{k}_{\mu}\cdot\mathbf{R}_0}\sigma_{-} , \quad (7c)$$

where

$$\sigma_{+}\equiv\sigma_{21}, \quad \sigma_{-}\equiv\sigma_{12} \quad (8)$$

are raising and lowering operators, respectively, for the atomic states. It is not necessary to write time-evolution equations for σ_{+}, σ_{11}, and $a_{\mu}^{\dagger}$ since these operators are readily determined from

$$\sigma_{11}=1-\sigma_{22} , \quad (9a)$$

$$\sigma_{+}=(\sigma_{-})^{\dagger} , \quad (9b)$$

and

$$a_{\mu}=(a_{\mu})^{\dagger} . \quad (9c)$$

It is possible to formally integrate Eq. (7c), substitute the resulting expression into Eqs. (7a) and (7b), and perform the summation over the field modes. When this procedure is carried out in the Weisskopf-Wigner approximation, one finds that Eqs. (7) may be rewritten as[5]

$$\dot{\sigma}_{-}=-(\tfrac{1}{2}\gamma_2+i\omega)\sigma_{-}+\sum_{\mu=1}^{3}f_{\mu}e^{i\mathbf{k}_{\mu}\cdot\mathbf{R}_0}(2\sigma_{22}-1)a_{\mu} , \quad (10a)$$

$$\dot{\sigma}_{22}=-\gamma_2\sigma_{22}-\sum_{\mu=1}^{3}(f_{\mu}e^{i\mathbf{k}_{\mu}\cdot\mathbf{R}_0}\sigma_{+}a_{\mu}+f_{\mu}^{*}e^{-i\mathbf{k}_{\mu}\cdot\mathbf{R}_0}a_{\mu}^{\dagger}\sigma_{-}) , \quad (10b)$$

$$a_{\mu}=a_{\mu}(t_0)e^{-i\Omega_{\mu}(t-t_0)}+\int_{t_0}^{t}f_{\mu}^{*}e^{-i\mathbf{k}_{\mu}\cdot\mathbf{R}_0}\sigma_{-}(t')e^{-i\Omega_{\mu}(t-t')}dt' , \quad (10c)$$

where γ_2 is the spontaneous decay rate of level 2, t_0 is some arbitrary initial time, and ω now is assumed to include any radiative level shifts. In writing Eq. (10a), we have neglected a term

$$+\sum_{\mu=1,2,3}f_{\mu}e^{i\mathbf{k}_{\mu}\cdot\mathbf{R}_0}(2\sigma_{22}-1)a_{\mu}$$

and in (10b) a term

$$-\sum_{\mu=1,2,3}(f_{\mu}e^{i\mathbf{k}_{\mu}\cdot\mathbf{R}_0}\sigma_{+}a_{\mu}+f_{\mu}^{*}e^{-i\mathbf{k}_{\mu}\cdot\mathbf{R}_0}a_{\mu}^{\dagger}\sigma_{-}) .$$

Such terms, while important for maintaining the integrity of various operator products and commutation relations, do not contribute to the four-wave-mixing signal to be calculated below.[5,6]

The physical observable that is calculated is the rate at which photons are generated in a field mode α_0 ($\alpha_0\neq 1,2,3$) which was originally unoccupied. The number operator $\hat{n}_{\alpha_0}(t)$ for field mode α_0 is given by

$$\hat{n}_{\alpha_0}(t)=a_{\alpha_0}^{\dagger}(t)a_{\alpha_0}(t) . \quad (11)$$

Using Eq. (10c) and averaging the number operator over the initial atomic and radiation field states (denoted by $\langle\ \rangle_i$), one finds that the average number of photons emitted into a field mode α_0 that was initially unoccupied is equal to

$$n_{\alpha_0}(t)=\langle\hat{n}_{\alpha_0}(t)\rangle_i$$
$$=|f_{\alpha_0}|^2\sum_{j,j'=1}^{N}\int_{t_0}^{t}dt'\int_{t_0}^{t}dt''\exp\{i[\mathbf{k}_{\alpha_0}\cdot(\mathbf{R}_{j'}-\mathbf{R}_j)-\Omega_{\alpha_0}(t'-t'')]\}\langle\sigma_{+}^{j}(t'')\sigma_{-}^{j'}(t')\rangle_i , \quad (12)$$

where we have now included contributions to $n_{\alpha_0}(t)$ from an ensemble of N "active" atoms, located at positions $\mathbf{R}=\mathbf{R}_j (j=1,\ldots,N)$.

In general, σ^j will vary from one atomic site to another since both the phase and amplitude of the incident fields change as the fields propagate through the atomic medium. To simplify the calculation, we neglect all effects related to field depletion (i.e., it is assumed that the sample is optically thin). In this limit, there is no $\mathbf{R}_j$ dependence for σ^j_{11} and σ^j_{22} while $\sigma^j_{\pm}$ mirrors the (unmodified) spatial phase variations of the incident fields. In particular, it is shown below that the contribution to $\sigma^j_-(t)$ associated with the generation of a four-wave-mixing signal in a direction $\mathbf{k}_s$ varies as

$$\sigma^j_-(t)=\tilde{\sigma}^j_- e^{i(\mathbf{k}_s\cdot\mathbf{R}_j-\Omega_s t)} , \tag{13}$$

where $\tilde{\sigma}^j$ is independent of $\mathbf{R}_j$ since field-depletion effects have been neglected. When this expression is substituted into Eq. (12), it is seen that the major contribution to $n_{\alpha_0}(t)$ occurs when $\Omega_{\alpha_0}\simeq\Omega_s$ and $\mathbf{k}_{\alpha_0}\simeq\mathbf{k}_s$. Both of these conditions can be satisfied only if

$$k_s=\Omega_s/c , \tag{14}$$

which is a phase-matching condition for four-wave mixing. Assuming that this condition is satisfied, that $k_s|\mathbf{R}_j-\mathbf{R}_{j'}|\gg 1$ for $j\neq j'$ and that the limit $t\sim\infty$ in Eq. (12) is taken, we show in Appendix A that the rate $\dot{n}_s$ at which photons are emitted into mode $(\mathbf{k}_s,\Omega_s)$ is proportional to

$$\dot{n}_s\propto\sum_{j,j'=1}^{N}\langle\tilde{\sigma}^j_+\tilde{\sigma}^{j'}_-\rangle_i . \tag{15}$$

Equation (15) can now be generalized to incorporate collisional effects. In the absence of collisions, $\tilde{\sigma}^j_{\pm}$ is independent of j and $\dot{n}_s(t)$ varies as N^2. With collisions present, Eq. (15) must also be averaged over collision histories. Since the collision histories at each active-atom site can be taken as independent, it follows that $\langle\tilde{\sigma}^j_+\tilde{\sigma}^{j'}_-\rangle_c=\langle\tilde{\sigma}^j_+\rangle_c\langle\tilde{\sigma}^{j'}_-\rangle_c$ for $j\neq j'$ ($\langle\ \rangle_c$ indicates an average over collision histories). For $j=j'$ the contribution to $\dot{n}_s(t)$ is of order N and can be neglected in comparison with the N^2 contribution for $j\neq j'$. The quantities $\langle\tilde{\sigma}^j_{\pm}\rangle_c$ are independent of j since each atom, on average, sees the same collision history. Consequently, one finds the photon emission rate given by (15) is proportional to a quantity I_s defined by

$$I_s=\langle\langle\tilde{\sigma}_+\rangle_c\langle\tilde{\sigma}_-\rangle_c\rangle_i , \tag{16}$$

where the outer brackets refer to an average over the initial atomic and radiation field states. We shall refer to I_s as "the signal."

It is now straightforward to introduce collisions into the operator equations (10), since the signal depends only on $\langle\sigma\rangle_c$. The collision model adopted is one in which collisions do not affect population operators σ_{11} and σ_{22}, but result in a decay of coherence operators $\langle\sigma_-\rangle_c$ and $\langle\sigma_+\rangle_c$ with rate Γ. In this model, Eqs. (10) are transformed into

$$\langle\dot{\sigma}_-\rangle_c=-[(\tfrac{1}{2}\gamma_2+\Gamma)+i\omega]\langle\sigma_-\rangle+\sum_{\mu=1}^{3}f_\mu e^{i\mathbf{k}_\mu\cdot\mathbf{R}_0}(2\langle\sigma_{22}\rangle_c-1)a_\mu , \tag{17a}$$

$$\langle\dot{\sigma}_{22}\rangle_c=-\gamma_2\langle\sigma_{22}\rangle_c-\sum_{\mu=1}^{3}(f_\mu e^{i\mathbf{k}_\mu\cdot\mathbf{R}_0}\langle\sigma_+\rangle_c a_\mu+f^*_\mu e^{-i\mathbf{k}_\mu\cdot\mathbf{R}_0}a^\dagger_\mu\langle\sigma_-\rangle_c) , \tag{17b}$$

$$a_\mu=a_\mu(t_0)e^{-i\Omega_\mu(t-t_0)},\quad \mu=1,2,3 , \tag{17c}$$

where $\mathbf{R}_0$ is the position of an arbitrary active atom. The remaining atomic operators are given by

$$\langle\sigma_+\rangle_c=(\langle\sigma_-\rangle_c)^\dagger,\quad \langle\sigma_{11}\rangle_c=1-\langle\sigma_{22}\rangle_c . \tag{18}$$

Owing to our neglect of field depletion, the last term in Eq. (10c) has been dropped in arriving at Eq. (17c).

Equations (15)–(17) determine the rate at which photons are generated via four-wave mixing into field mode s. It should be noted that the commutation relations (6) are no longer valid for the operators $\langle\sigma\rangle_c$.[7] In subsequent equations, the $\langle\cdots\rangle_c$ averaging symbol is dropped.

III. SOLUTION VIA OPERATOR APPROACH IN DRESSED BASIS

Equations (17) describe the collisionally averaged interaction of three incident field modes with a two-level atom. Each field mode μ ($\mu=1,2,3$) is characterized by a wave vector $\mathbf{k}_\mu$, polarization $\hat{\epsilon}_\mu$, and frequency Ω_μ, such that $k_\mu=\Omega_\mu/c$. For simplicity, all fields are assumed to be polarized in the $\hat{y}$ direction, fields 1 and 2 are assumed to be incident in the $\hat{z}$ direction and field 3 propagates at a small angle $\theta\ll 1$ relative to the z axis (see Fig. 1). In order to calculate the phase-matched emission with new wave vector

$$\mathbf{k}_s=\mathbf{k}_1+\mathbf{k}_2-\mathbf{k}_3 \tag{19}$$

to lowest order in perturbation theory, it is necessary to obtain a solution to Eqs. (17) for $\sigma_-(\infty)$ which varies as $f_1f_2f_3^*$. The quantities f_μ ($\mu=1,2,3$) can be related to the Rabi frequencies of the incident fields by

$$if_\mu(\bar{n}_\mu)^{1/2}=\chi_\mu , \tag{20}$$

where

$$\chi_\mu=(p_y)_{21}E_\mu/2\hbar , \tag{21}$$

p_y is the y component of the atomic dipole operator, E_μ is an effective field amplitude for field mode μ, and $\bar{n}_\mu$ is the average number of photons in mode μ.

It is rather straightforward to solve Eqs. (17) using a perturbative approach. One obtains all the standard results relating to the PIER4 resonances.[3] Rather than follow the direct, perturbative approach, we introduce a dressed-state approach which enables us to give a simple physical interpretation to both the collision-induced terms and the background signal. Our approach is perturbative in nature, since the dressed states are defined to lowest order in the initially incident fields.

To simplify the algebraic complexity of the solution of Eqs. (17), we limit our discussion to atom-field detunings and decay rates which satisfy

$$(\gamma_2+\Gamma)/|\Delta_\mu| \ll 1 , \tag{22}$$

where Δ_μ is the atom-field detuning for field mode μ defined by

$$\Delta_\mu = \omega - \Omega_\mu . \tag{23}$$

This so-called *secular approximation*[8] often corresponds to the experimental conditions under which PIER4 resonances are observed.[3] It is further assumed that the various Rabi frequencies are less than or comparable to the spontaneous decay rate γ_2, in order to justify the perturbation expansion that is used.

In the context of these approximations, it becomes extremely convenient to introduce dressed states. We first consider fields 1 and 3 as the "dressing" fields and neglect the presence of field 2. The appropriate dressed states are the eigenstates of the Hamiltonian describing the interaction of a two-level atom with field modes 1 and 3 in the absence of collisions and spontaneous decay. Specifically, this Hamiltonian is given by

$$H_d = H_0 - i\hbar \sum_{\mu=1,3} [f_\mu(\mathbf{R}_0)\sigma_{12} a_\mu - f_\mu^*(\mathbf{R}_0) a_\mu^\dagger \sigma_{21}] , \tag{24a}$$

where

$$H_0 = \hbar\omega\sigma_{22} + \sum_{\mu=1,3} \hbar\Omega_\mu (a_\mu^\dagger a_\mu + \tfrac{1}{2}) \tag{24b}$$

and

$$f_\mu(\mathbf{R}_0) = f_\mu e^{i\mathbf{k}_\mu\cdot\mathbf{R}_0} . \tag{25}$$

Consistent with our perturbative approach (see below), it is necessary to obtain the dressed-state eigenkets only to first order in the coupling constants f_μ ($\mu=1,3$). To this order, one finds that the dressed-state eigenkets can be specified by

$$|A;n_1,n_3\rangle = |1;n_1,n_3\rangle + i \sum_{\mu=1,3} \frac{f_\mu(\mathbf{R}_0)}{\Delta_\mu} a_\mu |2;n_1,n_3\rangle , \tag{26a}$$

$$|B;n_1,n_3\rangle = |2;n_1,n_3\rangle + i \sum_{\mu=1,3} \frac{f_\mu^*(\mathbf{R}_0)}{\Delta_\mu} a_\mu^\dagger |1;n_1,n_3\rangle , \tag{26b}$$

where $|i;n_1,n_3\rangle$ ($i=1,2$) is an eigenket of H_0.

In terms of these kets, one can define dressed-state operators $\sigma_{\alpha\beta}$ ($\alpha,\beta=A,B$) by

$$\sigma_{\alpha\beta} = \sum_{n_1,n_3} |\alpha;n_1,n_3\rangle\langle\beta;n_1,n_3| , \quad \alpha,\beta=A,B , \tag{27}$$

which, according to Eqs. (26), are linearly related to bare-state operators σ_{ij} defined by

$$\sigma_{ij} = \sum_{n_1,n_3} |i;n_1,n_3\rangle\langle j;n_1,n_3| , \quad i,j=1,2 . \tag{28}$$

The σ_{ij} defined by Eq. (28) are equivalent to those previously defined in Eq. (5). Using Eqs. (27), (28), and (17), we find that, to first order in the coupling constants and neglecting spontaneous and collisional decay, the time evolution of the dressed-state operators is given by

$$\dot\sigma_{AA} = \dot\sigma_{BB} = 0, \quad \dot\sigma_{AB} = (\dot\sigma_{BA})^\dagger = -i\omega\sigma_{AB} . \tag{29}$$

In order to specify the initial conditions for Eq. (29), it is assumed that, at $t=0$, the atoms are in their ground states and a distribution of field modes is present, but there is no atom-field interaction. The atom-field interaction is then turned on in a time that is long compared with $|\Delta|^{-1}$; with this adiabatic turn-on of the fields, Eqs. (29) retain their validity even though the atom-field interaction is not constant as has been assumed in their derivation. The initial conditions are determined by the density matrix ρ, which is constant in the Heisenberg representation. The density matrix corresponding to the initial conditions described above is

$$\rho = |A\rangle\langle A|\rho_f , \tag{30}$$

where ρ_f is the density matrix for the radiation fields, and the s superscript indicates that the bra and ket are given in the Schrödinger representation.

One must now add to Eqs. (29) the contributions to $\dot\sigma_{\alpha\beta}$ arising from spontaneous decay and collisions. To carry out this procedure, (1) equations for $\dot\sigma_{\alpha\beta}$ are written in terms of the bare-state operators $\dot\sigma_{ij}$ ($i,j=1,2$) using Eqs. (26) and (27); (2) the $\dot\sigma_{ij}$ are replaced by their contributions from spontaneous emission and collisional decay, i.e., $\dot\sigma_{11}=\gamma_2\sigma_{22}$, $\dot\sigma_{22}=-\gamma_2\sigma_{22}$, $\dot\sigma_{12}=-(\frac{1}{2}\gamma_2+\Gamma)\sigma_{12}$; (3) the σ_{ij} are rewritten in terms of the $\sigma_{\alpha\beta}$ using the inverse of Eqs. (26). (Note that greek indices are used to label dressed states and latin indices to label bare states).

When the above procedure is carried out, the resultant expressions are algebraically complicated. In the so-called secular approximation (22), however, the equations take on a simplified form. As long as condition (22) is satisfied, one can neglect contributions from σ_{AB} and σ_{BA} to lowest order in $(\gamma_2+\Gamma)/|\Delta|$. In that limit, σ_{AB} may be set equal to 0, and the time evolution of σ_{BB}, obtained by the procedure outlined above, is given by[9]

$$\dot\sigma_{BB} = -\gamma_2\sigma_{BB} + 2\Gamma \sum_{\mu,\mu'=1,3} \frac{f_\mu(\mathbf{R}_0) f_{\mu'}^*(\mathbf{R}_0)}{\Delta_\mu\Delta_{\mu'}} a_\mu^\dagger a_{\mu'} \sigma_{11} . \tag{31}$$

It is necessary to calculate σ_{BB} only, since σ_{11} may be obtained from σ_{BB} using

$$\sigma = 1 - \sigma_{BB} . \tag{32}$$

Note that Eq. (31) is correct to second order in the coupling constants even though the dressed states are defined only to first order in the coupling constants. For the initial conditions (30) in which $\langle\sigma_{BB}(0)\rangle_i = 0$, second-order corrections to the dressed-state eigenkets lead to contributions to Eq. (31) which are at least *third* order in the coupling constants.

We are not interested in the most general solution of Eq. (31). To calculate the four-wave-mixing signal in the

$\mathbf{k}_s$ direction, we seek only that component of σ_{BB} which varies as $f_1 f_3^*$. We set σ_{AA} equal to $\sigma^0_{AA}=|A\rangle\langle A|$ and $a_\mu(t)$ equal to $a_\mu(0)\exp(-i\Omega_\mu t)$ in Eq. (31) to obtain the appropriate perturbative solution for σ_{BB}. The component of the "steady-state" solution for σ_{BB} which varies as $f_1 f_3^*$, obtained from Eq. (31) and denoted by $\sigma_{BB}(f_1 f_3^*)$, is found to be

$$\sigma_{BB}(f_1 f_3^*)=2\Gamma\frac{f_1(\mathbf{R}_0)f_3^*(\mathbf{R}_0)a_3^\dagger(0)a_1(0)}{\Delta_1\Delta_3(\gamma_2+i\delta)}e^{i\delta t}\sigma^0_{AA}\ , \tag{33}$$

where the fact that $\Omega_3-\Omega_1=\delta$ [Eq. (1)] has been used. Note that σ_{BB} vanishes in the absence of collisions.

It is now necessary to consider the effect of field 2 to lowest order. It is convenient to return to the bare picture and write

$$\dot\sigma_{\ \ }=-(\tfrac{1}{2}\gamma_2+\Gamma+i\omega)\sigma_{\ \ }+f_2(\mathbf{R}_0)(2\sigma_{22}-1)a_2(0)e^{\ \ i\Omega_2 t}\ . \tag{34}$$

This equation is to be solved to first order in f_2. The "1" term in Eq. (34) can be neglected since it corresponds to linear absorption of field 2, which does not contribute to the four-wave-mixing signal. In the remaining equation, we take only the component of σ_{22} which varies as $(f_1 f_3^*)$ since it is this component that contributes to the four-wave-mixing signal of interest. Denoting this component by $\sigma_{22}(f_1 f_3^*)$, we find that the appropriate equation to be solved is

$$\dot\sigma_{\ \ }=-(\tfrac{1}{2}\gamma_2+\Gamma+i\omega)\sigma_{\ \ }+2f_2(\mathbf{R}_0)\sigma_{22}(f_1 f_3^*)a_2(0)e^{\ \ i\Omega_2 t}\ . \tag{35}$$

It remains to express $\sigma_{22}(f_1 f_3^*)$ in terms of the dressed-state operators. The inverse of Eq. (26b) is

$$|2;n_1,n_3\rangle=|B;n_1,n_3\rangle-i\sum_{\mu=1,3}\frac{f_\mu^*(\mathbf{R}_0)}{\Delta_\mu}a_\mu^\dagger|A;n_1,n_3\rangle \tag{36}$$

which allows us to construct

$$\sigma_{22}=\sum_{n_1 n_3}|2;n_1,n_3\rangle\langle 2;n_1,n_3|\ .$$

Using the fact that $\sigma_{AB}=\sigma_{BA}^\dagger\approx 0$, and keeping terms which vary only as $f_1 f_3^*$, one finds

$$\sigma_{22}(f_1 f_3^*)=\sigma_{BB}(f_1 f_3^*)+\frac{f_1(\mathbf{R}_0)f_3^*(\mathbf{R}_0)a_3^\dagger(0)a_1(0)e^{i\delta t}}{\Delta_1\Delta_3}\sigma^0_{AA}\ , \tag{37}$$

where $\sigma_{BB}(f_1 f_3^*)$ is given by Eq. (33), $a_\mu(t)$ has been replaced by $a_\mu(0)\exp(-i\Omega_\mu t)$, and σ^0_{AA} is σ_{AA} evaluated to zeroth order in f_1 and f_3, i.e.,

$$\sigma^0_{AA}=|A\rangle\langle A|\ . \tag{38}$$

From Eqs. (35) and (37), it is seen that $\sigma_{\ \ }$ has two driving terms. One of the terms is proportional to $\sigma_{BB}(f_1 f_3^*)$. This term, given by Eq. (33), corresponds to a collision-induced population of dressed state B which is modulated at frequency δ. The second contribution, also modulated at frequency δ, corresponds to a modification of the initial dressed-state population σ^0_{AA} and is present even in the absence of collisions. The $\sigma_{BB}(f_1 f_3^*)$ term leads to the PIER4 resonance and the σ^0_{AA} term to the background contribution in the four-wave-mixing signal. This separation of the two contributions to the four-wave-mixing signal is essentially the same as the one presented in our earlier paper using a semiclassical dressed-atom approach.[2] The pressure-induced resonances result from a collision-induced population modulation of dressed state B, while the background term results from the field-induced modification of dressed state A.

It is now a simple matter to obtain the four-wave-mixing signal. Using Eqs. (35)–(38), one obtains the steady-state solution

$$\sigma_{\ \ }=\frac{2f_1 f_2 f_3^* a_3^\dagger(0)a_2(0)a_1(0)}{\Delta_1\Delta_3(\Delta_2+\delta)}\times\left[\frac{2\Gamma}{\gamma_2+i\delta}+1\right]\sigma^0_{AA}e^{i(\mathbf{k}_s\cdot\mathbf{R}_0-\Omega_s t)}\ , \tag{39}$$

where $\mathbf{k}_s=\mathbf{k}_1+\mathbf{k}_2-\mathbf{k}_3$ and $\Omega_s=\Omega_1+\Omega_2-\Omega_3$. Combining this result with Eqs. (16), (13), (30), and (38), and assuming that $|\delta|<|\Delta|$ such that $\Delta_1=\Delta_2\sim\Delta_3\equiv\Delta$, one finds a four-wave-mixing signal

$$I_s=\Delta^{-6}|f_1 f_2 f_3^*|^2\bar n_1\bar n_2\bar n_3\left|\frac{2\Gamma}{\gamma_2+i\delta}+1\right|^2 \tag{40a}$$

$$=|\chi_1\chi_2\chi_3^*/\Delta^3|^2\left|\frac{2\Gamma}{\gamma_2+i\delta}+1\right|^2\ , \tag{40b}$$

where $\bar n_\mu$ is the average number of photons in mode μ. As has been mentioned in an earlier paper, the four-wave-mixing signal is produced even for temporally incoherent fields, since the signal depends only on the product of the $\bar n_\mu$'s. The result (40) is the same as that obtained by standard, semiclassical methods.[1–3] What has been achieved in our approach is an interpretation of the result in terms of the quantized dressed-state operators. Our perturbative approach is valid provided that $|\chi_\mu/\Delta|^2(\Gamma+\gamma_2)/\gamma_2\ll 1$ $(\mu=1,2,3)$.

Equation (40) is not complete. Although fields 1 and 3 have been used as the dressing field, one could have equally well used fields 2 and 3 as the dressing fields and arrive at a contribution to the signal in the $\mathbf{k}_s=\mathbf{k}_1+\mathbf{k}_2-\mathbf{k}_3$ direction. Thus, a term $1\cdots 2$ should be added to Eq. (40). The resulting equation can be generalized somewhat to allow for atomic motion if one makes the replacements

$$\begin{aligned}\Delta_\mu&\cdots\Delta_\mu+\mathbf{k}_\mu\cdot\mathbf{v}\ ,\\ \delta&\cdots\delta-\mathbf{k}_{31}\cdot\mathbf{v}\ ,\end{aligned} \tag{41}$$

where

$$\mathbf{k}_{ij}=\mathbf{k}_i-\mathbf{k}_j \tag{42}$$

and $\mathbf{v}$ is an active atom velocity. Assuming that $|\Delta_\mu|$ is much greater than the Doppler width associated with the 1-2 transition, one finds a signal

$$I_s=|\chi_1\chi_2\chi_3^*/\Delta^3|^2\left|\left\langle\frac{2\Gamma}{\gamma_2+i(\delta-\mathbf{k}_{31}\cdot\mathbf{v})}\right\rangle_v+1\right|^2+\{1\leftrightarrow2\}\ , \tag{43}$$

where $\langle\ \rangle_v$ indicates an average over a Maxwellian velocity distribution[10] and $\{1\leftrightarrow2\}$ represents a term in which field indices 1 and 2 are interchanged.

IV. SOLUTION VIA OCCUPATION-NUMBER APPROACH

It is possible to give an alternative interpretation for the pressure-induced resonances if the occupation-number states are explicitly specified. In this approach, the pressure-induced resonances can be viewed as resulting from transitions between the various dressed states.

The signal is given by Eq. (16). In the Heisenberg picture, the density operator ρ is constant in time. We shall assume that at $t=0$, the density operator is given by

$$\rho=\rho(0)$$
$$=\sum_{n_1n_2n_3}P(n_1,n_2,n_3)|1;n_1,n_2,n_3\rangle\langle1;n_1,n_2,n_3|\ , \tag{44}$$

that is, the atom is in its ground state and the field modes are described by a density matrix diagonal in their occupation numbers. The quantity $P(n_1,n_2,n_3)$ is the joint probability for n_μ photons in mode μ ($\mu=1,2,3$), which is assumed to be a slowly varying function of n_1, n_2, and n_3 (i.e., we assume that $\bar{n}_\mu\gg\Delta n_\mu\gg1$, where Δn_μ is the standard deviation of n_μ). In this section, all bras and kets are written in the (time-independent) Schrödinger picture. On taking the trace in Eq. (16), one finds

$$I_s=\sum_{i=1,2}\sum_{\substack{n_1n_2n_3\\m_1m_2m_3}}P(n_1,n_2,n_3)\times\langle1;n_1,n_2,n_3|\sigma_{-}|i;m_1,m_2,m_3\rangle\times\langle i;m_1,m_2,m_3|\sigma_{+}|1;n_1,n_2,n_3\rangle\ . \tag{45}$$

Of all the terms which contribute in Eq. (45), the terms corresponding to the four-wave-mixing signal having propagation vector $\mathbf{k}_s=\mathbf{k}_1+\mathbf{k}_2-\mathbf{k}_3$ are those for which

$$i=1,\quad m_1=n_1-1,\quad m_2=n_2-1,\quad m_3=n_3+1\ . \tag{46}$$

Thus, the signal generated in direction $\mathbf{k}_s$ is given by

$$I_s=\sum_{n_1n_2n_3}P(n_1,n_2,n_3)\times|\langle1;n_1-1,n_2-1,n_3+1|\sigma_{+}|1;n_1,n_2,n_3\rangle|^2 \tag{47}$$

and the problem reduces to evaluating

$$\langle1;n_1-1,n_2-1,n_3+1|\sigma_{-}|1;n_1,n_2,n_3\rangle\ .$$

Of course, the signal calculated from Eq. (47) is identical to that calculated in Sec. III [Eq. (40a)].

From Eqs. (35) and (37), it follows that this matrix element of σ_{-} has two driving terms. The first of these terms varies as

$$D_1=(f_2/\Delta)\langle1;n_1-1,n_2,n_3+1|\sigma_{BB}|1;n_1,n_2,n_3\rangle\ . \tag{48a}$$

It is shown in Appendix B that this term is proportional to a matrix element of the density operator $\tilde{\rho}_s(t)$ in the Schrödinger picture (the tilde indicates a field-interaction representation[11]), namely,

$$D_1\propto(f_2/\Delta)\times\langle B;n_1-1,n_2-1,n_3+1|\tilde{\rho}_s(t)|B;n_1,n_2-1,n_3\rangle\ , \tag{48b}$$

provided one takes the contribution to this term originating from an initial population in state $|1;n_1,n_2-1,n_3+1\rangle$. The second term varies is

$$D_2=(f_1f_2f_3^*/\Delta^3)e^{i\delta t}\times\langle1;n_1,n_2,n_3|\sigma_{AA}^0|1;n_1,n_2,n_3\rangle \tag{49a}$$
$$\propto(f_1f_2f_3^*/\Delta^3)e^{i\delta t}\times\langle A;n_1,n_2-1,n_3+1|\tilde{\rho}_s(t)|A;n_1,n_2-1,n_3+1\rangle\ . \tag{49b}$$

Let us consider each of these terms separately.

The term D_1 vanishes in the absence of collisions [see Eq. (33)]. For this contribution to exist, a collision-induced coherence between states $|B;n_1-1,n_3+1\rangle$ and $|B;n_1,n_3\rangle$ must be formed. As shown in Fig. 2(a), these states differ in frequency by a detuning δ. Field mode 2 can then act on the $(B;n_1,n_2-1,n_3)-(B;n_1-1,n_2-1,n_3+1)$ coherence to create a dipolelike coherence $\langle2;n_1-1,n_2-1,n_3+1|\rho_s(t)|1;n_1,n_2,n_3\rangle$ that oscillates at frequency $\Omega_s=\Omega_2-\delta$. It is this coherence which is the origin of the four-wave-mixing signal. As δ is varied, there is a level crossing resonance in the four-wave-mixing signal having width (full width at half maximum) $2\gamma_2$ which corresponds to the PIER4 resonance. Thus, in this picture, the PIER4 resonance arises from a level-crossing between dressed states that are coherently populated as a result of the combined action of the incident fields and collisions. The amplitude of the resonance depends on the amount of $(B;n_1-1,n_3+1)-(B_1;n_1,n_3)$ coherence produced, which, in turn, depends linearly on the collision rate Γ. The entire process, which is reminiscent of that encountered in trilevel echoes[12] and coherent Raman beats,[13] can be interpreted rather loosely in terms of a coherent Raman scattering [Fig. 2(a)]. The term "coherent" is used since the various density matrix elements have a well-defined macroscopic spatial phase associated with them.

In contrast to the D_2 contribution, the D_1 term [Eq. (49)] is nonvanishing even in the absence of collisions. In

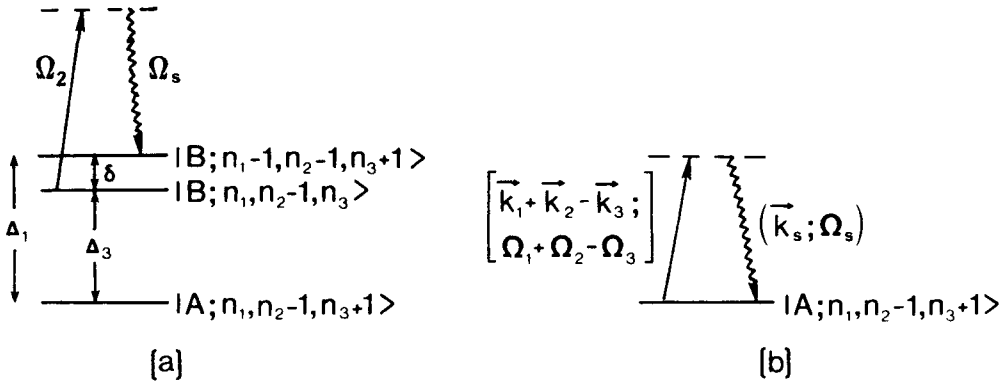

FIG. 2. (a) Collisions create a coherence between dressed states $|B;n_1,n_2-1,n_3\rangle$ and $|B;n_1-1,n_2-1,n_3+1\rangle$, starting from state $|A;n_1,n_2-1,n_3+1\rangle$. The four-wave-mixing signal in direction $\mathbf{k}_s$ having frequency $\Omega_s=\Omega-\delta$ appears as a type of coherent Raman scattering originating in state $|B;n_1,n_2-1,n_3\rangle$ and terminating in state $|B;n_1-1,n_2-1,n_3+1\rangle$, with field 2 acting as the driving field for this transition. This contribution to the signal exhibits a level-crossing resonance centered at $\delta=0$. The effect of field 2 is shown schematically; the actual role of field 2 is to create a coherence $\langle 2;n_1-1,n_2-1,n_3+1|\tilde{\rho}(\cdots)|1;n_1,n_2,n_3\rangle$ which is responsible for the coherent emission at frequency $\Omega-\delta$. (b) Another contribution to the signal originates in state $|A;n_1,n_2-1,n_3+1\rangle$, which is populated even in the absence of collisions. This contribution to the signal can be viewed as a type of coherent Rayleigh scattering driven by an effective field having propagation vector $\mathbf{k}_1+\mathbf{k}_2-\mathbf{k}_3$ and frequency $\Omega_1+\Omega_2-\Omega_3=\Omega-\delta$. There is no resonant structure centered at $\delta=0$ associated with this contribution. These figures are drawn assuming that fields 1 and 3 are the dressing fields; in arriving at the final signal, one must also consider analogous diagrams in which fields 2 and 3 act as the dressing fields.

some sense, this contribution corresponds to a coherent Rayleigh scattering from dressed state $|A;n_1,n_2-1,n_3+1\rangle$ via an effective three-photon operator represented in Eq. (49) by the product $f_1f_2f_3^*/\Delta^3$. The frequency of emission is $\Omega_s=\Omega_1+\Omega_2-\Omega_3$ [see Fig. 2(b)]. This contribution to the four-wave-mixing signal is insensitive to small variations in δ.

The interpretation given above in terms of the density operator in the Schrödinger picture is not meant to be taken too literally. It is intended mainly to provide some initial link between the Heisenberg and Schrödinger approaches to the problem and to connect the present calculation with one given in a previous paper.[1] In that work, collision-induced resonant structures produced in the excitation of a three-level atom by four fields were interpreted as arising from transitions between the various dressed states.

We plan to present a detailed calculation of the four-wave-mixing signal using the Schrödinger representation in a future work. For arbitrary initial states of the radiation fields, it would seem that the calculation of the four-wave-mixing signal is most conveniently carried out using the Heisenberg representation, as was done in this work. However, the Schrödinger picture may lead to an alternative physical interpretation as to the origin of the pressure-induced resonances.

V. SUMMARY

Using a fully quantized approach, we have presented a theory and interpretation of the pressure-induced resonances in four-wave-mixing signals (PIER4) that can arise when three radiation fields are incident on an ensemble of two-level atoms. In an operator approach, the PIER4 resonances were attributed to a collision-induced creation of a modulated dressed-state population. In an occupation-number picture, these resonances were interpreted as arising from a level crossing between collisionally populated dressed states. This type of fully quantized approach can also be applied to the theory and interpretation of the complementary problem of the absorption and amplification spectrum experienced by a probe beam acting on a given atomic transition that is simultaneously driven by a "pump" field.

ACKNOWLEDGMENTS

This research was supported, in part, by National Science Foundation International Grants (Nos. INT 8413300 and INT 8815036). The research of PRB was supported by the U.S. Office of Naval Research and the National Science Foundation (Grant Nos. PHY-8415781 and PHY-8814423). The Laboratoire de Spectroscopie Hertzienne de l'Ecole Normale Supérieure is "associé au Centre National de la Recherche Scientifique."

APPENDIX A

In this Appendix, we outline the derivation of Eq. (15) from Eq. (12). We first note that the solution we seek is one for observation times $(t-t_0)\gg\gamma_2^{-1}$, since it is in this limit only that the steady-state solutions are applicable. We substitute (12) into (13), set $t_0=0$, change variables to $(\tau=t'-t'',\ t'=t')$, and differentiate with respect to t to obtain

$$\dot{n}_{\alpha_0}=|f_{\alpha_0}|^2\sum_{j,j'}^{N}\int_0^t d\tau\exp[i\mathbf{k}_{\alpha_0}-\mathbf{k}_s)\cdot(\mathbf{R}_{j'}-\mathbf{R}_j) -i(\Omega_{\alpha_0}-\Omega_s)\tau]\langle\tilde{\sigma}^{\dagger}_{j'}\tilde{\sigma}^{\prime\prime}_{j}\rangle_s\ . \tag{A1}$$

The summations over $\mathbf{R}_j$ and $\mathbf{R}_{j'}$ are converted to in-

tegrals over the interaction volume V using the prescription

$$\sum_{j,j'=1}^{N} \Longrightarrow (N/V)^2 \int d\mathbf{R} \int d\mathbf{R}' \ . \tag{A2}$$

Equation (A1) is to be summed over a small range of $\Delta\mathbf{k}_{\alpha_0}$ centered about $\mathbf{k}_{\alpha_0}=\mathbf{k}_s$. To carry out this summation, we use the explicit form for $|f_{\alpha_0}|^2$, namely,

$$|f_{\alpha_0}|^2=\frac{2\pi\Omega_{\alpha_0}|(p_y)_{21}|^2}{\hbar V_Q} \ , \tag{A3}$$

where $(p_y)_{21}$ is a dipole moment matrix element (the incident fields are assumed to be polarized parallel to the y axis) and V_Q is the *quantization* volume, which is not necessarily equal to the interaction volume V. The sum over $\mathbf{k}_{\alpha_0}$ is converted to an integral using

$$\sum_{\mathbf{k}_{\alpha_0}} \Longrightarrow [V_Q/(2\pi)^3] \int d\mathbf{k}_{\alpha_0} \ . \tag{A4}$$

Combining Eqs. (A1)–(A4) and setting $\bar{\mathbf{R}}=\mathbf{R}-\mathbf{R}'$, $\bar{\mathbf{k}}=\mathbf{k}_{\alpha_0}-\mathbf{k}_s$, and $\bar{\Omega}=\Omega_{\alpha_0}-\Omega_s$, one obtains the rate

$$\dot{n}_s=\sum_{\Delta\mathbf{k}_{\alpha_0}} \dot{n}_{\alpha_0} \Longrightarrow (N/V)^2 \left[\frac{\Omega_s|(p_y)_{21}|^2}{(2\pi)^2\hbar}\right] \int_{\Delta\mathbf{k}} d\bar{\mathbf{k}} \int d\mathbf{R}' \int d\mathbf{R} \int_{-T}^{T} d\tau\, e^{i(\bar{\mathbf{k}}\cdot\bar{\mathbf{R}}-\bar{\Omega}\tau)} \langle \tilde{\sigma}_+^j \tilde{\sigma}_-^{j'} \rangle_i \ , \tag{A5}$$

where T is the observation time and $\Delta\bar{\mathbf{k}}$ is centered about $\bar{\mathbf{k}}=0$. (As noted in the text, $\langle \sigma_+^j \sigma_-^{j'} \rangle_i$ is independent of $\mathbf{R}$ and $\mathbf{R}'$ when field depletion is neglected.)

A typical geometry is one in which $\mathbf{k}_s$ is along the axis of a cylindrical interaction volume of length L and cross sectional area A. The integration (A5) is carried out for such an integration volume assuming that $cT \gg L$, but $cT/k^2A<1$. If one expands $\bar{\Omega}\tau$ as

$$\{[\bar{k}_x^2+\bar{k}_y^2+(\bar{k}_z+k_s)^2]^{1/2}c-\Omega_s\}\tau$$

and compares it with $\bar{\mathbf{k}}\cdot\bar{\mathbf{R}}=\bar{k}_x\bar{x}+\bar{k}_y\bar{y}+\bar{k}_z\bar{z}$, one finds that, if $cT \gg L$ and $cT/k^2A<1$, then the spatial phase dominates for the transverse directions and the temporal phase for the longitudinal direction. The consequence of this is that one can integrate over x,x' and y,y' to get $(2\pi)^2 A\,\delta(\bar{k}_x)\delta(\bar{k}_y)$ and over τ to get

$$2\pi\delta([\bar{k}_x^2+\bar{k}_y^2+(\bar{k}_z+k_s)^2]^{1/2}c-\Omega_s) \ .$$

When the subsequent integration over $\bar{k}$ is performed, one finds

$$\dot{n}_s=[\mathcal{N}^2 2\pi\Omega_s A|(p_y)_{21}|^2/\hbar c] \times \int\int_{-L/2}^{L/2} dz\,dz'\, e^{-i[k_s-(\Omega_s/c)](z-z')} \langle \tilde{\sigma}_+^j \tilde{\sigma}_0^{j'} \rangle_i \ , \tag{A6}$$

where $\mathcal{N}=N/V$ is the active-atom density. When phase matching is satisfied ($k_s=\Omega_s/c$), Eq. (A6) reduces to

$$\dot{n}_s=[\mathcal{N}^2 2\pi\Omega_s A|(p_y)_{21}|^2/\hbar c]L^2 \langle \tilde{\sigma}_+^j \tilde{\sigma}^{j'} \rangle_i \ . \tag{A7}$$

Electromagnetic energy density in mode s is produced in the sample at a rate

$$dW_s/dt=(\hbar\Omega_s/V)\dot{n}_s \tag{A8}$$

and the power exiting the sample is equal to

$$I_s=L\,dW_s/dt \ . \tag{A9}$$

Combining Eqs. (A7)–(A9), one arrives at

$$I_s=2\pi c\mathcal{N}^2 k_s^2 L^2 |(p_y)_{21}|^2 \langle \tilde{\sigma}_+^j \tilde{\sigma}_-^{j'} \rangle_i \ . \tag{A10}$$

APPENDIX B

In this Appendix, we sketch the transitions from Eqs. (48a) to (48b) and (49a) to (49b). In essence, we wish to show how to relate matrix elements of σ to those of ρ. In this Appendix, all bras and kets, as well as the density operator ρ, are written in the Schrödinger representation, while σ is defined in the Heisenberg representation. Although the calculation in the text involves three fields, the basic ideas can be illustrated by considering a single incident field. To simplify the notation, we replace $f_1\exp[i(\mathbf{k}_1\cdot\mathbf{R}_0-\Omega_1 t)]$ appearing in Eq. (10) by the single symbol f.

Taking matrix elements of Eq. (10) (along with the corresponding equations for σ_{11} and σ_+) between states $\langle 1;n|$ and $|1;n'\rangle$, we find

$$\langle 1;n|\dot{\sigma}_{11}|1;n'\rangle=\gamma_2\langle 1;n|\sigma_{22}|1;n'\rangle + f\sqrt{n'}\langle 1;n|\sigma_+|1;n'-1\rangle + f^*\sqrt{n}\,\langle 1;n-1|\sigma_-|1;n'\rangle \ , \tag{B1a}$$

$$\langle 1;n|\dot{\sigma}_{22}|1;n'\rangle=-\gamma_2\langle 1;n|\sigma_{22}|1;n'\rangle - f\sqrt{n'}\langle 1;n|\sigma_+|1;n'-1\rangle - f^*\sqrt{n}\,\langle 1;n-1|\sigma_-|1;n'\rangle \ , \tag{B1b}$$

$$\langle 1;n|\dot{\sigma}_-|1;n'\rangle=-(\tfrac{1}{2}\gamma_2+i\omega)\langle 1;n|\sigma_-|1;n'\rangle + f\sqrt{n'}\langle 1;n|\sigma_{22}|1;n'-1\rangle - f\sqrt{n'}\langle 1;n|\sigma_{11}|1;n'-1\rangle \ , \tag{B1c}$$

$$\langle 1;n|\dot{\sigma}_+|1;n'\rangle=-(\tfrac{1}{2}\gamma_2-i\omega)\langle 1;n|\sigma_+|1;n'\rangle + f^*\sqrt{n}\,\langle 1;n-1|\sigma_{22}|1;n'\rangle - f^*\sqrt{n}\,\langle 1;n-1|\sigma_{11}|1;n'\rangle \ . \tag{B1d}$$

Using the relationship $\dot{\rho}=-(i/\hbar)[H,\rho]+$(relaxation terms), one can obtain equations for density-matrix elements of ρ. In a field-interaction representation defined by

$$\langle j;q|\rho|j';q'\rangle=\langle j;q|\tilde{\rho}|j';q'\rangle e^{-i(q-q')\Omega_1 t} \quad (j,j'=1,2) ,$$

matrix elements of $\tilde{\rho}$ evolve as

$$\langle 1;q|\dot{\tilde{\rho}}|1;q'\rangle=\gamma_2\langle 2;q|\rho|2;q'\rangle+f\sqrt{q'}\langle 1;q|\tilde{\rho}|2;q'-1\rangle+f^*\sqrt{q}\langle 2;q-1|\tilde{\rho}|1;q'\rangle , \tag{B2a}$$

$$\langle 2;q|\dot{\tilde{\rho}}|2;q'\rangle=-\gamma_2\langle 2;q|\tilde{\rho}|2;q'\rangle-f\sqrt{q+1}\langle 1;q+1|\tilde{\rho}|2;q'\rangle-f^*\sqrt{q'+1}\langle 2;q|\tilde{\rho}|1;q'+1\rangle , \tag{B2b}$$

$$\langle 2;q|\dot{\tilde{\rho}}|1;q'\rangle=-(\tfrac{1}{2}\gamma_2+i\omega)\langle 2;q|\tilde{\rho}|1;q'\rangle+f\sqrt{q'}\langle 2;q|\tilde{\rho}|2;q'-1\rangle-f\sqrt{q+1}\langle 1;q+1|\tilde{\rho}|1;q'\rangle , \tag{B2c}$$

$$\langle 1;q|\dot{\tilde{\rho}}|2;q'\rangle=-(\tfrac{1}{2}\gamma_2-i\omega)\langle 1;q|\tilde{\rho}|2;q'\rangle+f^*\sqrt{q}\langle 2;q-1|\tilde{\rho}|2;q'\rangle-f^*\sqrt{q'+1}\langle 1;q|\tilde{\rho}|1;q'+1\rangle . \tag{B2d}$$

In order to compare Eqs. (B1) and (B2), we note that $[a,\sigma]=[a^\dagger,\sigma]=0$. If field-depletion effects are neglected, a is equal to $a(0)e^{-i\Omega_1 t}$. By taking matrix elements of $a\sigma$ and σa (or $a^\dagger\sigma$ and $\sigma a^\dagger$), one finds

$$\sqrt{n'}\langle 1;n|\sigma|1;n'-1\rangle=\sqrt{n+1}\langle 1;n+1|\sigma|1;n'\rangle , \tag{B3a}$$

$$\sqrt{n}\langle 1;n-1|\sigma|1;n'\rangle=\sqrt{n'+1}\langle 1;n|\sigma|1;n'+1\rangle , \tag{B3b}$$

where σ is any of $\sigma_{11},\sigma_{22},\sigma_+$, or σ_-. If Eqs. (B3) are substituted into Eqs. (B1), one arrives at

$$\langle 1;n|\dot{\sigma}_{11}|1;n'\rangle=\gamma_2\langle 1;n|\sigma_{22}|1;n'\rangle+f\sqrt{n'}\langle 1;n|\sigma_+|1;n'-1\rangle+f^*\sqrt{n}\langle 1;n-1|\sigma_-|1;n'\rangle , \tag{B4a}$$

$$\langle 1;n|\dot{\sigma}_{22}|1;n'\rangle=-\gamma_2\langle 1;n|\sigma_{22}|1;n'\rangle-f\sqrt{n+1}\langle 1;n+1|\sigma_+|1;n'\rangle-f^*\sqrt{n'+1}\langle 1;n|\sigma_-|1;n'+1\rangle , \tag{B4b}$$

$$\langle 1,n|\dot{\sigma}_-|1;n'\rangle=-(\tfrac{1}{2}\gamma_2+i\omega)\langle 1;n|\sigma_-|1;n'\rangle+f\sqrt{n'}\langle 1;n|\sigma_{22}|1;n'-1\rangle-f\sqrt{n+1}\langle 1;n+1|\sigma_{11}|1;n'\rangle , \tag{B4c}$$

$$\langle 1;n|\dot{\sigma}_+|1;n'\rangle=-(\tfrac{1}{2}\gamma_2-i\omega)\langle 1;n|\sigma_+|1;n'\rangle+f^*\sqrt{n}\langle 1;n-1|\sigma_{22}|1;n'\rangle-f^*\sqrt{n'+1}\langle 1;n|\sigma_{11}|1;n'+1\rangle . \tag{B4d}$$

One sees immediately that Eqs. (B2) and (B5) are now identical provided one makes the identifications

$$\langle 1;n|\sigma_{ii}|1;n'\rangle=\langle i;q|\tilde{\rho}|i;q'\rangle, \quad i=1,2 , \tag{B5a}$$

$$\langle 1;n|\sigma_-|1;n'\rangle=\langle 2;q|\tilde{\rho}|1;q'\rangle , \tag{B5b}$$

$$\langle 1;n|\sigma_+|1;n'\rangle=\langle 1;q|\tilde{\rho}|2;q'\rangle . \tag{B5c}$$

Although the equations for matrix elements of σ and $\tilde{\rho}$ are identical, the *solutions* to these equations differ owing to different initial conditions. For example, $\langle 1;n|\sigma_{11}+\sigma_{22}|1;n'\rangle$ is identically equal to $\delta_{nn'}$ whereas $\langle 1;q|\tilde{\rho}|1;q'\rangle+\langle 2;q|\tilde{\rho}|2;q'\rangle$ is not even a conserved quantity owing to cascades associated with spontaneous emission.

Although the solutions differ, it is still possible to interpret the results in a way that enables us to identify matrix elements of σ with those of $\tilde{\rho}$. First we assume that

$$\langle 2;q|\tilde{\rho}|2;q'\rangle\approx\langle 1;q-1|\tilde{\rho}|2;q'-1\rangle$$

based on the fact that $\Delta q\gg 1$. In that limit, the ρ equations are closed in the subspace involving kets $|1;q\rangle$ and $|2;q-1\rangle$, with

$$\langle 1;q|\tilde{\rho}|1;q\rangle+\langle 2;q-1|\tilde{\rho}|2;q-1\rangle=\text{const.}$$

By artificially setting this constant equal to unity, one arrives at equations which are identical to those for $\langle 1;n|\sigma|1;n'\rangle$, provided one adopts the initial condition $\langle 1;q|\tilde{\rho}|1;q'\rangle=\delta_{qq'}$. Thus Eqs. (B5) can be considered to give the correspondence between matrix elements of σ and $\tilde{\rho}$, in the limit that all population is locked in the $|1;q\rangle$, $|2;q-1\rangle$ subspace. If one wants to calculate $\langle 1;n-1|\sigma_-|1;n\rangle$ in this scheme, it is simply equal to $\langle 2;n-1|\tilde{\rho}|1;n\rangle$, assuming initial unit probability for the state $|1;n\rangle$.

The generalization to three incident fields is straightforward. Again the matrix elements of σ and $\tilde{\rho}$ obey identical equations. One finds that

$$\langle 1;n_1-1,n_2-1,n_3+1|\sigma_-|1;n_1,n_2,n_3\rangle$$

can be identified with

$$\langle 2;n_1-1,n_2-1,n_3+1|\tilde{\rho}|1;n_1,n_2,n_3\rangle ,$$

provided that initial state $|1;n_1,n_2-1,n_3+1\rangle$ is assumed to have unit probability. The element

$$\langle 2;n_1-1,n_2-1,n_3+1|\tilde{\rho}|1;n_1,n_2,n_3\rangle$$

is proportional to

$$(f_2/\Delta)\langle 2;n_1-1,n_2-1,n_3+1|\tilde{\rho}|2;n_1,n_2-1,n_3\rangle ,$$

which can be reexpressed in terms of the dressed states. This provides the connection between matrix elements of σ and $\tilde{\rho}$ used in Eqs. (48) and (49).

[1]P. R. Berman and G. Grynberg, Phys. Rev. A **39**, 570 (1989).

[2]G. Grynberg and P. R. Berman, Phys. Rev. A **39**, 4016 (1989).

[3]N. Bloembergen, H. Loten, and R. T. Lynch, Jr., Indian J. Pure Appl. Phys. **16**, 151 (1978); A. R. Bogdan, Y. Prior, and N. Bloembergen, Opt. Lett. **6**, 82 (1981); A. R. Bogdan, M. W. Downer, and N. Bloembergen, *ibid.* **6**, 348 (1981). For recent reviews of PIER4, see L. Rothberg, in *Progress in Optics*, edited by E. Wolf (Elsevier Scientific, Amsterdam, 1987), pp. 39–101; G. Grynberg, in *Spectral Line Shapes*, edited by R. Exton (Deepak, Hampton, VA, 1987), Vol. 4 , pp. 503–521.

[4]V. Mizrahi, Y. Prior, and S. Mukamel, Opt. Lett. **8**, 145 (1983); Y. Prior and A. N. Weiszmann, Phys. Rev. A **29**, 2700 (1984); M. Sargent III, D. A. Holm, and M. S. Zubairy, *ibid.* **31**, 3112 (1985); S. Stenholm, D. A. Holm, and M. Sargent III, *ibid.* **31**, 3124 (1985); D. A. Holm and M. Sargent III, *ibid.* **35**, 2150 (1987); S. T. Ho, P. Kumar, and J. H. Shapiro, *ibid.* **35**, 3982 (1987); **37**, 2017 (1988).

[5]See, for example, J. R. Ackerhalt and J. H. Eberly, Phys. Rev. D **10**, 3350 (1974).

[6]Note that Eqs. (10a) and (10b) contain $a_\mu(t)$ ($\mu=1,2,3$) rather than $a_\mu(0)\exp(-i\Omega_\mu t)$, as is conventionally found in these equations (see Ref. 5). Which form is preferable depends to some extent on the physical system being modeled. In this work, it is assumed that the average number of photons in each of the incident field modes is large, implying that the two forms can be interchanged without significant error.

[7]Even in the absence of collisions, the commutator relations (6) are no longer valid for operators obeying Eqs. (10), since terms involving initially unoccupied modes have been dropped from Eqs. (10a) and (10b).

[8]See, for example, C. Cohen-Tannoudji, in *Frontiers in Laser Spectroscopy*, edited by R. Balian, S. Haroche, and S. Liberman (North-Holland, Amsterdam, 1977), pp. 3–104, and references therein; S. Reynaud and C. Cohen-Tannoudji, J. Phys. (Paris) **43**, 1021 (1982).

[9]Within the limits of our approximations, one can set the commutators $[a_\mu,a_\mu^\dagger]$ ($\mu=1,2,3$) equal to zero, since this substitution introduces errors of order $\bar{n}_\mu^{-1} \ll 1$.

[10]One can further generalize Eq. (43) to allow for the collisional narrowing of the bracketed expression in Eq. (43) which can result from collision-induced changes in the velocity associated with atomic state populations. See, for example, M. Gorlicki, P. R. Berman, and G. Khitrova, Phys. Rev. A **37**, 4340 (1988).

[11]The field interaction representation we are using is defined by

$$\langle j;n_1,n_2,n_3|\rho|j';n_1',n_2',n_3'\rangle = \langle j;n_1,n_2,n_3|\tilde{\rho}|j';n_1',n_2',n_3'\rangle \times\exp\{-i[(n_1-n_1')\Omega_1+(n_2-n_2')\Omega_2+(n_3-n_3')\Omega_3]t\}$$

$(j,j'=1,2)$.

[12]See, for example, T. Mossberg, A. Flusberg, R. Kachru, and S. R. Hartmann, Phys. Rev. Lett. **39**, 1523 (1977); T. W. Mossberg, R. Kachru, S. R. Hartmann, and A. M. Flusberg, Phys. Rev. A **20**, 1976 (1979); P. R. Berman and E. Giacobino, *ibid.* **28**, 2900 (1983).

[13]See, for example, R. L. Shoemaker and R. G. Brewer, Phys. Rev. Lett. **28**, 1430 (1972); R. G. Brewer and E. L. Hahn, Phys. Rev. A **8**, 464 (1973).

Pressure-induced extra resonances in nonlinear spectroscopy

G. Grynberg
Laboratoire de Spectroscopie Hertzienne de l'Ecole Normale Supérieure, Université Pierre et Marie Curie, 75252 Paris CEDEX 05, France

P. R. Berman
Department of Physics, New York University, 4 Washington Place, New York, New York 10003
(Received 21 September 1989)

We present three examples of pressure-induced extra resonances that can be observed in nonlinear spectroscopy: fluorescence of a "three-level atom" driven by two laser fields, two-photon ionization of a "three-level atom" (plus continuum) driven by two laser fields, and excitation of a "four-level atom" driven by four laser fields. We show that all these extra resonances can be interpreted in terms of quantum pathways, each pathway involving a collisionally aided excitation. We also demonstrate that the two first extra resonances can be obtained with incoherent fields, while relatively coherent fields are required in the last example.

INTRODUCTION

The field of extra resonances triggered by collisional relaxation has for a long time mainly concentrated on the resonances occurring in four-wave mixing generation.[1] However, similar resonances have also been predicted in nonlinear spectroscopy,[2-4] the main differences being that in this case, the signal originates from atomic state populations rather than from a coherent collective emission.

The aim of this paper is to present other examples of pressure-induced extra resonances (PIER) occurring in nonlinear spectroscopy. We examine PIER which arise in (a) the fluorescence of a "three-level" atom driven by two laser fields, (b) the two-photon ionization of a "three-level" atom driven by two laser fields, and (c) the excitation of a "four-level" atom driven by four laser fields.

Apart from their intrinsic interest, we show that each of these examples allows one to specify the role of the relaxation process in the generation of extra resonances. In particular, we show that the extra resonances can be understood in terms of quantum-mechanical interference between two pathways, each of these pathways involving a collisionally aided excitation. In addition, the influence of the phase of the applied fields will be stressed. We show that some extra resonances can be obtained with number states for the applied fields while, in other cases, relatively coherent fields are required.

I. NOTATION AND ASSUMPTIONS

Let us first consider a three-level atom with a ground state a and two excited states b and b' (see Fig. 1). This atom interacts with two electromagnetic fields of frequencies ω_1 and ω_2. The first field is nearly resonant with the a-b transition and we denote by $\Delta_1=\omega_1-\omega_0$ the frequency detuning from resonance. The second field is nearly resonant with the a-b' transition and we define its detuning $\Delta_2'=\omega_2-\omega_0'$. The amplitudes of these two fields, and their associated resonance Rabi frequencies, are denoted by E_1 and E_2, and Ω_1 and Ω_2' ($\Omega_1=-d_{ab}E_1/\hbar$, $\Omega_2'=-d_{ab'}E_2/\hbar$, where d_{ab} and $d_{ab'}$ are dipole-moment matrix elements).

The radiative lifetimes of the excited states b and b' are Γ_b^{-1} and $\Gamma_{b'}^{-1}$, respectively. Apart from radiative relaxation, the atoms undergo collisional relaxation. We assume that the active atoms are perturbed by a buffer gas and that the collisions are dephasing in nature, inducing a decay of the atomic state coherences, but not of the atomic state population. The relaxation rate of the atomic state coherence i-j due to collisions is denoted by γ_{ij}. We assume that the conditions of the impact approximation are satisfied and, in particular, that $|\Delta_1|$ and $|\Delta_2'|$ are small compared to τ_c^{-1}, where τ_c is the typical duration of a collision. On the other hand, we assume that $|\Delta_1|$ and $|\Delta_2'|$ are large compared to the widths of the a-b and a-b' transitions, but that $|\Delta_1-\Delta_2'|$ remains small compared to $|\Delta_1|$ and $|\Delta_2'|$. To simplify matters somewhat, we shall also assume that $|\Omega_1/\Delta_1|$ and $|\Omega_2'/\Delta_2'|$ are very small compared to unity. With this assumption, the density-matrix equations can be solved using a perturbative approach.[5]

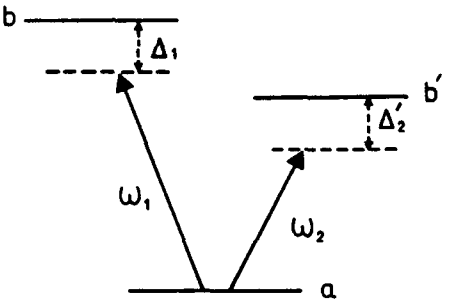

FIG. 1. Three-level atom driven by two laser fields.

The calculations are carried out using either a semiclassical approach (classical fields and quantum-mechanical atoms) or a (fully quantized) dressed-atom picture. In the first case, the atomic density-matrix elements evolve as[6]

$$\frac{d}{dt}\rho_{ij}=\frac{1}{i\hbar}[H,\rho]_{ij}-\Gamma_{ij}\rho_{ij}+(\Gamma_b\rho_{bb}+\Gamma_{b'}\rho_{b'b'})\delta_{ia}\delta_{ja} , \tag{1}$$

where

$$\Gamma_{ij}=\tfrac{1}{2}(\Gamma_i+\Gamma_j)+\gamma_{ij} \tag{2}$$

is the sum of the radiative and collisional relaxation rates and

$$H=H_0+V \tag{3a}$$

is the Hamiltonian for the system without relaxation. The quantity H_0 is the free-atom Hamiltonian and V is the electric dipole interaction between the atom and the field

$$V=-\mathbf{d}\cdot\mathbf{E}_T . \tag{3b}$$

$\mathbf{d}$ is the atomic dipole operator and $\mathbf{E}_T$ is the sum of the incident fields.

To second order in the incident fields, we find that the populations and the coherence of the excited states are

$$\rho_{bb}^{(2)}=\frac{\Omega_1^2}{4\Delta_1^2}\left[1+\frac{\gamma_{ba}+\gamma_{ba}^*}{\Gamma_b}\right] , \tag{4a}$$

$$\rho_{b'b'}^{(2)}=\frac{\Omega_2'^2}{4\Delta_2'^2}\left[1+\frac{\gamma_{b'a}+\gamma_{b'a}^*}{\Gamma_{b'}}\right] , \tag{4b}$$

$$\rho_{bb'}^{(2)}=\frac{\Omega_1\Omega_2'}{4\Delta_1\Delta_2'}\left[1+\frac{\gamma_{ba}+\gamma_{ba}^*-\gamma_{bb'}}{\Gamma_{bb'}-i\delta}\right]e^{-i(\omega_1-\omega_2)t}e^{i(\theta_1-\theta_2)} , \tag{4c}$$

$$\rho_{b'b}^{(2)}=\rho_{bb'}^{(2)*} , \tag{4d}$$

where

$$\delta=\Delta_1-\Delta_2' . \tag{5}$$

In these expressions, θ_1 and θ_2 correspond to the phase of the fields E_1 and E_2. If these fields propagate in the $\mathbf{k}_1$ and $\mathbf{k}_2$ directions, we have $\theta_1=\mathbf{k}_1\cdot\mathbf{r}+\varphi_1$ and $\theta_2=\mathbf{k}_2\cdot\mathbf{r}+\varphi_2$, where φ_1 and φ_2 are some additional phases associated with fields 1 and 2, respectively. The quantities ρ_{bb} and $\rho_{b'b'}$ appear as the sum of a collision-free term and a collisionally aided term. The collision-free term has been shown to be connected with Rayleigh scattering at the laser frequency while the collisionally aided terms leads to fluorescence at the resonance frequency.[7] A similar separation exists for $\rho_{bb'}$, the collisionally aided term being proportional to the factor $(\gamma_{ba}+\gamma_{b'a}^*-\gamma_{bb'})$, which has been originally introduced by Bloembergen, Loten and Lynch.[8]

Another approach uses a dressed-atom basis. In the perturbative limit the eigenstates of the dressed-atom Hamiltonian are[9]

$$|1(N_1,N_2)\rangle=-\frac{\Omega_1}{2\Delta_1}|a,N_1+1,N_2+1\rangle+|b,N_1,N_2+1\rangle , \tag{6a}$$

$$|2(N_1,N_2)\rangle=-\frac{\Omega_2'}{2\Delta_2'}|a,N_1+1,N_2+1\rangle+|b',N_1+1,N_2\rangle , \tag{6b}$$

$$|3(N_1,N_2)\rangle=|a,N_1+1,N_2+1\rangle+\frac{\Omega_1}{2\Delta_1}|b,N_1,N_2+1\rangle+\frac{\Omega_2'}{2\Delta_2'}|b',N_1+1,N_2\rangle , \tag{6c}$$

where $|i,N_1,N_2\rangle$ describes an atom in state $|i\rangle$ with N_1 photons of frequency ω_1 and N_2 photons of frequency ω_2. The quantities Ω_1 and Ω_2' are evaluated at $\overline{N_1}$ and $\overline{N_2}$, where $\overline{N_1}$ and $\overline{N_2}$ are the mean number of photons in these two modes of the field. (Ω_1 and Ω_2' should be replaced by $\Omega_1 e^{i\theta_1}$ and $\Omega_2' e^{i\theta_2}$ to describe propagation effects. Since the paper is devoted to single atom effects, we omit the phase factors). Within the approximations made in this paper, the stages $|1(N_1,N_2)\rangle$, $|2(N_1,N_2)\rangle$, and $|3(N_1,N_2)\rangle$ are very close in energy, the separation between $|1(N_1,N_2)\rangle$ and $|3(N_1,N_2)\rangle$ being $-\hbar\Delta_1$ and the separation between $|2(N_1,N_2)\rangle$ and $|3(N_1,N_2)\rangle$ being $-\hbar\Delta_2'$. In the dressed-atom approach, collisions induce transitions between the dressed states. The steady-state values ρ_{11} and ρ_{22} of the populations of the levels $|1(N_1,N_2)\rangle$ and $|2(N_1,N_2)\rangle$ and of the coherence ρ_{12} between $|1(N_1,N_2)\rangle$ and $|2(N_1,N_2)\rangle$ are[10]

$$\rho_{11}=\frac{\Omega_1^2}{4\Delta_1^2}\frac{\gamma_{ba}+\gamma_{ba}^*}{\Gamma_b} , \tag{7a}$$

$$\rho_{22}=\frac{\Omega_2'^2}{4\Delta_2'^2}\frac{\gamma_{b'a}+\gamma_{b'a}^*}{\Gamma_{b'}} , \tag{7b}$$

$$\rho_{12}=\frac{\Omega_1\Omega_2'}{4\Delta_1\Delta_2'}\frac{\gamma_{ba}+\gamma_{b'a}^*-\gamma_{bb'}}{\Gamma_{bb'}-i\delta} . \tag{7c}$$

One recognizes in (7c) the collisional factor $(\gamma_{ba}+\gamma_{b'a}^*-\gamma_{bb'})$, which is associated with the creation of a coherence between dressed states through collisional excitation.[9] The values of ρ_{11} and ρ_{22} result from an equilibrium between the collisional excitation of the level and decay by spontaneous emission.[7]

Actually, the results presented above are only valid for stationary atoms. For a Doppler broadened medium, the detuning δ appearing in Eqs. (4c) and (7c), as well as elsewhere in this paper, should be replaced by $[\delta-(\mathbf{k}_1-\mathbf{k}_2)\cdot\mathbf{v}]$, where $\mathbf{v}$ is the atomic velocity. For the time being, we assume that $|(\mathbf{k}_1-\mathbf{k}_2)\cdot\mathbf{v}|\ll\Gamma_{bb'}$ for all atoms in the sample, justifying our neglect of the residual Doppler shift $(\mathbf{k}_1-\mathbf{k}_2)\cdot\mathbf{v}$. The modifications of the results that would occur if $|(\mathbf{k}_1-\mathbf{k}_2)\cdot\mathbf{v}|>\Gamma_{bb'}$ is discussed in the Conclusion.

II. FLUORESCENCE OF A THREE-LEVEL ATOM

A. PIER resonance in atomic states populations

The aim of this section is to show how the fluorescence originating from level b is modified by the field E_2 acting on the a-b' transition. Consequently, we seek a term in the population of level b which depends on both E_1 and E_2. Furthermore, we are interested only in the PIER resonance occurring around $\delta=0$. This term should originate from $\rho^{(2)}_{bb'}$ given in (4c).

Solving the density-matrix equation to fourth order, we find that the term of interest is equal to

$$\rho^{(I)}_{bb}=\frac{\Omega_1^2\Omega_2'^2}{16\Delta_1^2\Delta_2'\Gamma_b}i\left[\frac{(\gamma^a_{bb'})^*}{\Gamma^*_{bb'}+i\delta}-\frac{\gamma^a_{bb'}}{\Gamma_{bb'}-i\delta}\right], \tag{8}$$

where $\gamma^a_{bb'}$ is the collisional factor of PIER 4

$$\gamma^a_{bb'}=\gamma_{ba}+\gamma^*_{b'a}-\gamma_{bb'}\ . \tag{9}$$

Equation (8) is valid in the limit that

$$\left|\frac{\Omega_1\Omega_2'}{\Delta_1(\Gamma_{bb'}-i\delta)}\right|\ll 1\ . \tag{10}$$

Let us split $\gamma^a_{bb'}$ into its real and imaginary parts

$$\gamma^a_{bb'}=(\gamma^a_{bb'})'+i(\gamma^a_{bb'})''\ .$$

We also assume that the imaginary part of $\Gamma_{bb'}$ (which corresponds to a shift of the line) is included in δ. We thus take $\Gamma_{bb'}$ real and obtain for $\rho^{(I)}_{bb}$

$$\rho^{(I)}_{bb}=\frac{\Omega_1^2}{8\Delta_1^2}\frac{\Omega_2'^2}{\Delta_2'\Gamma_b}\left[\frac{(\gamma^a_{bb'})'\delta}{\Gamma^2_{bb'}+\delta^2}-\frac{(\gamma^a_{bb'})''\Gamma_{bb'}}{\Gamma^2_{bb'}+\delta^2}\right]. \tag{11}$$

This pressure-induced contribution to the fluorescence from state b can have either a positive or negative sign (of course, the *total* fluorescence from level b is positive). The ratio of the relative magnitude of the PIER given by (11) and of the background given by (4a) is

$$\frac{\rho^{(I)}_{bb}}{\rho^{(2)}_{bb}}\sim\frac{\Omega_2'^2}{\Delta_2'\Gamma_{bb'}}. \tag{12}$$

Although it is assumed that $|\Omega_2'/\Delta_2'|\ll 1$, the ratio (12) is not necessarily very small compared to unity[11] since Ω_2' can be larger than $\Gamma_{bb'}$. Furthermore, when Δ_2' varies, the background remains constant while $\rho^{(I)}_{bb}$ exhibits a narrow resonance around $\Delta_2'-\Delta_1=0$. Thus the PIER should be observable on the fluorescence from the excited state. To have an image of how such resonance should appear, we have plotted in Fig. 2 the variation of the fluorescence I_F emitted from level b versus the frequency ω_2 for several values of the buffer-gas pressure. The frequency ω_1 of the first source is assumed to remain constant and I_F is calculated from the sum $\rho^{(2)}_{bb}+\rho^{(I)}_{bb}$.

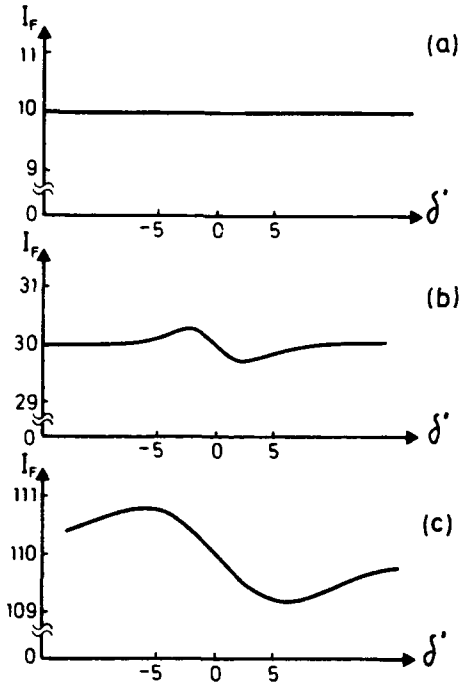

FIG. 2. Variation of the fluorescence I_F emitted from the level b vs the frequency ω_2 for various buffer-gas pressures. The curves have been obtained by assuming that $\gamma^a_{bb'}$, γ_{ba}, $\gamma_{b'a}$, and $\gamma_{bb'}$ are real and by taking $\gamma^a_{bb'}=\gamma_{b'a}=\gamma_{ba}$. We have $\Omega_1\ll\Omega_2'$ and $|\Omega_2'/\Delta_2'|=10^{-2}$. We take $\Gamma_b=\Gamma_{b'}$ and $\Omega_2'/\Gamma_{b'}=20$. The curve a is obtained in absence of buffer gas ($\gamma_{bb'}=0$). The curve b is obtained for a pressure of buffer gas such that $\gamma_{bb'}=\Gamma_b$ and the curve c for a higher pressure ($\gamma_{bb'}=5\Gamma_b$). The same arbitrary unit is used on the vertical axis of the three curves. The abscissa corresponds to $\delta'=(\omega_2-\omega_1-\omega_0'+\omega_0)/\Gamma_b$. One can note that in the range of pressure considered here the signal and the background increases with pressure. For higher pressure, the signal saturates while the background still increases.

B. Interpretation in the uncoupled states basis

We first interpret this resonance in terms of interference between transition amplitudes. A transition amplitude will be represented by a diagram which, at this stage, should be considered a qualitative method for understanding the physics rather than a complete method for calculating the signal. If we consider the excitation of level b, two possible paths can be considered. The first possibility [Fig. 3(a)] is a direct collisionally aided excitation with absorption of one photon ω_1. The population of level b resulting from this process is proportional to the intensity of the field having frequency ω_1, i.e., to Ω_1^2. In fact, it is this process that leads to the collision-induced component of formula (4a) [or to formula (7a)]. A second possibility is a collisionally aided excitation of level b' followed by a two-photon transition from b' to b [Fig. 3(b)]. This process alone would lead to a population of the level b proportional to the square of the intensity of the field having frequency ω_2 multiplied by the intensity of the field having frequency ω_1, i.e., proportional to $\Omega_2'^4\Omega_1^2$. To get the population ρ_{bb}, however, one must also consider the possibility of an interference between these two pathways. Indeed, the quantum states of the fields and of the internal degrees of freedom of the atom are the same in the initial ($|a,N_1,N_2\rangle$) and final ($|b,N_1-1,N_2\rangle$) states

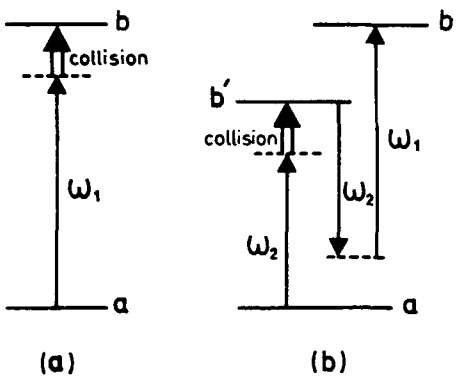

FIG. 3. Collisionally aided excitation of level b. (a) Direct pathway and (b) pathway with intermediate excitation of level b'. The pressure-induced extra resonance on the population of level b comes from the interference between these two pathways.

(in the second pathway the absorption of a photon ω_2 is followed by an emission of a photon ω_2 with the net result that N_2 is not changed). The transition amplitude for the second pathway should exhibit a resonance when the two-photon transition from b' to b becomes resonant, i.e., when $\delta=0$ [see Fig. 3(b)]. This resonance should also appear in the interference term. In some sense, the interference between the two pathways of Fig. 3 has an effect similar to that of an heterodyne detection since the effect associated with the pathway of Fig. 3(b) appears at a lower order of perturbation because of the interference with the pathway of Fig. 3(a).

The origin of the PIER resonance at $\delta=0$ can also be interpreted by a complementary argument. To have interference effect between the two pathways of Fig. 3, we should also consider the external degrees of freedom since the atom is not isolated but undergoes a collision. Indeed, energy is exchanged between the active atom and its collision partner. In the pathway shown in Fig. 3(a), the energy received by the atom is $E_{ba}-\hbar\omega_1$. In the pathway shown in Fig. 3(b), the energy received is $E_{b'a}-\hbar\omega_2$. In order to have the same change of kinetic energy of the colliding atoms for each pathway, we must have

$$E_{ba}-\hbar\omega_1=E_{b'a}-\hbar\omega_2 , \tag{13}$$

i.e.,

$$\delta=0 . \tag{14}$$

Thus the interference between the two pathways of Fig. 3 only occurs around $\delta=0$.

C. Interpretation in the dressed-state basis

We can also interpret this resonance using the dressed-state basis. More precisely, when the two-photon coupling between $|b,N_1,N_2+1\rangle$ and $|b',N_1+1,N_2\rangle$ becomes important, the states $|1(N_1,N_2)\rangle$ and $|2(N_1,N_2)\rangle$ should be written[9]

$$\begin{aligned}|1(N_1,N_2)\rangle=&-\left[\frac{\Omega_1}{2\Delta_1}\cos\theta+\frac{\Omega_2'}{2\Delta_2'}\sin\theta\right]\\&\times|a,N_1+1,N_2+1\rangle\\&+(\cos\theta)|b,N_1,N_2+1\rangle\\&+(\sin\theta)|b',N_1+1,N_2\rangle ,\end{aligned} \tag{15a}$$

$$\begin{aligned}|2(N_1,N_2)\rangle=&-\left[\frac{\Omega_2'}{2\Delta_2'}\cos\theta-\frac{\Omega_1}{2\Delta_1}\sin\theta\right]\\&\times|a,N_1+1,N_2+1\rangle\\&-(\sin\theta)|b,N_1,N_2+1\rangle\\&+(\cos\theta)|b',N_1+1,N_2\rangle ,\end{aligned} \tag{15b}$$

with

$$\tan2\theta=\frac{\Omega_1\Omega_2'}{2\Delta_1\delta} . \tag{16}$$

Let us now assume that initially, the system is in the state $|3(N_1,N_2)\rangle$. We calculate the probability of finding the system in the state $|1(N_1,N_2)\rangle$ after a collision, our demonstration being very similar to the one originally done for the PIER resonances in four-wave mixing.[9] We call Φ and Φ' the phase factors due to a collision of relative velocity v and impact parameter b on the transitions a-b and a-b', respectively. The state $|\psi\rangle$ of the system after a collision is

$$\begin{aligned}|\psi\rangle=&|a,N_1+1,N_2+1\rangle+\frac{\Omega_1}{2\Delta_1}e^{-i\Phi}|b,N_1,N_2+1\rangle\\&+\frac{\Omega_2'}{2\Delta_2'}e^{-i\Phi'}|b',N_1+1,N_2\rangle .\end{aligned} \tag{17}$$

From (15a) and (17), we deduce the transition amplitude to find the system in the state $|1(N_1,N_2)\rangle$ after a collision,

$$\begin{aligned}\langle 1(N_1,N_2)|\psi\rangle=&\frac{\Omega_1}{2\Delta_1}(\cos\theta)(e^{-i\Phi}-1)\\&+\frac{\Omega_2'}{2\Delta_2'}(\sin\theta)(e^{-i\Phi'}-1) .\end{aligned} \tag{18}$$

The transition probability is thus

$$\begin{aligned}|\langle 1(N_1,N_2)|\psi\rangle|^2=&\frac{\Omega_1^2}{2\Delta_1^2}(\cos^2\theta)(1-\cos\Phi)\\&+\frac{\Omega_1\Omega_2'}{4\Delta_1\Delta_2'}(\cos\theta)(\sin\theta)\\&\times[(1-e^{-i\Phi})(1-e^{i\Phi'})+\text{c.c.}]\\&+\frac{\Omega_2'^2}{2\Delta_2'^2}(\sin^2\theta)(1-\cos\Phi') .\end{aligned} \tag{19}$$

When we average the various phase factors over all possible collisions, we find[9]

$$\langle 1-e^{-i\Phi}\rangle=\gamma_{ba} , \tag{20a}$$

$$\langle (1-e^{-i\Phi})(1-e^{i\Phi'})\rangle=\gamma_{ba}+\gamma^{*}_{b'a}-\gamma_{bb'} =\gamma^{a}_{bb'} , \tag{20b}$$

$$\langle 1-e^{-i\Phi'}\rangle=\gamma_{b'a} . \tag{20c}$$

Thus the mean collisionally aided excitation of level $|1(N_1,N_2)\rangle$ in steady state is

$$\Lambda_1=\frac{\Omega_1^2}{4\Delta_1^2}(\cos^2\theta)(\gamma_{ba}+\gamma^{*}_{ba}) +\frac{\Omega_1\Omega_2'}{4\Delta_1\Delta_2'}(\cos\theta)(\sin\theta)(\gamma^{a}_{bb'}+\gamma^{a*}_{bb'}) +\frac{\Omega_2'^2}{4\Delta_2'^2}(\sin^2\theta)(\gamma_{b'a}+\gamma^{*}_{b'a}) . \tag{21}$$

In the secular approximation $|\delta|\gg\Gamma_{bb'}$, the steady-state population of state $|1(N_1,N_2)\rangle$, denoted by ρ_{11}, is equal to Λ_1/Γ_b. To compare this result with Eq. (11), we note that the validity condition for Eq. (11) [Eq. (10)] is equivalent to $\theta\ll 1$ when $|\delta|\gg\Gamma_{bb'}$. In the limit $\theta\ll 1$, we obtain

$$\rho_{11}=\frac{\Omega_1^2}{4\Delta_1^2}\frac{(\gamma_{ba}+\gamma^{*}_{ba})}{\Gamma_b}+\frac{\Omega_1^2\Omega_2'^2}{16\Delta_1^2\Delta_2'\delta}\frac{(\gamma^{a}_{bb'}+\gamma^{a*}_{bb'})}{\Gamma_b} . \tag{22}$$

The second term of (22) coincides with the result of formula (11) for $|\delta|\gg\Gamma_{bb'}$. This shows that, in this approach, the PIER resonance results from the contamination of the dressed state $|1(N_1,N_2)\rangle$ by a small amount of the state $|b'\rangle$. The contamination is maximum when the two uncoupled states $|b',N_1+1,N_2\rangle$ and $|b,N_1,N_2+1\rangle$ have the same energy, i.e., when the resonance condition for the two-photon transition is fulfilled.[12]

Finally, we note that the phase of the fields does not appear in the formula (11), which give $\rho^{(I)}_{bb'}$. This is an indication that the observation of this effect does not require coherent fields. This indication is supported by the physical discussion given above, which is done in terms of number states for the field.

III. TWO-PHOTON IONIZATION

We still consider the three-level atom a,b,b', but now consider the possibility that a second photon is absorbed to a state k in the continuum. More precisely, we study the case where an absorption of a photon ω_2 from state b or an absorption of a photon ω_1 from state b' leads to ionization of the atom (Fig. 4).

In the dressed-state basis, we have to add to the states given by formulas (6) the states $|k(N_1,N_2)\rangle$ corresponding to the continuum (see Fig. 5)

$$|k(N_1,N_2)\rangle=|k,N_1,N_2\rangle . \tag{23}$$

With respect to $|3(N_1,N_2)\rangle$, the state $|k(N_1,N_2)\rangle$ has an energy

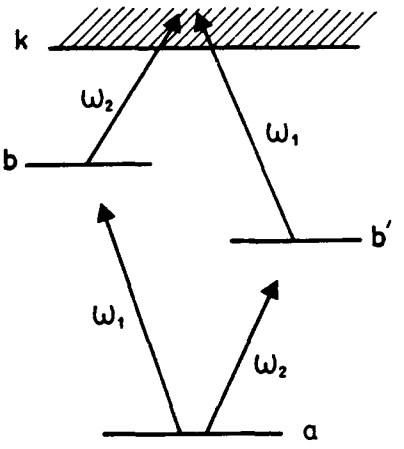

FIG. 4. Three-level atom plus continuum driven by two laser fields.

$$-\hbar\Delta_k=E_{ka}-\hbar(\omega_1+\omega_2) . \tag{24}$$

The coupling between $|1(N_1,N_2)\rangle$, $|2(N_1,N_2)\rangle$ and $|k(N_1,N_2)\rangle$ is produced by the electric dipole interaction having matrix elements

$$\langle k(N_1,N_2)|V|1(N_1,N_2)\rangle=-\frac{d_{kb}E_2}{2}=\hbar\frac{\Omega_2}{2} , \tag{25a}$$

$$\langle k(N_1,N_2)|V|2(N_1,N_2)\rangle=-\frac{d_{kb'}E_1}{2}=\hbar\frac{\Omega_1'}{2} . \tag{25b}$$

Recall that states $|1(N_1,N_2)\rangle$ and $|2(N_1,N_2)\rangle$ are populated only in the presence of collisions.

The state $|3(N_1,N_2)\rangle$ is also coupled to $|k(N_1,N_2)\rangle$ through its small components depending on the atomic states b and b' [see formula (6c)]

$$\langle k(N_1,N_2)|V|3(N_1,N_2)\rangle=\frac{\hbar}{4}\left[\frac{\Omega_1\Omega_2}{\Delta_1}+\frac{\Omega_2'\Omega_1'}{\Delta_2'}\right] . \tag{26}$$

This term corresponds to the direct coupling between the dressed state $|3(N_1,N_2)\rangle$ (adiabatically connected to the atomic ground state) and the continuum. In the absence of collisions, the photoionization results from this two-

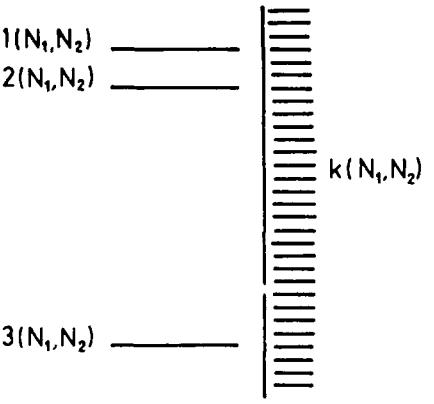

FIG. 5. Energy levels in the dressed-state picture.

photon coupling. The states of the continuum that are reached by this direct photoionization mechanism are those that have the same energy as $|3(N_1,N_2)\rangle$, i.e., those for which

$$E_{ka}=\hbar(\omega_1+\omega_2)\ . \tag{27}$$

On the other hand, in presence of collisional damping, two other photoionization processes are possible. First, we can have a collisionally aided excitation of $|1(N_1,N_2)\rangle$ followed by an absorption of a photon $\hbar\omega_2$ [Fig. 6(a)]. The states of the continuum that are reached by this process have energies

$$E_{k'b}=\hbar\omega_2\ . \tag{28}$$

The second process [Fig. 6(b)] is a collisionally aided excitation of $|2(N_1,N_2)\rangle$ followed by an absorption of a photon $\hbar\omega_1$. The states of the continuum that are reached by this process have energies

$$E_{k''b'}=\hbar\omega_1\ . \tag{29}$$

If we compare the states of the continuum that can be reached by the different processes, we find, by comparing formulas (27) and (28) on one hand and formulas (27) and (29) on the other hand,

$$E_{kk'}=\hbar\omega_1-\hbar\omega_0=\hbar\Delta_1, \tag{30a}$$

$$E_{kk''}=\hbar\omega_2-\hbar\omega_0'=\hbar\Delta_2'\ . \tag{30b}$$

Thus it can be deduced from the assumptions of our model that the states of the continuum reached by direct photoionization and by collisionally aided photoionization are well separated in energy and can be (at least theoretically) distinguished by measuring the kinetic energy of the ejected electron. On the other hand,

$$E_{k''k'}=\hbar(\Delta_1-\Delta_2')=\hbar\delta \tag{31}$$

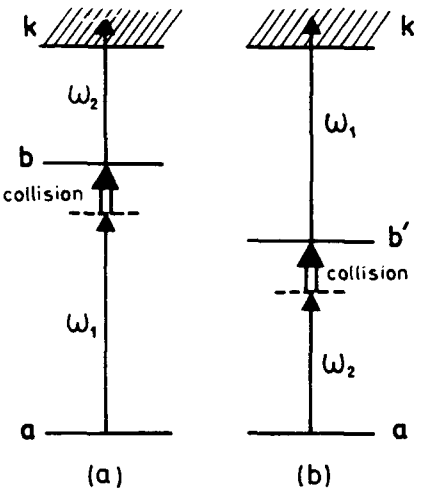

FIG. 6. Collisionally aided two-photon ionization. The pathway (a) involves the intermediate excitation of level b and the pathway (b) the intermediate excitation of level b'. Note that one photon of each mode is absorbed in each process. The pressure-induced extra resonance in two-photon ionization comes from the interference between the pathways (a) and (b).

is a small quantity and the two collisionally aided photoionization processes have to be handled together. In the following, we consider only the electrons that originate from the collisionally aided processes.

Let us consider a time interval t which is large compared to the time necessary to reach the steady-state values for ρ_{11}, ρ_{12}, and ρ_{22} [formula (7)]. We assume that the states of the field are number states. The number of photoelectrons of energy E_k generated is equal to

$$\rho_{kk}=\frac{\Omega_2^2}{4}\rho_{11}\frac{\sin^2[(\Delta_1-\Delta_k)t/2]}{[(\Delta_1-\Delta_k)/2]^2}+\frac{\Omega_1'^2}{4}\rho_{22}\frac{\sin^2[(\Delta_2'-\Delta_k)t/2]}{[(\Delta_2'-\Delta_k)/2]^2}$$
$$+\frac{\Omega_1'\Omega_2}{4}\left[\rho_{12}\int_0^t dt' e^{-i(\Delta_k-\Delta_1)t'}\int_0^t dt'' e^{i(\Delta_k-\Delta_2')t''}+\text{c.c.}\right]\ . \tag{32}$$

If we call $\rho(E_k)$ the density of states in the continuum, the total number of photoelectrons obtained through a collisionally aided process is

$$N^{(\text{coll})}=\int dE_k\rho(E_k)\rho_{kk}\ . \tag{33}$$

We assume that the continuum is sufficiently flat so that we can replace $\rho(E_k)$ by $\rho(\bar{E})$ with $\bar{E}\simeq E_b+\hbar\omega_1\simeq E_{b'}+\hbar\omega_2$. The integration of formula (33) with ρ_{kk} given by formula (32) then leads to

$$N^{(\text{coll})}=\frac{2\pi}{\hbar}\rho(\bar{E})\left[\left[\frac{\Omega_2^2}{4}\rho_{11}+\frac{\Omega_1'^2}{4}\rho_{22}\right]t+\frac{\Omega_1'\Omega_2}{4}\left[\rho_{12}\int_0^t dt' e^{i\delta t'}+\text{c.c.}\right]\right]\ . \tag{34}$$

The two first terms of formula (34) (proportional to ρ_{11} and ρ_{22}) correspond to the photoionization processes described by the diagrams of Figs. 6(a) and 6(b), respectively. The last term of formula (34) describes the interference between these two diagrams. Here again, we see

that an interference occurs around $\delta \simeq 0$, i.e., in a situation where the energy exchanged with the collision partner is the same for the two pathways of Fig. 6.

More precisely, when $|\delta| t \gg 1$ the interference term contributes negligibly and we obtain, using formulas (7) and (34),

$$\frac{N^{(\mathrm{coll})}}{t} = \frac{2\pi}{\hbar}\rho(\bar{E})\left[\frac{\Omega_1^2\Omega_2^2}{16\Delta_1^2}\frac{\gamma_{ba}+\gamma_{ba}^*}{\Gamma_b} + \frac{\Omega_1'^2\Omega_2'^2}{16\Delta_2'^2}\frac{\gamma_{b'a}+\gamma_{b'a}^*}{\Gamma_{b'}}\right] . \tag{35}$$

On the other hand, when $|\delta| t \ll 1$, there is an interference between the two pathways and we find

$$\frac{N^{(\mathrm{coll})}(\delta=0)}{t} = \frac{2\pi}{\hbar}\rho(\bar{E})\left[\left[\frac{\Omega_1^2\Omega_2^2}{16\Delta_1^2}\frac{\gamma_{ba}+\gamma_{ba}^*}{\Gamma_b} + \frac{\Omega_1'^2\Omega_2'^2}{16\Delta_2'^2}\frac{\gamma_{b'a}+\gamma_{b'a}^*}{\Gamma_{b'}}\right] + \frac{\Omega_1\Omega_1'\Omega_2\Omega_2'}{16\Delta_1\Delta_2'}\left[\frac{\gamma_{bb'}^a}{\Gamma_{bb'}}+\mathrm{c.c.}\right]\right] . \tag{36}$$

Here again, the initial state $|a, N_1+1, N_2+1\rangle$ and the final state $|k, N_1, N_2\rangle$ of the excitation processes shown in Fig. 6 correspond to pure number states for the field. The pressure-induced extra resonance predicted in two-photon ionization does not require coherent fields.

We should also note that the effect calculated here would probably not be easy to observe. It is essentially a "gedanken" experiment suited to show the influence of the interference between collisionally aided diagrams. Even if the interference process appears more intelligible in Fig. 6 than in Fig. 3, we think that the process described in Sec. II is more suited to an experimental investigation.

IV. TWO-PHOTON ABSORPTION OF A FOUR-LEVEL ATOM

The last example that we will consider is a four-level atom (Fig. 7) driven by four laser fields. The new fields E_3 and E_4 (having frequencies ω_3 and ω_4, respectively) drive the b-c and b'-c transitions, respectively.[13] The detunings from resonance are denoted by Δ_3 and Δ_4',

$$\hbar\Delta_3 = \hbar\omega_3 - \hbar\omega_{cb} , \tag{37a}$$

$$\hbar\Delta_4' = \hbar\omega_4 - \hbar\omega_{cb'} . \tag{37b}$$

We assume that the single-photon detunings $|\Delta_3|$ and $|\Delta_4'|$ and the two-photon detunings $|\Delta_1+\Delta_3|$ and $|\Delta_2+\Delta_4'|$ are much smaller than τ_c^{-1}. For the sake of simplicity, we also assume that

$$\omega_1+\omega_3 = \omega_2+\omega_4 . \tag{38}$$

The detunings from the two-photon resonance are thus the same for the two possible excitation paths ($\Delta_1+\Delta_3 = \Delta_2'+\Delta_4'$). We calculate the population $\rho_{cc}^{(4)}$ to fourth order in the field amplitudes. We denote by Ω_3 and Ω_4' the Rabi frequencies for the b-c and b'-c transitions ($\Omega_3 = -d_{bc}E_3/\hbar$, $\Omega_4' = -d_{b'c}E_4/\hbar$). Besides the terms proportional to $\Omega_1^2\Omega_3^2$, which correspond to the excitation through level b, and those proportional to $\Omega_2'^2\Omega_4'^2$, which correspond to the excitation through b', there are terms depending on $\Omega_1\Omega_2'\Omega_3\Omega_4'$ which correspond to an interference between these two pathways. It is those terms, denoted by $\rho_{cc}^{(I)}$, that we consider now. Using perturbation theory, we find

$$\rho_{cc}^{(I)} = \frac{\Omega_1\Omega_2'\Omega_3\Omega_4'}{16\Gamma_c}e^{i(\theta_1+\theta_3-\theta_2-\theta_4)}\left[\frac{1}{\Gamma_{ba}-i\Delta_1}\frac{1}{\Gamma_{ca}-i(\Delta_1+\Delta_3)}\frac{1}{\Gamma_{cb'}-i\Delta_4'} + \frac{1}{\Gamma_{b'a}^*+i\Delta_2'}\frac{1}{\Gamma_{ca}^*+i(\Delta_2'+\Delta_4')}\frac{1}{\Gamma_{cb}^*+i\Delta_3} + \left[1+\frac{\gamma_{bb'}^a}{\Gamma_{bb'}-i\delta}\right]\frac{1}{\Gamma_{ba}-i\Delta_1}\frac{1}{\Gamma_{b'a}^*+i\Delta_2'}\left[\frac{1}{\Gamma_{cb'}-i\Delta_4'}+\frac{1}{\Gamma_{cb}^*+i\Delta_3}\right]\right]+\mathrm{c.c.} \tag{39}$$

Regrouping the terms, this expression can be written

$$\rho_{cc}^{(I)} = \frac{\Omega_1\Omega_2'\Omega_3\Omega_4'}{16\Gamma_c}e^{i(\theta_1+\theta_3-\theta_2-\theta_4)} \times \left[\frac{1}{\Gamma_{ba}-i\Delta_1}\frac{1}{\Gamma_{cb'}-i\Delta_4'}\left[\frac{1}{\Gamma_{ca}-i(\Delta_1+\Delta_3)}+\frac{1}{\Gamma_{b'a}+i\Delta_2'}\right] + \frac{1}{\Gamma_{b'a}^*+i\Delta_2'}\frac{1}{\Gamma_{cb}^*+i\Delta_3}\left[\frac{1}{\Gamma_{ca}^*+i(\Delta_2'+\Delta_4')}+\frac{1}{\Gamma_{ba}-i\Delta_1}\right] + \frac{\gamma_{bb'}^a[\Gamma_{cb'}+\Gamma_{cb}^*+i(\Delta_3-\Delta_4')]}{(\Gamma_{bb'}-i\delta)(\Gamma_{ba}-i\Delta_1)(\Gamma_{b'a}^*+i\Delta_2')(\Gamma_{cb'}-i\Delta_4')(\Gamma_{cb}^*+i\Delta_3)}\right]+\mathrm{c.c.} \tag{40}$$

Using the relation $(\Delta_3-\Delta_4') = -(\Delta_1-\Delta_2') = -\delta$, we finally obtain

$$\rho_{cc}^{(I)}=\frac{\Omega_1\Omega_2'\Omega_3\Omega_4' e^{i(\theta_1+\theta_3-\theta_2-\theta_4)}}{16\Gamma_c(\Gamma_{ba}-i\Delta_1)(\Gamma_{b'a}^*+i\Delta_2')}\left[\frac{2\Gamma_{ca}}{(\Gamma_{ca})^2+(\Delta_1+\Delta_3)^2}+\frac{\gamma_{cb'}^a}{[\Gamma_{ca}-i(\Delta_1+\Delta_3)][\Gamma_{cb'}-i\Delta_4']}+\frac{(\gamma_{cb}^a)^*}{[\Gamma_{ca}^*+i(\Delta_1+\Delta_3)][\Gamma_{cb}^*+i\Delta_3]}+\frac{\gamma_{bb'}^a}{(\Gamma_{cb'}-i\Delta_4')(\Gamma_{cb}^*+i\Delta_3)}\left[1+\frac{\Gamma_c+\gamma_{bb'}^c}{\Gamma_{bb'}-i\delta}\right]\right]+\text{c.c.}\ , \tag{41}$$

where $\gamma_{cb'}^a$ and γ_{cb}^a are defined by expressions similar to formula (9) and

$$\gamma_{bb'}^c=\gamma_{cb}^*+\gamma_{cb'}-\gamma_{bb'}\ . \tag{42}$$

Let us now discuss Eq. (41). In the absence of collisions, all the γ_{ij}^k are equal to zero and the only term that remains is the two-photon term centered at $\Delta_1+\Delta_3=0$.[14] This term represents the interference between the two pathways for two-photon excitation via fields $\omega_1+\omega_3$ or $\omega_2+\omega_4$. Once collisions occur, there are several new resonant features centered at $\Delta_4'=0$, $\Delta_3=0$, and $\delta=0$. Let us first note that the second term of formula (41) is related to a collisionally aided excitation of the coherence between levels c and b' (see Fig. 8) identical to the one used in the four-wave mixing generation of Ref. 15. In other words, the two pathways that interfere are associated with a collisionally aided two-photon absorption [Fig. 8(a)] and a collisionally aided single-photon absorption followed by the absorption of a photon ω_4 [Fig. 8(b)]. Similarly, the third term of formula (41) is related to an interference between the two pathways shown in Fig. 9.

Finally, we find that the resonance centered at $\delta=0$ (which is analogous to the PIER 4 resonance[1]) arises from the last term of formula (41). In particular, if we assume that the fields are detuned from the single-photon and two-photon resonances ($|\Delta_3|\gg\Gamma_{cb}$, $|\Delta_4'|\gg\Gamma_{cb'}$, $|\Delta_1|\gg\Gamma_{ba}$, $|\Delta_2'|\gg\Gamma_{b'a}$, $|\Delta_1+\Delta_3|\gg\Gamma_{ca}$) we find that Eq. (41) reduces to

$$\rho_{cc}^{(I)}=\frac{\Omega_1\Omega_2'\Omega_3\Omega_4' e^{i(\theta_1+\theta_3-\theta_2-\theta_4)}}{16\Gamma_c\Delta_1\Delta_2'\Delta_3\Delta_4'}\left[A+\gamma_{bb'}^a\frac{\Gamma_c+\gamma_{bb'}^c}{\Gamma_{bb'}-i\delta}\right], \tag{43}$$

where

$$A=2\Gamma_{ca}\frac{\Delta_3\Delta_4'}{(\Delta_1+\Delta_3)^2}+\gamma_{bb'}^a-\gamma_{cb'}^a\frac{\Delta_3}{\Delta_1+\Delta_3}-\gamma_{cb}^{a*}\frac{\Delta_4'}{\Delta_1+\Delta_3}\ . \tag{44}$$

The background term A grows linearly with the pressure. The term exhibiting a resonance at $\delta=0$ has a numerator which grows quadratically with the pressure, while the width of the resonance increases linearly with pressure.

The resonance at $\delta=0$ is also obtained if we consider the situation where the two single-photon transitions from b to c and from b' to c are nearly resonant, but that $|\Delta_1|$ and $|\Delta_2'|$ are very large. In this case, the resonance at $\delta=0$ is very similar to the one described in Sec. III for the two-photon ionization. However, there are some different features. In particular, there is a phase dependence in formulas (41) and (43) that was not present in formula (36). Let us first note that $\rho_{cc}^{(I)}$ is a function of the point $\mathbf{r}$ unless one assumes that

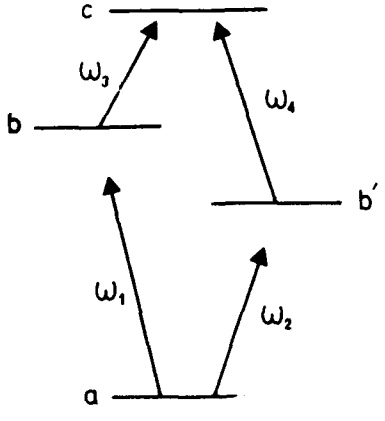

FIG. 7. Four-level atom driven by four applied laser fields.

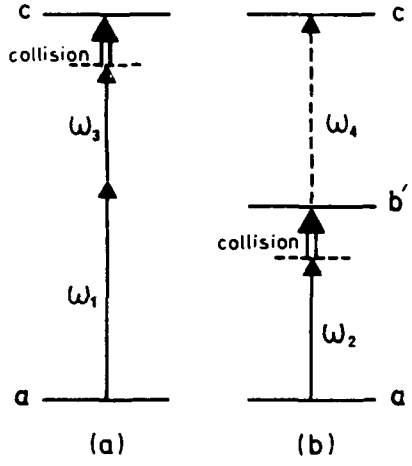

FIG. 8. Collisionally aided excitation of level c. The pathway (a) corresponds to a collisionally aided two-photon excitation, while the pathway (b) is associated to a collisionally aided two-step process with intermediate excitation of level b'. The interference between these pathways leads to a pressure-induced extra resonance centered at $\Delta_4'=0$.

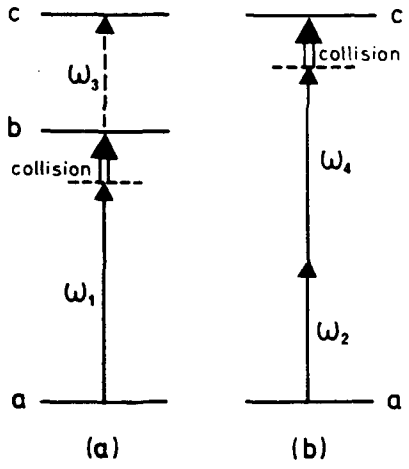

FIG. 9. Collisionally aided excitation of level c. The interference between the two pathways leads to a pressure-induced extra resonance centered at $\Delta_3=0$.

$$\mathbf{k}_1+\mathbf{k}_3=\mathbf{k}_2+\mathbf{k}_4 .$$

If this condition (similar to the phase-matching condition of four-wave mixing generation) is fulfilled, $\rho_{cc}^{(I)}$ is independent of $\mathbf{r}$, but still remains a function of the phases of the field through a factor $e^{i(\varphi_1+\varphi_3-\varphi_2-\varphi_4)}$. This means that the resonance centered at $\delta=0$ vanishes unless the fields are relatively coherent.

This feature can be understood if we try to describe the resonance at $\delta=0$ as an interference between quantum pathways similar to the one of Fig. 6. Let us first assume that all the fields are in number states and that the initial state of the system is $|a,N_1,N_2,N_3,N_4\rangle$. The two pathways that should be considered now are associated with the absorption of one photon ω_1 and one photon ω_3 [Fig. 10(a)] or with the absorption of one photon ω_2 and one photon ω_4 [Fig. 10(b)]. In the first case, the final state is $|c,N_1-1,N_2,N_3-1,N_4\rangle$, while in the second case, the final state is $|c,N_1,N_2-1,N_3,N_4-1\rangle$. Since the final state is not the same for the two pathways, there is no possible interference between these pathways.[16] On the other hand, if the nondiagonal matrix elements for the density matrix of the fields are not zero (as it is the case for quasiclassical fields),[17] then the number of photons is not fixed in the initial state and the interference can be restored. For example, let us assume that the initial state is

$$|\psi_i\rangle=\sum_{N_1',N_2',N_3',N_4'} c_1(N_1')c_2(N_2')c_3(N_3')c_4(N_4') \times|a,N_1',N_2',N_3',N_4'\rangle . \quad (45)$$

The probability of finding the system in the final state $|\psi_f\rangle=|c,N_1,N_2,N_3,N_4\rangle$ is proportional to

$$|\langle\psi_f|U|\psi_i\rangle|^2\sim|c_1(N_1+1)c_2(N_2)c_3(N_3+1) \times c_4(N_4)[(N_1+1)(N_3+1)]^{1/2} +c_1(N_1)c_2(N_2+1)c_3(N_3)c_4(N_4+1) \times[(N_2+1)(N_4+1)|^2]^{1/2} . \quad (46)$$

To obtain the probability to find the atom in state c, we have to sum formula (46) over N_1, N_2, N_3, and N_4. We see that the interference term is equal to zero unless we have $c_i(N_i)$ and $c_i(N_i+1)$ simultaneously different from zero for the four fields.

In other words, to obtain a resonance on the population of the c level, we have to start with a coherence

$$\langle A,N_1+1,N_2,N_3+1,N_4|\rho|A,N_1,N_2+1,N_3,N_4+1\rangle ,$$

where $|A,N_1,N_2,N_3,N_4\rangle$ is the dressed state adiabatically connected to the uncoupled state $|a,N_1,N_2,N_3,N_4\rangle$. Then collisions act on this coherence to create

$$\langle B,N_1,N_2,N_3+1,N_4|\rho|B',N_1,N_2,N_3,N_4+1\rangle ,$$

where $|B,N_1,N_2,N_3,N_4\rangle$ and $|B',N_1,N_2,N_3,N_4\rangle$ are the dressed states connected to $|b,N_1,N_2,N_3,N_4\rangle$ and $|b',N_1,N_2,N_3,N_4\rangle$, respectively. Finally, the action of the fields 3 and 4 leads to a population $\langle c,N_1,N_2,N_3,N_4|\rho|c,N_1,N_2,N_3,N_4\rangle$. In this approach, which is essentially similar to the one already developed in Ref. 4, the resonance at $\delta=0$ arises from the collisionally aided excitation of the coherence between the dressed states B and B'.

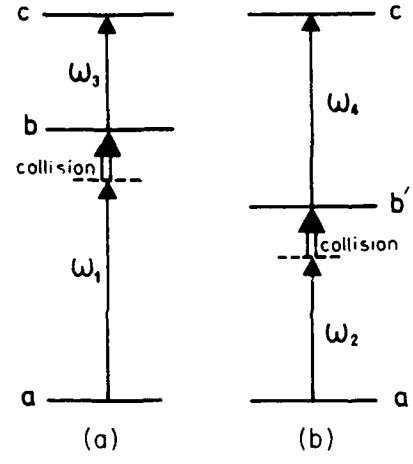

FIG. 10. Collisionally aided excitation of level c. The pathway (a) corresponds to a collisionally aided two-step excitation with intermediate excitation of level b. The pathway (b) is associated to a similar process with intermediate excitation of level b'. The interference between these pathways leads to a pressure-induced extra resonance centered at $\delta=0$.

CONCLUSION

In conclusion, we have presented three different examples of pressure-induced extra resonances that can be observed in nonlinear spectroscopy. We have shown that all these resonances can be qualitatively interpreted in terms of interference between quantum pathways, each pathway involving a collisionally aided excitation. Finally, we have shown that the resonances can be obtained in some cases with incoherent fields while, in other cases, coherent fields are required.

Implicit in our approach has been the neglect of any effects arising from the atoms' velocity. As long as the single-photon and two-photon detunings Δ_1, Δ_2', Δ_3,

$|\Delta_4'|$, $|\Delta_1+\Delta_3|$ are all much greater than the Doppler widths associated with their corresponding transitions, one is at liberty to neglect the Doppler shifts associated with these terms. On the other hand, $|\delta|$ is a small quantity compared with $|\Delta_1|$ or $|\Delta_2'|$, consequently, one should include any effects of residual Doppler shifts in all terms containing δ. The results are then modified by replacing δ by $\delta-(\mathbf{k}_1-\mathbf{k}_2)\cdot\mathbf{v}$ and averaging over a Maxwellian distribution of velocities having most probable speed u. If $Ku \ll \Gamma_{bb'}$ ($\mathbf{K}=\mathbf{k}_1-\mathbf{k}_2$), none of the results are changed. If $Ku \gg \Gamma_{bb'}$, the results are modified as follows: (a) In Eq. (11), the first term no longer contributes and the second term becomes a Gaussian of width Ku; (b) in Eq. (34), the PIER contribution no longer varies as t for $\delta \sim 0$; (c) in Eq. (43), the PIER contribution is again proportional to a Gaussian having width Ku. The ratio $Ku/\Gamma_{bb'}$ is determined in a large part by the energy separation of levels b and b'. To observe PIER, it is thus best to have two nearby energy levels.

ACKNOWLEDGMENTS

This research was supported, in part by the National Science Foundation (NSF) International Grants (No. INT 841 33 00 and INT 881 50 36). The research of P.R.B. is supported by the U.S. Office of Naval Research and the NSF (Grant No. PHY 84 15 781 and PHY 88 14 423). The Laboratoire de Spectroscopie Hertzienne de l'Ecole Normale Supérieure is "associé au Centre National de la Recherche Scientifique, à l'Ecole Normale Supérieure, et à l'Université Pierre et Marie Curie."

---

[1]Y. Prior, A. R. Bogdan, M. Dagenais, and N. Bloembergen, Phys. Rev. Lett. **46**, 111 (1981). For a recent review see L. J. Rothberg, in *Progress in Optics*, edited by E. Wolf, (Elsevier Scientific, Amsterdam, 1987), pp. 39–101.

[2]V. Mizrahi, Y. Prior, and S. Mukamel, Opt. Lett. **8**, 145 (1983).

[3]G. S. Agarwal, Opt. Commun. **57**, 129 (1986).

[4]P. R. Berman and G. Grynberg, Phys. Rev. A **39**, 570 (1989); G. Grynberg and P. R. Berman, *ibid.* **39**, 4016 (1989).

[5]In fact, the conditions $|\Omega_1/\Delta_1| \ll 1$ and $|\Omega_2'/\Delta_2'| \ll 1$ are necessary conditions to justify a perturbative expansion, but they are not sufficient. Other conditions [see formula (10) and Ref. 11) should also be verified.

[6]In the relaxation terms, we neglect the coupling between the coherence $\rho_{bb'}$ and the population ρ_{aa}. Such an assumption is generally justified because the term that has been neglected leads to nonsecular contributions. However, there are a few cases where this term should be kept [see G. Grynberg and M. Pinard, Europhys. Lett. **1**, 129 (1986)].

[7]A. Omont, E. W. Smith, and J. Cooper, Astrophys. J. **175**, 185 (1972); J. L. Carlsten and A. Szöke, J. Phys. B **9**, L231 (1976); C. Cohen-Tannoudji, J. Dupont-Roc, and G. Grynberg, *Processus d'interaction entre Photons et Atomes* (InterEditions, Paris, 1988), Complément B VI.

[8]N. Bloembergen, H. Loten, and R. T. Lynch, Jr., Indian J. Pure Appl. Phys. **16**, 151 (1978).

[9]G. Grynberg, J. Phys. B **14**, 2089 (1981).

[10]Actually the coherences given by Eqs. (7) are the reduced coherences, which are related to the real coherences $\langle i(N_1,N_2)|\rho|j(N_1,N_2)\rangle$ by the relation $\rho_{ij} = \sum_{N_1,N_2}\langle i(N_1,N_2)|\rho|j(N_1,N_2)\rangle$.

[11]The ratio (12) should, however, remain smaller than 1 if one wants the perturbation expansion to be correct. In particular, the higher-order terms are negligible only if the ratio (12) is smaller than unity.

[12]The calculation for $\delta \sim 0$ in the dressed-state basis requires one to solve the coupled equations of evolution in the subspace generated by $|1(N_1,N_2)\rangle$ and $|2(N_1,N_2)\rangle$.

[13]A practical way to realize such an excitation would be to have two light sources of frequencies ω_1 and ω_3 and two acousto-optic modulators to obtain the other frequencies ω_2 and ω_4 by shifting the frequencies ω_1 and ω_3. Because of the small value of $|\omega_1-\omega_2|$ and $|\omega_3-\omega_4|$, the levels b and b' would be fine or hyperfine sublevels, or even Zeeman sublevels whose degeneracy can be shifted by applying a static magnetic field.

[14]The shift of the two-photon resonance due to the imaginary part of Γ_{ca} has been included in $(\Delta_1+\Delta_3)$ when we have written formula (41).

[15]E. Giacobino and P. R. Berman, Phys. Rev. Lett. **58**, 21 (1987).

[16]The same argument can be applied for the diagrams of Figs. 7 and 8.

[17]See, for example, R. J. Glauber, in *Quantum Optics and Electronics*, edited by C. de Witt, A. Blandin, and C. Cohen-Tannoudji (Gordon and Breach, New York, 1965), p. 63.

Laser Spectroscopy IX,
edited by M. Feld, J. Thomas,
A. Mooradian

Dressed-Atom Approach to Collision-Induced Resonances

P. R. Berman
Physics Department, New York University, 4 Washington Place,
New York, NY 10003, USA
C. Grynberg
Laboratoire de Spectroscopie Hertzienne de l'Ecole Normale
Supérieure, Université Pierre et Marie Curie,
75252 Paris CEDEX 05, France

Motivated in large part by the work of Bloembergen and coworkers, there has been considerable interest over the past ten years in the study of pressure-induced extra resonances, a class of resonant structures that appear in spectroscopic line shapes only in the presence of collisions (1). What is particularly intriguing about the pressure-induced resonances is that collisions, which are often thought to broaden and destroy coherent structures, are essential for producing these resonances. Moreover, the pressure-induced resonances can be very narrow, in some cases having widths equal to the inverse lifetime of the ground states of the atoms which are interacting with the laser fields. It is relatively simple to obtain theoretical expressions for the pressure-induced resonances. What has been more elusive, however, is a physical explanation of their origin.

We present an interpretation of pressure-induced resonances based on a dressed-atom picture of the atom-field interaction (2)-(4). Both semiclassical (classical fields - quantum-mechanical atoms) and fully-quantized (quantized fields - quantum-mechanical atoms) dressed-state theories are employed. Using this dressed-atom approach, we are able to show that the vanishing of the pressure-induced resonances in the absence of collisions is a direct consequence of the conservation of energy. The positions and widths of the resonances can be attributed either to a modulated dressed-state population or to a level-crossing of the dressed states.

In order to illustrate the physical concepts, we consider a pressure-induced resonance that is produced in fluorescence beats (4),(5). A two-level atom is subjected to two copropagating laser fields (Fig. 1). The first field has frequency Ω and is detuned by $\Delta = \omega - \Omega$ from the atomic resonance, while the second field has frequency $\Omega+\delta$. It is assumed that $|\delta| \leq \gamma_2 \ll |\Delta|$ (γ_2 is the decay rate of the excited state) and that $|\Delta|$ is much greater than the Doppler width associated with the 1-2 transition. If the incident fields are relatively coherent, it is found that part of the fluorescence from level 2 is modulated at frequency δ. To lowest order in the applied fields, this component of the fluorescence, denoted by $I(\delta)$, is given by

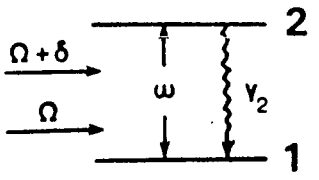

Fig. 1. Copropagating laser fields having frequencies Ω and $\Omega+\delta$ are incident on on a two-level atom. Modulated fluorescence from level 2 is monitored as a function of δ.

$$I(\delta) = \frac{\chi_1 \chi_2^*}{\Delta^2} e^{i\delta t}\left[1 + \frac{2\Gamma}{\gamma_2 + i\delta}\right] + \text{c.c.},$$

where χ_i is a Rabi frequency associated with field i and Γ is a collision rate associated with the atomic coherence ρ_{12}. The modulated fluorescence consists of a background term (present even in the absence of collisions) and a pressure-induced term which exhibits a resonant structure centered at $\delta=0$, having width γ_2.

To explain the physical origin of this resonance, we use a fully-quantized dressed-atom approach. To lowest order in the applied fields, the appropriate dressed states are given by

$$|A;n_1,n_2\rangle = |1;n_1,n_2\rangle + \theta(n_1)|2;n_1-1,n_2\rangle + \theta(n_2)|2;n_1,n_2-1\rangle$$

$$|B;n_1,n_2\rangle = |2;n_1,n_2\rangle - \theta^*(n_1+1)|1;n_1+1,n_2\rangle - \theta^*(n_2+1)|1;n_1,n_2+1\rangle,$$

where the n's label the photon number states of the fields,

$$\theta(n) = ig\sqrt{n}/\Delta,$$

and g is a coupling constant. Some of the dressed energy levels are shown in Fig. 2

The structure of the fluorescence beats can now be understood as follows: In the absence of collisions, all population remains in the "A" dressed states, since there is no physical mechanism to provide the energy difference Δ to transfer population from states A to B. Since states $|A;n_1,n_2\rangle$ and $|A;n_1,n_2+1\rangle$ each contain an admixture of state $|2;n_1,n_2\rangle$, they can undergo a radiative decay to state $|A;n_1,n_2\rangle$. The component of the modulated fluorescence associated with this collision-free contribution is

$$I_{cf}(\delta) = \sum_{n_1 n_2} \theta(n_1+1)\theta^*(n_2+1)\rho^F_{n_1+1,n_2;n_1,n_2+1}(t) + \text{c.c.},$$

where $\rho^F(t)$ is the free-field density matrix. There is no resonant structure centered at $\delta=0$. As can be seen in Fig. 2, the collision-free contribution to the fluorescence occurs at the laser frequencies.

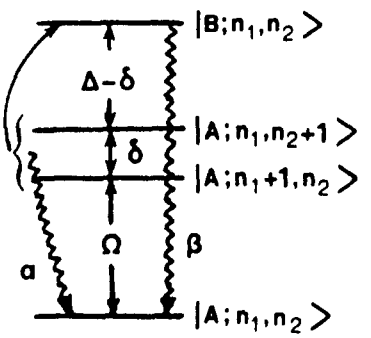

Fig. 2. Dressed states of the atom-field system. Collisions couple states A and B within a given manifold (curved arrow). A coherence between states $|A;n_1,n_2+1\rangle$ and $|A;n_1+1,n_2\rangle$ produced by the incident fields leads to background (α) and pressure-induced (β) modulated fluorescence.

With collisions present, states $|A\rangle$ and $|B\rangle$ within a given dressed-state manifold are coupled since the collisional interaction can provide the energy mismatch $\hbar\Delta$ between these states. Radiative decay from level $|B;n_1,n_2\rangle$ to $|A;n_1,n_2\rangle$ results in fluorescence centered at the *atomic* frequency (see Fig. 2 – recall that $\Delta+\Omega=\omega$). The modulated component of this fluorescence is given by

$$I_C(\delta) = \theta(n_1+1)\theta^*(n_2+1)\,[2\Gamma/(\gamma_2+i\delta)] \times \rho^F_{n_1+1,n_2;n_1,n_2+1}(t) + \text{c.c.}$$

The amplitude of this collision-induced component vanishes in the absence of collisions. Owing to the modulation of ρ_{BB}, the fluorescence exhibits a resonant structure centered at $\delta=0$, having width γ_2. The modulated fluorescence can be traced to a combined collisional-radiative process that couples the initial coherence $\rho_{A,n_1+1,n_2;A,n_1,n_2+1}$ to the dressed-state population $\rho_{B,n_1,n_2;B,n_1,n_2}$.

It is seen that the fluorescence vanishes unless $\rho_{n+1,n} \neq 0$ for each of the incident fields. In other words, the incident fields must be phase coherent to produce the fluorescence beats. The same conclusion would have been reached had we used a semiclassical dressed atom approach (4). In that case, the collision-induced modulated signal is proportional to $\chi_1\chi_2^*$ which vanishes, on average, for uncorrelated fields. In a manner analogous to that presented for fluorescence beats, one can use a dressed-atom approach to explain the pressure-induced resonances that can be produced when (a) a three-level atom is excited by four incident fields (3); (b) a four-level atom is excited by four incident fields (6); an atom is ionized by four fields (6); and (d) four-wave mixing signals are generated in active media of two or three-level atoms. In contrast to cases (a)-(c), in case (d) the signal depends only on the average number of photons in each incident field; the incident fields need only be spatially coherent to generate the appropriate phase-matched emission.

Acknowledgments. This research is supported in part by NSF Grants INT-8413300 and INT-8815036. The research of PRB is supported by the U. S. Office of Naval Research and NSF Grant PHY-8814423. The Laboratoire de Spectroscopie Hertzienne de l'Ecole Normale Supérieure is "associé au Centre National de la Recherche Scientifique."

References

1. For recent reviews of pressure-induced resonances, see L. Rothberg, in *Progress in Optics*, edited by E. Wolf (Elsevier Scientific, Amsterdam, 1987), pp. 39-101; G. Grynberg, in *Spectral Line Shapes*, edited by R. Exton (A. Deepak, Hampton, VA, 1987), Vol. 4, pp. 503-521.
2. G. Grynberg, J. Phys. B14, 2089 (1981).
3. P. R. Berman and G. Grynberg, Phys. Rev. A39, 570 (1989).
4. G. Grynberg and P. R. Berman, Phys. Rev. A39, 4016 (1989).
5. G. S. Agarwal, Opt. Comm. 57, 129 (1986).
6. G. Grynberg and P. R. Berman, submitted to Phys. Rev. A.